AL.Z.1986-729

Information Series No. 63
February, 1974

TDA-RCA Capsule Pipeline Project

Phase 2 Report

edited by
Erik J. Jensen

Contributors
H. S. Ellis
Jan Kruyer
A. A. Roehl

Alberta
RESEARCH

Digitized by the Internet Archive
in 2017 with funding from
University of Alberta Libraries

https://archive.org/details/tdarcacapsulepip63albe

TDA-RCA CAPSULE PIPELINE PROJECT

SEP 15 1975
c. 1

PHASE II REPORT

edited by
Erik J. Jensen

contributors,
H. S. Ellis, Jan Kruyer, A.A. Roehl

Alberta Research

Information Series No. 63

February, 1974

LIST OF CONTENTS

Chapter I	Introduction and Summary	2
Chapter II	Nomenclature, Definition of Terms and Experimental Details	7
Chapter III	Hydrodynamics of Cylindrical Capsules	13
Chapter IV	Hydrodynamics of Spherical Capsules	32
Chapter V	A Model Which Relates the Capsule Pressure Gradient, Capsule Velocity and Liquid Velocity for Cylinders	47
Chapter VI	Friction and Surface Roughness of Cylinders in Capsule Pipelines	75
Chapter VII	Methods of Minimizing Pressure Gradients	91
Chapter VIII	Further Work Required	106
Appendix A	Data Acquisition and Control of an Experimental Four Inch Pipeline	108
Appendix B	Operation and Data Acquisition of a Ten Inch Experimental Pipeline	120

CHAPTER I

Introduction and Summary

CHAPTER I

Introduction

In January 1971, the Federal Ministry of Transport, through the Transportation Development Agency, granted a 3-year contract for the purpose of developing reliable design equations for the movement of bulk commodities in capsule form in liquid media. The equations would be based on hydrodynamic studies using experimental pipelines ranging in diameter from one-half to ten inches.

The report on Phase I of the project, published in two parts in February 1973, reiterated details of the Work Statement of the contract and covered activities from January 1971 to April 1972. Part 1 reported the analytical work, the University Support Program, and the experimental program formulated during that period, while Part 2 contained drawings of the pipelines, outlines of the computer programs and other documentation.

The present Phase II report deals with experimental and analytical results obtained during the period April 1972 to April 1973, and presents interpretations and conclusions of the work done during this period. The report may be considered a comprehensive progress report. The conclusions reached during this time will be expanded in the Phase III report, which will be submitted after the conclusion of the project.

During the period under review some personnel changes have taken place. Mr. R. Cushing, Northern Natural Gas Company, Omaha, resigned from the Project Advisory Committee due to pressure of work. Mr. R.A. King, ShelPac, Toronto, was replaced by Mr. G.H. Durham of the same company.

The only R.C.A. staff change occurred when Mr. G.E. Johanson resigned in 1973 and Mr. M.L. Blachut joined the team that operates the ten-inch pipeline facility.

The experimental results obtained have shown that there is a very definite relationship between the capsule pressure gradient, the capsule velocity and the liquid velocity and that one of these can be predicted when the other two are known. It has also been shown that so far as cylindrical capsules are concerned, the capsule pressure gradient is affected by three factors: the roughness of the surfaces, the coefficient of friction between the surfaces and the distortion of the velocity profile of the liquid.

An important conclusion is that the determination of the hydrodynamics of a capsule pipeline is very dependent upon the types of materials and pipe used, and a verified correlation of the power requirements, pressure gradients and velocities will be limited to materials tested.

Summary

The nomenclature used in the report, the data acquisition and reduction procedures are presented in Chapter II. A description of the experimental facilities has already been given in the Phase I report. Additional details of experimental techniques are contained in Appendix A and B of the Phase II report.

Chapter III deals with the hydrodynamics of cylindrical capsules, and the effects of bulk velocity, diameter ratio, capsule specific gravity and pipe diameter are considered individually. It has been found that the pressure gradient due to a train of flowing capsules can increase or decrease, depending mainly on the buoyed specific gravity and the capsule-pipe interface. This is contrary to the pipeline flow of liquids where the pressure gradient increases with increasing velocity.

The effect of the diameter ratio is that the capsule pressure gradient at a given bulk velocity appears to be directly proportional to the square of the diameter ratio. The capsule pressure gradient is also directly proportional to the buoyed specific gravity at low capsule velocities but becomes decreasingly dependent on it as the velocity increases.

The experimentation related to the effect of pipe diameter has not been completed, but the results in hand indicate that the pressure gradient is inversely related to the square root of the pipe diameter.

In Chapter IV the hydrodynamics of spherical capsules are discussed. It has been found that the pressure gradients for spherical capsules generally are smaller than for cylindrical capsules for the same mass throughput, and spheres are increasingly attractive hydrodynamically as the specific gravity of the solid material increases.

In Chapter V a model which relates the capsule pressure gradient, the capsule velocity and the liquid velocity for cylinders is presented and evaluated. The model

allows the prediction of the bulk velocity when both the capsule velocity and the capsule pressure gradient are known and thus enables the calculation of the amount of liquid required to move a given quantity of solids. It also allows the prediction of the capsule pressure gradient when both the capsule velocity and the bulk velocity are known, but the measurement of these velocities must be very accurate before the capsule pressure gradient can be predicted to a reasonable accuracy.

Chapter VI deals with friction and surface roughness effects in capsule pipelines. It is shown that the pressure gradients for cylindrical capsules with densities different from that of the carrier liquid are influenced by the interaction between the surfaces of the capsule and the pipe. Pressure gradients for capsules at the point of incipient motion can be calculated directly from the coefficient of friction. For moving capsules, however, the pressure gradients are a function of the capsule velocity, the surface roughnesses of the capsule and pipe walls and the coefficient of friction. Data are presented to show how capsule pressure gradients change with velocity for various degrees of capsule and pipe surface polish.

The methods that can be employed to minimize pressure gradients, and therefore power requirements in capsule pipelining, are discussed in Chapter VII. It is concluded that if the solid to be transported has a specific gravity greater than 1.25, spheres are the most advantageous form of capsules. If cylindrical capsules have to be used, the most advantageous pressure gradients are obtained by using one or a combination of the following methods:

(1) Reduction of the coefficient of friction by applying a low-friction coating to the capsule and/or pipe.
(2) The use of smooth capsule and pipe surfaces.
(3) Fitting the capsules with collars. This is the most effective way of reducing the power required for the transport of cylinders other than method (4).
(4) Manufacturing the capsules with voids. This can reduce the power requirements by an order of magnitude.

Chapter VIII briefly outlines further work required on the hydrodynamics of capsule flow for the remainder of the project, based on the conclusions of the research results analyzed to date. Work required in some areas of the complete capsule pipeline

system is also indicated.

Two recent papers detailing the methods of measurement in the four-inch and ten-inch pipeline facilities form Appendix A and B.

CHAPTER II

Nomenclature, Definition of Terms and Experimental Details

CHAPTER II

Nomenclature, Definition of Terms and Experimental Details

2.1 Nomenclature

A	cross sectional area of pipe		ft^2
C	a dimensional constant	144/62.34 =	2.31 $in^2/ft/lb.$
d	capsule diameter		in.
D	pipe internal diameter		in.
F	force		lb.
f	Fanning friction factor		-
g	gravitational acceleration		$ft./sec.^2$
g_o	gravitational conversion factor		$lb_m\ ft/lb_f\ sec.^2$
k	capsule/pipe diameter ratio, d/D		-
L	length		ft.
N	number of capsules		-
P	pressure		$lb./in.^2$
Q	volumetric flow rate		$ft^3/sec.$
R	a ratio		-
Re	Reynolds number		-
T	solid throughput		millions of tons/yr.
V	velocity		ft/sec.
w	width		ft.
y	distance between two surfaces		ft.

Subscripts

a	annular
b	bulk
c	capsule
f	fluid
m	fluid and capsule
p	pipe test section
t	train

Greek letters

β	buoyed specific gravity = $\frac{\sigma - \rho}{62.36}$	-
	[When water at 60°F is the transporting liquid, ρ = 62.36 and β = (S.G. of capsule) - 1.]	
Δ	differential between two points	-
η	coefficient of friction	-
λ	linear fill = (sum of the lengths of the capsules)/pipeline length	
ν	kinematic viscosity	$ft^2/sec.$
ρ	weight density of liquid	$lb/ft.^3$
σ	weight density of capsule	$lb/ft.^3$
τ	shear stress	$lb/in.^2$

2.2 Data Acquisition and reduction

The data acquisition apparatus for the four-inch laboratory pipe and the ten-inch pipe were described in the Phase I Report, Part 1, Chapters V to VII and Part 2. The apparatus for the half-inch pipe was almost identical to that of the four-inch pipe. The following notes summarize the calculation of the principal parameters and variables discussed in this report. Further details of experimental procedures and techniques are given in Appendix A and B.

Pressure gradients. The pressure gradients due to the liquid were obtained by dividing the pressure differential when only liquid was flowing, by the distance between the pressure taps. The calculation of pressure gradients along a capsule train is more involved, since experimental trains usually do not fully occupy the distance between the pressure taps. It was found convenient to convert the pressure gradients to represent a linear line fill of 100%. For example, if 60% of the distance between the pressure taps was filled by liquid, 60% of the pressure differential for liquid alone was subtracted from the pressure differential measured while the capsule train moved between the pressure taps; the result was then divided by the train length. In mathematical terms:

$$\left(\frac{\Delta P}{L}\right)_c = \left[(\Delta P)_m - \frac{(L_p - L_c)}{L_p} (\Delta P)_f \right] / L_c$$

where $\left(\frac{\Delta P}{L}\right)_c$ is the pressure gradient due to the capsule train for 100% linear line fill, $(\Delta P)_m$ and $(\Delta P)_f$ are the pressure drops between the taps due to the capsules plus liquid and liquid alone respectively, and L_p and L_c the distance between the taps and the length of the capsule train respectively. Accordingly, $\left(\frac{\Delta P}{L}\right)_c$ refers to the capsules and the annular liquid and includes any pressure effects due to the ends of the capsules.

Capsule velocities, V_c, were measured by timing the nose of the first capsule of the train between several pairs of light-photocell assemblies at intervals along the pipeline so that the constancy of the velocity could be checked. See Appendix I. In the four-inch pipe it was found advisable to

hold the cylindrical capsules of a train together with magnets or hooks. In the ten inch-pipe the capsules were free, and maintaining a continuous train generally presented little problem, though some difficulty was experienced with capsules with collars. (See Chapter 7.) Any breaks in the continuity of the train were recorded and taken into account.

The bulk velocity, V_b, is defined as Q/A, where Q is the volumetric flow rate at any pipeline section (cu.ft./sec.), and A is the cross-sectional area of the pipeline ($ft.^2$). Q is constant at any section of the pipeline whether it contains liquid alone or capsules and annular liquid. Measurement of the liquid flow rate with a magnetic flowmeter therefore gives Q which, when divided by A, gives not only the mean liquid velocity in capsule-free sections of the pipeline but also the total bulk velocity in the capsule-filled sections. Accordingly the symbol V_{av} which was used in previous papers to denote the average velocity of the liquid in the free pipe has been replaced by the symbol V_b. It is numerically equal to V_{av}.

In order to calibrate the flowmeter a plunger or an inflated sphere was timed between several pairs of light-photocell assemblies. The volumetric flow rate was calculated from this "pig" velocity multiplied by the average cross-sectional area of the pipe.

Buoyed specific gravity. The force exerted by a stationary capsule on the pipe is proportional to the weight density of the capsule (σ) minus that of the liquid (ρ), i.e. to the buoyed weight density of the capsules ($\sigma - \rho$) lb./cu.ft. ($\sigma - \rho$) multiplied by the volume of the capsule in cubic feet gives the normal gravity force. This is the force which gives rise to friction when the capsule is stationary or moving very slowly. It is also a significant parameter when the capsule is moving rapidly. However, this force, $(\sigma - \rho)\,\pi d^2\, L_c /4 \times 144$ is not a convenient parameter when capsules of different diameters and lengths are used. It was therefore decided to use the dimensionless "buoyed specific gravity", $\beta = \frac{\sigma - \rho}{62.36}$, the constant being

the weight density of water at 60°F. β allows the comparison of the performance of capsules of different dimensions without involving the length and diameter. When water at 60°F is the transporting liquid, as in most of the experimental work reported in this Phase: specific gravity of the solid = $1 + \beta$. A table of specific gravities and weight densities follows.

TABLE 1

Table of specific gravities and weight densities.

S.G. of solid	S.G. of liquid *	β	σ (lb/ft^3)	ρ (lb/ft^3) *	($\sigma - \rho$) (lb/ft^3) *
3.000	1.000	2.000	187.08	62.36	124.72
2.000	"	1.000	124.72	"	62.36
1.500	"	0.500	93.54	"	31.18
1.250	"	0.250	77.95	"	15.59
1.125	"	0.125	70.16	"	7.80
1.062	"	0.062	66.23	"	3.87
1.031	"	0.031	64.29	"	1.93
1.000	"	0.000	62.36	"	0.00
0.969	"	-0.031	60.43	"	-1.93
0.938	"	-0.062	58.49	"	-3.87
0.875	"	-0.125	54.57	"	-7.80
0.750	"	-0.250	46.77	"	-15.59

* For water at 60°F used as the transporting liquid; for the experiments at elevated viscosity ρ is somewhat different, but for these σ was adjusted to maintain the same values of β as with the experiments in water.

2.3 Experimental Testing Schedule

Table 2 gives details of the pipe test sections and capsules used in the experiments.

TABLE 2

Experimental Schedule

Nominal pipe size (in.)	$\frac{1}{2}$	4	4	4	10
Average diameter (in.)	0.62	4.026	4.029	4.029	10.02
Material of test section	stainless steel	cellulose acetate butyrate	stainless steel	stainless steel	mild steel
Conveying liquid	water	water	water	water-glycol mixtures	water
Material of cylinder surfaces	stainless steel	stainless steel	stainless steel or butyrate	butyrate	mild steel
Material of spheres	stainless steel	-	P.V.C. (hollow)	P.V.C. (data not yet available)	aluminum and iron

CHAPTER III

Hydrodynamics of Cylindrical Capsules

CHAPTER III

Hydrodynamics of Cylindrical Capsules

Summary

The effects of bulk velocity, diameter ratio, capsule specific gravity and pipe diameter are considered individually.

1. The effect of bulk velocity.

In conventional pipe flow the pressure gradient due to a flowing liquid increases with an increase of bulk velocity; however, the pressure gradient due to a train of flowing capsules can increase or decrease, depending mainly on the buoyed specific gravity and the capsule-pipe interface.

2. The effect of diameter ratio.

For capsule/pipe diameter ratios between 0.80 and 0.95, which are the ratios most likely to be used in commercial pipelines, the capsule pressure gradient at a given bulk velocity appears to be directly proportional to the square of the diameter ratio.

3. The effect of capsule specific gravity.

The capsule pressure gradient is directly proportional to the buoyed specific gravity at low capsule velocities but becomes decreasingly dependent on it as the velocity increases.

4. The effect of pipe diameter.

At the same capsule velocity the pressure gradient data from the stainless steel capsules in the four inch stainless steel pipe and the steel capsules in the ten inch steel pipe appear to be inversely related to the square root of the pipe diameter. The data for the half-inch pipe cannot be used for comparison until they have been satisfactorily related to the capsule specific gravity. It is likely that most represent laminar flow.

3.1 The Effect of Bulk Velocity

Fig. 3-1 is a plot of the variations of capsule pressure gradient with bulk velocity in the half-inch pipe due to trains of eight stainless steel cylinders of four specific gravities; the test section was of stainless steel and the conveying liquid, water. The data are capsule pressure gradients at 100% linear fill, as explained under "Data Acquisition and Reduction", Chapter 2.2. The plain line at the bottom of the Figure indicates the pressure gradients for the water alone and shows the familiar upward curve for turbulent flow.

At a buoyed specific gravity, $\beta = 0.031$ (S.G. = 1.031) for medium and high velocities the pressure gradients due to the capsules and the annular liquid are lower than those of the liquid alone. This phenomenon is discussed in Chapter 7. As β increases, the curves change from concave, like that of the liquid, through a linear configuration to convex.

In Chapter 6 it is suggested that the pressure gradient is due to the distortion of the velocity profile and to solid and liquid friction. The distortion of the profile is almost independent of β, but the solid friction is directly proportional to β, and the liquid friction under the capsule is strongly influenced by it through the variation of clearance. As the capsule velocity increases, the increasing lift on the capsule reduces the effect of β, and the pressure gradient due to it is reduced; however the pressure gradient due to the distortion of the velocity profile increases with increasing velocity. The reduction of pressure gradient due to increasing lift is more evident with denser capsules and the increase due to the liquid profile distortion is more noticeable with less dense capsules. Both effects can be seen clearly in Fig. 3-1.

Fig. 3-2 presents data from three diameter ratios for each of three specific gravities of cylinders in the four inch pipe. The trend towards independence of β at high velocities is evident again. Although this Figure shows the pressure gradient to be rather constant with increase of V_b for a given specific gravity, Chapter 6 establishes the fact that if the capsule-pipe interface is very smooth, very considerable reductions of pressure gradient can occur with increasing velocity. See Fig. 6-2 for example.

The ten-inch pipe data of Fig. 3-3 show the same rather constant pattern as Fig. 3-2. There is an initial fall of pressure gradient as the velocity increases which is probably due to a reduction of solid friction since the clearance between the capsule and the bottom of the pipe may increase with velocity. With some metal capsule-pipe surface conditions the dip is absent, and for capsules with a vinyl surface the reduction continues until a much higher velocity is reached (see Fig. 7-5).

It appears that the most significant parameters in determining the variation of pressure gradient with bulk velocity are the buoyed specific gravity of the capsules, the capsule-pipe interface conditions and the distortion of the liquid profile due to the moving capsule.

3.2 The Effect of Diameter Ratio

Only one diameter of capsules was tested in the half-inch pipe so that the effect of capsule diameter in this line cannot be determined, but the data of Fig. 3-2 for the four-inch pipe provide a good opportunity. In Fig. 3-4 the pressure gradients of Fig. 3-2 have been divided by k^2 and plotted against V_c instead of V_b. Whereas in Fig. 3-2 at a particular specific gravity the pressure gradient increased with k, the variation in Fig. 3-4 is independent of k. If the possible variations of pressure gradient due to the coefficient of friction and roughness illustrated in Chapter VI are taken into account, the correlation of this Figure may be considered good.

A force balance in Chapter VI shows that if the capsule and pipe shear stresses are assumed to be equal when the capsule is stationary, the pressure gradient for this condition is proportional to k rather than k^2, as indicated for a moving capsule by Fig. 3-4. This would mean that as V_c approached zero the ordinate would increase as the diameter ratio decreased. There is some sign of this for the two higher specific gravities, but the result is indeterminate.

A similar diameter ratio correlation for the data from the ten-inch pipe is shown in Fig. 3-5. The results seem more consistent than those for the four-inch pipe, probably because there was less variation in capsule-pipe interaction in the ten-inch pipe.

The data from both the four-inch and ten-inch pipes indicate that for moving capsules at all capsule specific gravities and bulk velocities tested the pressure gradient

is closely proportional to the square of the diameter ratio. While this relationship appears to militate against large diameter capsules it should be pointed out that the throughput of solid at the same capsule velocity is also proportional to k^2. Thus at the same capsule velocity the capsule pressure gradient per unit throughput is independent of diameter ratio. In addition the annular liquid flow is considerably reduced with an increase in diameter ratio, so that less liquid is required for the same solid throughput.

3.3 The Effect of Capsule Specific Gravity

In Fig. 3-6 the pressure gradients in the half-inch pipe divided by the buoyed specific gravity as well as by k^2 are plotted against V_c. The diameter ratio was constant in this pipe, but k^2 has been included to confirm with the Figures for the four-inch and ten-inch pipes. The division by β makes the ordinate dimensionless when a constant $C = 2.31$ in.^{2}ft/lb. is introduced to relate the pressure and density units. The pressure gradients are correlated at very low capsule velocities (compare Fig. 3-1); however, as the velocity increases, the curves for the different specific gravities diverge widely. This indicates that the divisor representing the effect of specific gravity needs to be gradually eliminated with increasing velocity. Fig. 3-1 shows that as the velocity rises the pressure gradient becomes increasingly independent of β so that apparently at very high velocities no specific gravity correlation would be needed. The reasons for this were discussed in section 3.1. The curves for the low specific gravity capsules of Fig. 3-6 undergo upward changes of slope which have been magnified by division of the pressure gradient by the small fractional values of β.

Fig. 3-7 presents similar plots of the pressure gradients in the four-inch pipe divided by the diameter ratio and buoyed specific gravity. The three diameter ratios of Fig. 3-4 at each buoyed specific gravity have been plotted with a single symbol so that the three symbols represent the three buoyed specific gravities. Data points further than $\pm$ 20% from the mean line of any particular specific gravity have been ignored for the sake of clarity. As in the previous Figure the data converge towards a point on the y axis ($V_c = 0$). The data for the highest specific gravity capsules curve downward as the velocity reaches high values, while those for the smaller specific gravity capsules continue to rise slightly, showing the results of the decrease of the effect of β and the increase of profile distortion, as discussed in 3.1.

Corresponding plots for capsules of β = 0.031 and 0.062 are similar when the capsule velocity is small but rise more steeply at medium and high velocities than those of β = 0.125 and 0.250. Therefore, dividing $(\Delta P/L)_c / k^2$ by β correlates the data near the threshold velocity as it did for the half-inch pipe data, but again separates the data increasingly as the velocity rises; this is an indication of the need to separate the effects of β from that of profile distortion, so that the two effects can be considered separately. However, the effects due to the velocity profile distortion for the four-inch pipe data are less than for the half-inch pipe data.

The data for the ten-inch pipe have been related to k^2 and β in a similar way in Fig. 3-8. The profile distortion effects are even less than for the four-inch pipe, the points from the three specific gravities being well distributed with less scatter; however, the data for β = 0.500 fall off at high velocities and those for the lowest specific gravity (β = 0.125) rise as in Figs. 3-6 and 3-7 for the smaller diameter lines.

Data from all three pipes indicate the need for an expression which will give correct weight to the two components of the pressure gradient, and this will be a task for the next Phase of the project.

3.4 The Effect of Pipe Diameter

The ordinates of Fig. 3-6 for the half-inch pipe have been divided by the Froude number, $V_c / \sqrt{gD}$ and plotted against V_c in Fig. 3-9 in order to compare them with corresponding plots for the bigger diameter pipes. The correlation of Fig. 3-9 is similar to that for the buoyed specific gravity (Fig. 3-6), being good at low capsule velocities but becoming very poor at high velocities, especially for the lower specific gravities, due to the lack of a specific gravity correlation which varies with V_c.

A similar plot for the three specific gravities and three diameter ratios of the four-inch pipe data (Fig. 3-10) shows considerable improvement. No diameter ratio or specific gravity trends are apparent and the scatter is understandable in view of the differences of roughness discussed in Chapter VI. The similar plot for the ten-inch pipe (Fig. 3-11) shows an even better correlation.

The curves for the four-inch and ten-inch pipes, both referring to steel capsules in a steel pipe, are very similar, and indeed the value of $\sqrt{D}$ was chosen for comparison for this reason, V_c being introduced to complete the Froude number and restore the ordinate to a dimensionless group.

A better correlation of the half-inch pipe data with the specific gravity will have to be found before data from that pipe can be included in an estimate of the effect of pipe diameter. This will have to show a gradual reduction of the effect of specific gravity as the capsule velocity increases.

Though V_c has been used to complete the Froude number, the bulk velocity, V_b, is more properly used, since it is more closely connected with the pipe diameter. A good correlation is obtained for both the four-inch and the ten-inch lines if V_b is used in both the ordinate and abscissa, i.e. if $C\sqrt{gD}\,(\Delta P/L)_c/\beta k^2\ V_b$ is plotted against V_b as in Fig. 3-12.

V_b is less convenient than V_c as an independent variable since V_c can readily be calculated from the required throughput of solid; V_b and the pressure gradient are usually the unknown quantities. However, from Figs. 3-11 and 3-12 the pressure gradient may be obtained from either the capsule or bulk velocity in four-inch and ten-inch pipes under the conditions of the tests.

The present correlations apply to trains of steel-shelled capsules of specific gravities from 1.125 to 1.50 and diameter ratios from 0.85 to 0.95 in four-inch and ten-inch steel pipes; they allow the pressure gradient to be determined from either the capsule or bulk velocity, the capsule specific gravity and diameter and the pipe diameter. The reductions of pressure gradient to be achieved by smoothing the capsule surface and by other methods are discussed in Chapter 7.

3.5 Conclusions

Though surface effects can completely mask those of diameter ratio and pipe diameter (Chapter 6), for similar capsule and pipe surfaces the pressure gradient appears to be proportional to (diameter ratio)^2 and inversely proportional to $\sqrt{\text{pipe diameter}}$. At very low velocities the pressure gradient is proportional to the buoyed specific gravity of the capsules, but at high velocities becomes increasingly independent of specific gravity and this independence increases with a decrease in pipe diameter. The pressure gradients correlated for steel cylinders and steel pipes happen to be the highest recorded for any pair of materials, but so far insufficient data is available to enable correlations to be made for smoother capsules and pipes.

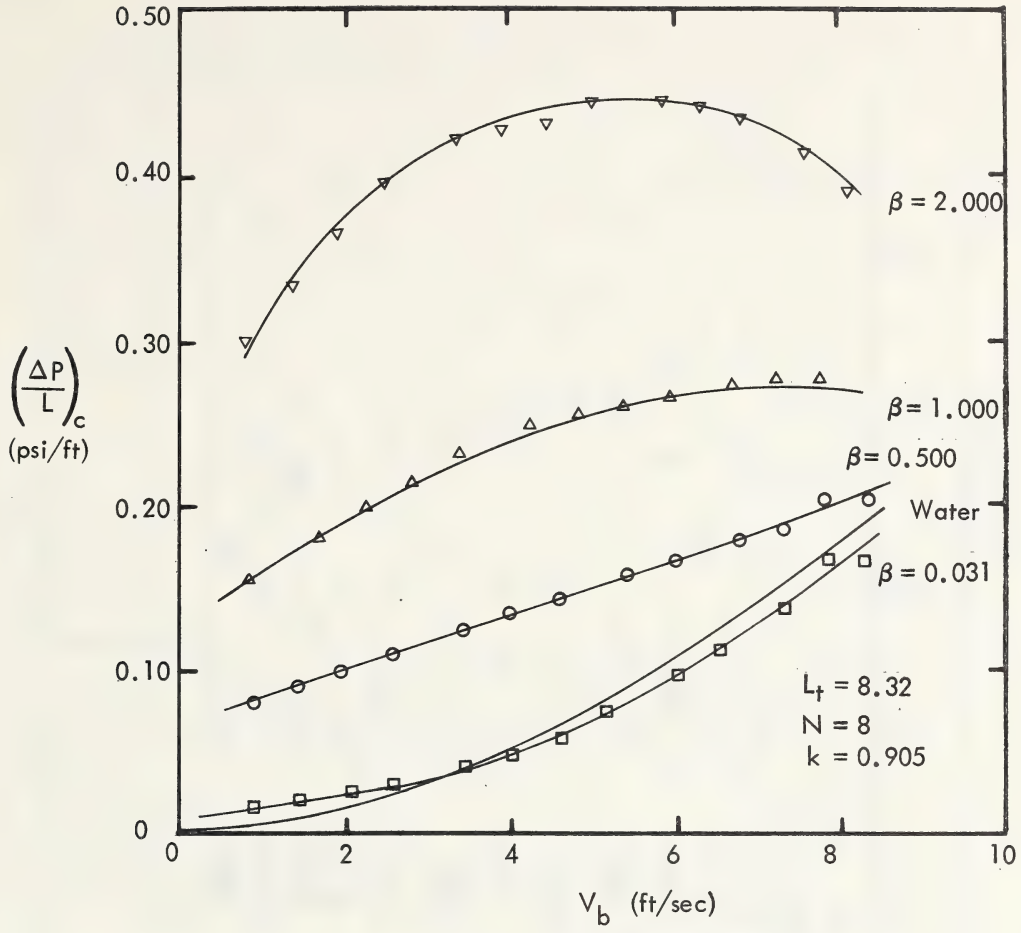

$\frac{1}{2}$ INCH PIPE WITH WATER
VARIATION OF PRESSURE GRADIENT WITH BULK VELOCITY

Figure 3 -1

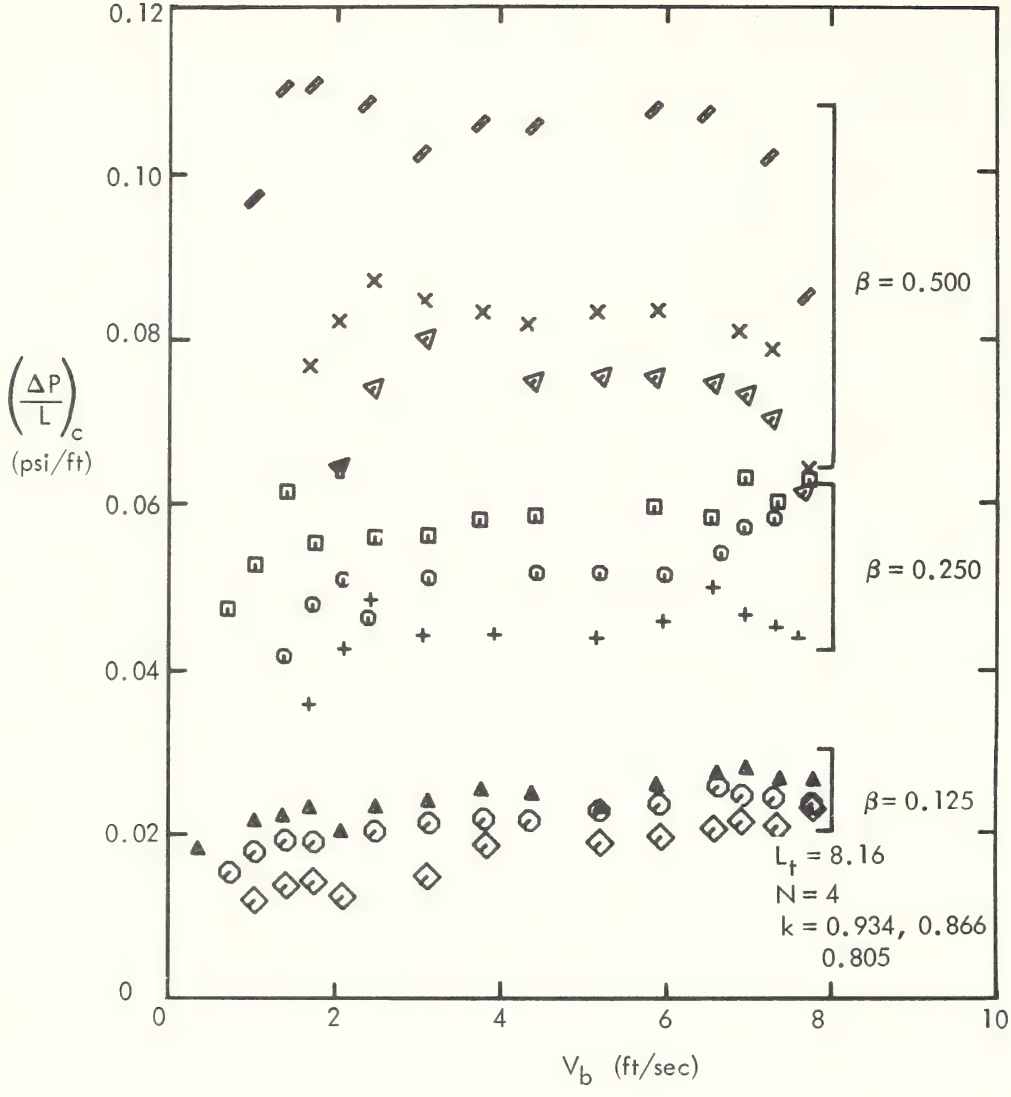

4 INCH PIPE WITH WATER
VARIATION OF PRESSURE GRADIENT WITH BULK VELOCITY

3 diameters of stainless steel cylinders in the stainless steel test section.

Figure 3 -2

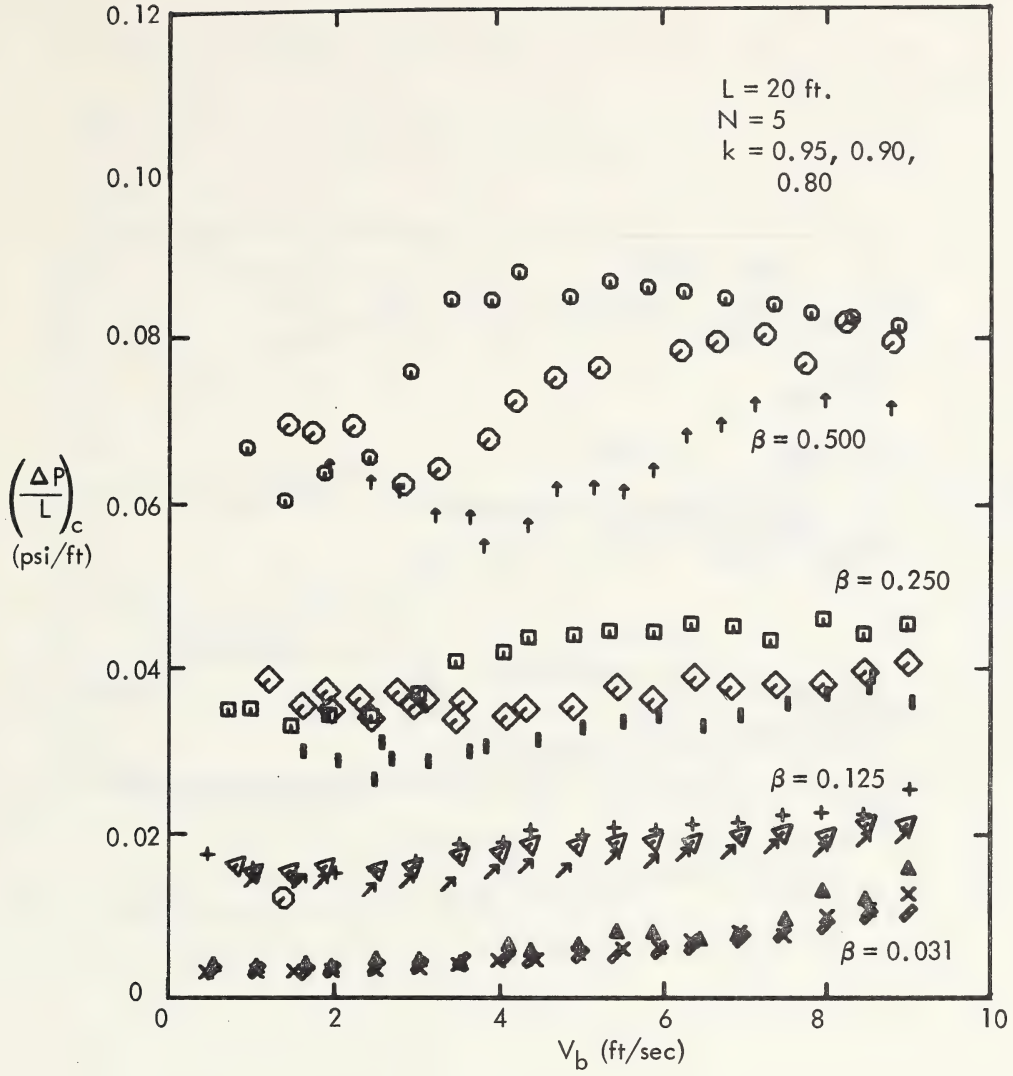

10 INCH PIPE WITH WATER
VARIATION OF PRESSURE GRADIENT WITH BULK VELOCITY

3 diameters of steel cylinders. Figure 3 -3

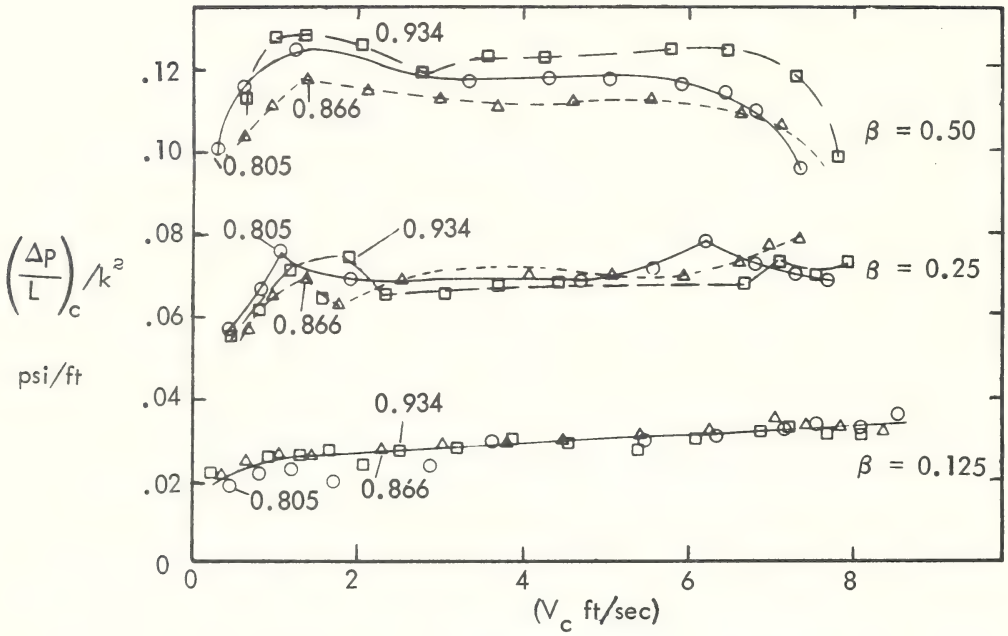

4 INCH STAINLESS STEEL PIPE

Correlation of pressure gradients for diameter ratios 0.805, 0.866 and 0.934 as functions of capsule buoyed specific gravity and velocity.

FIGURE 3-4

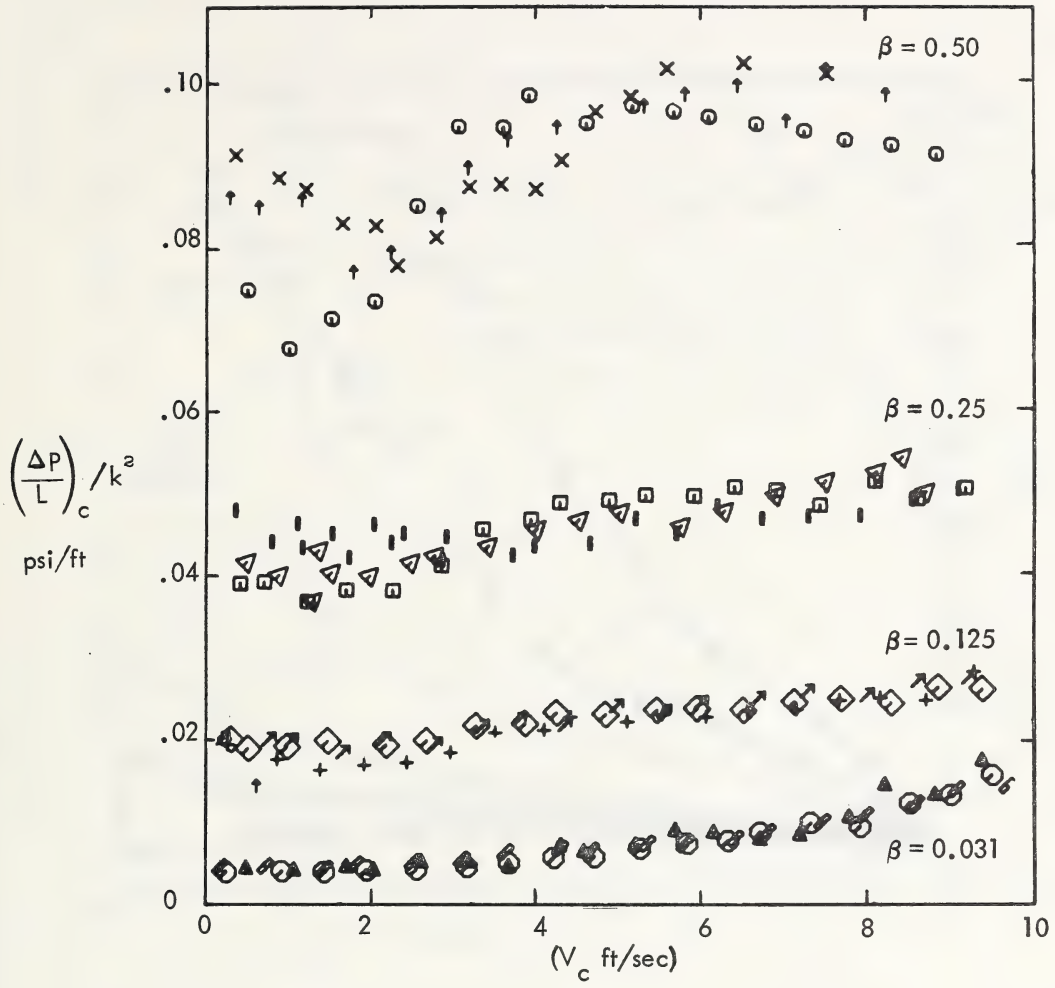

10 INCH STEEL PIPE

Correlation of pressure gradients for diameter ratios 0.80, 0.90 and 0.95 as functions of capsule buoyed specific gravity and velocity.

FIGURE 3-5

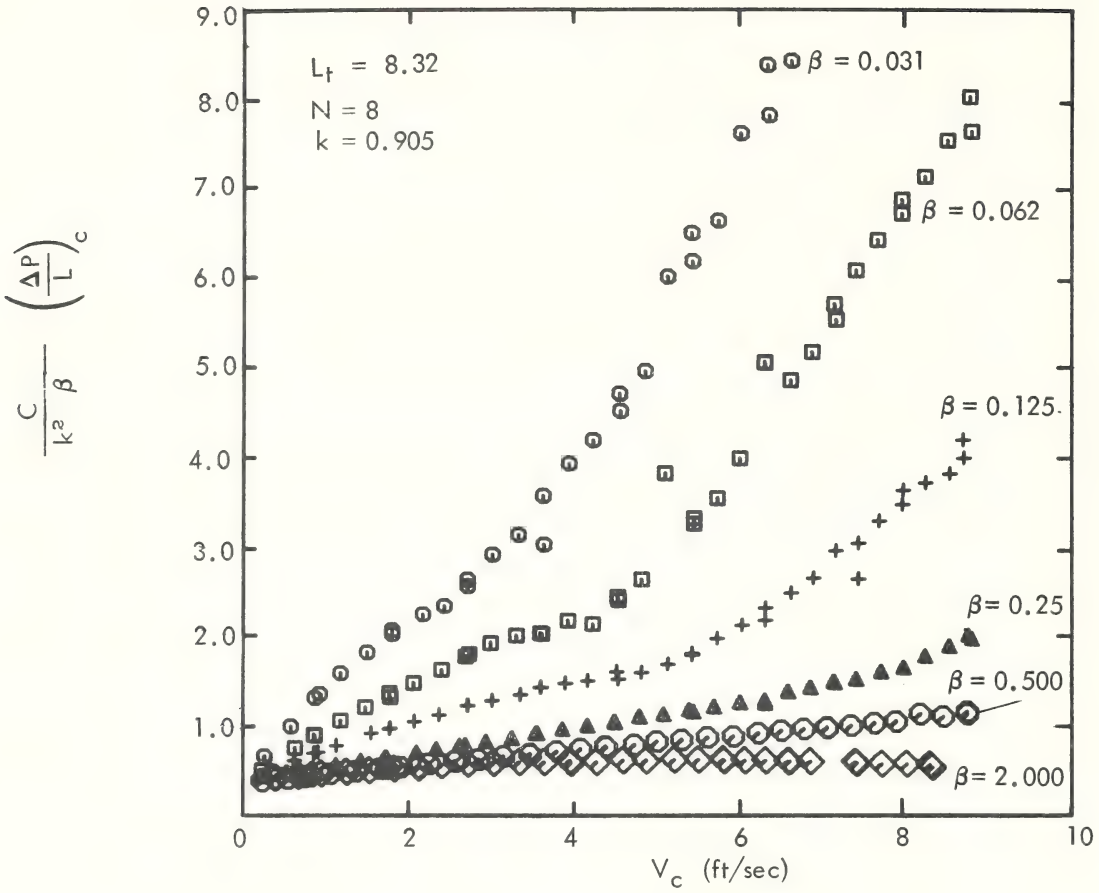

$\frac{1}{2}$ INCH PIPE WITH WATER
CORRELATION OF PRESSURE GRADIENT WITH DIAMETER RATIO AND BUOYED DENSITY AS A FUNCTION OF CAPSULE VELOCITY

Figure 3 -6

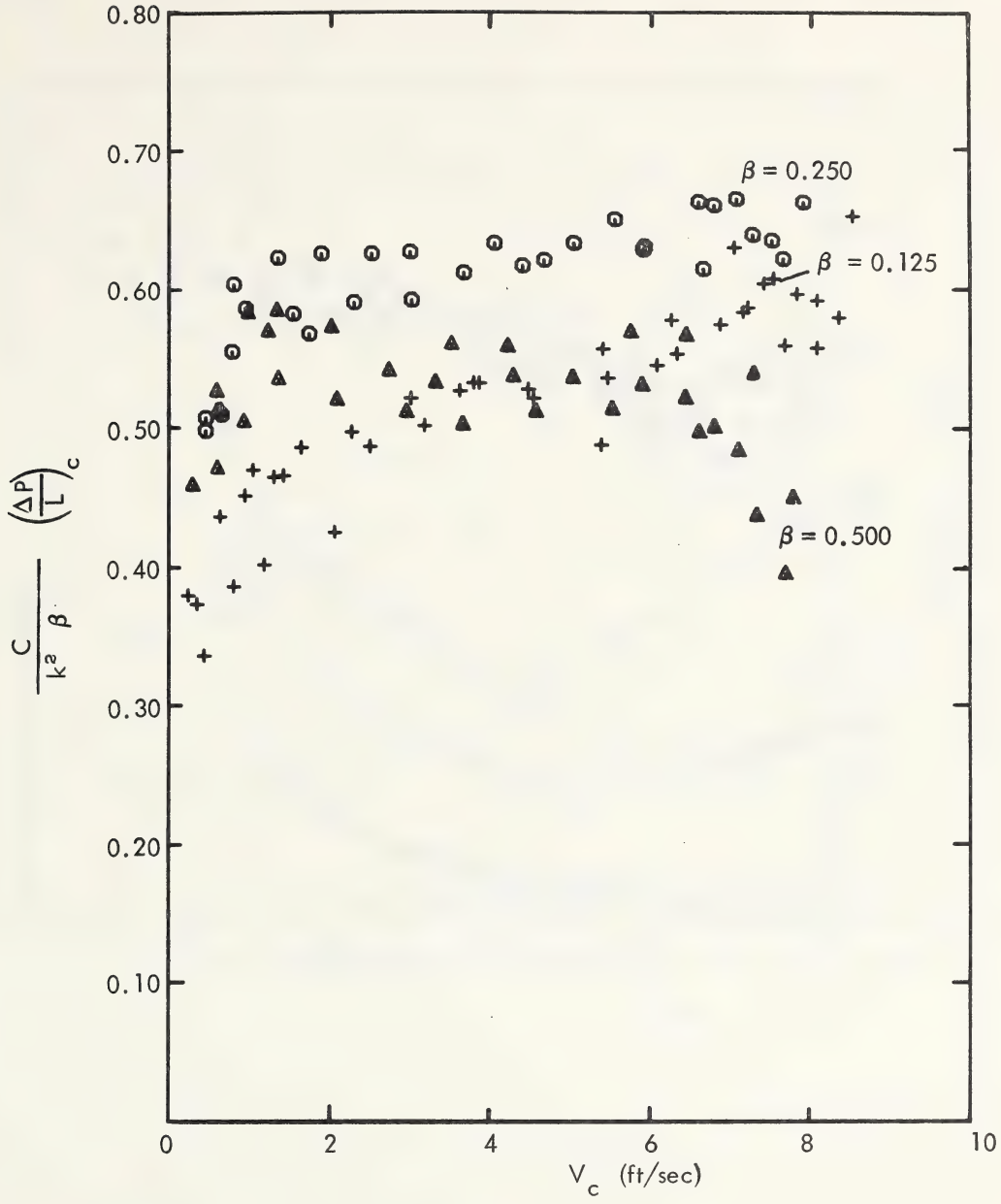

4 INCH PIPE WITH WATER
CORRELATION OF PRESSURE GRADIENT WITH DIAMETER RATIO AND BUOYED DENSITY AS A FUNCTION OF CAPSULE VELOCITY.
Stainless steel capsules in stainless steel test section.
Data as for Figures 3 -2 and 3 -4

Figure 3 -7

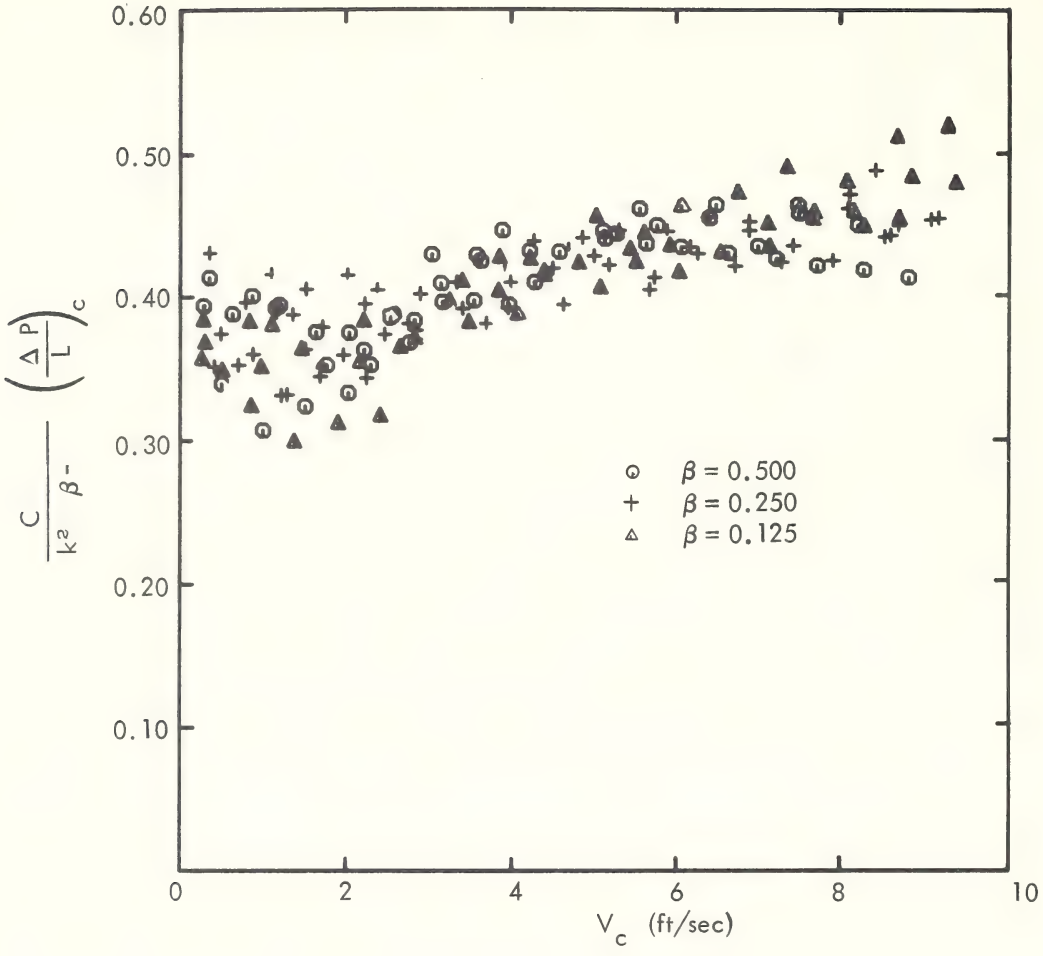

10 INCH PIPE WITH WATER
CORRELATION OF PRESSURE GRADIENT WITH DIAMETER RATIO AND BUOYED DENSITY AS A FUNCTION OF CAPSULE VELOCITY.
Steel capsules. Data as for Figures 3-3 and 3-5.

Figure 3-8

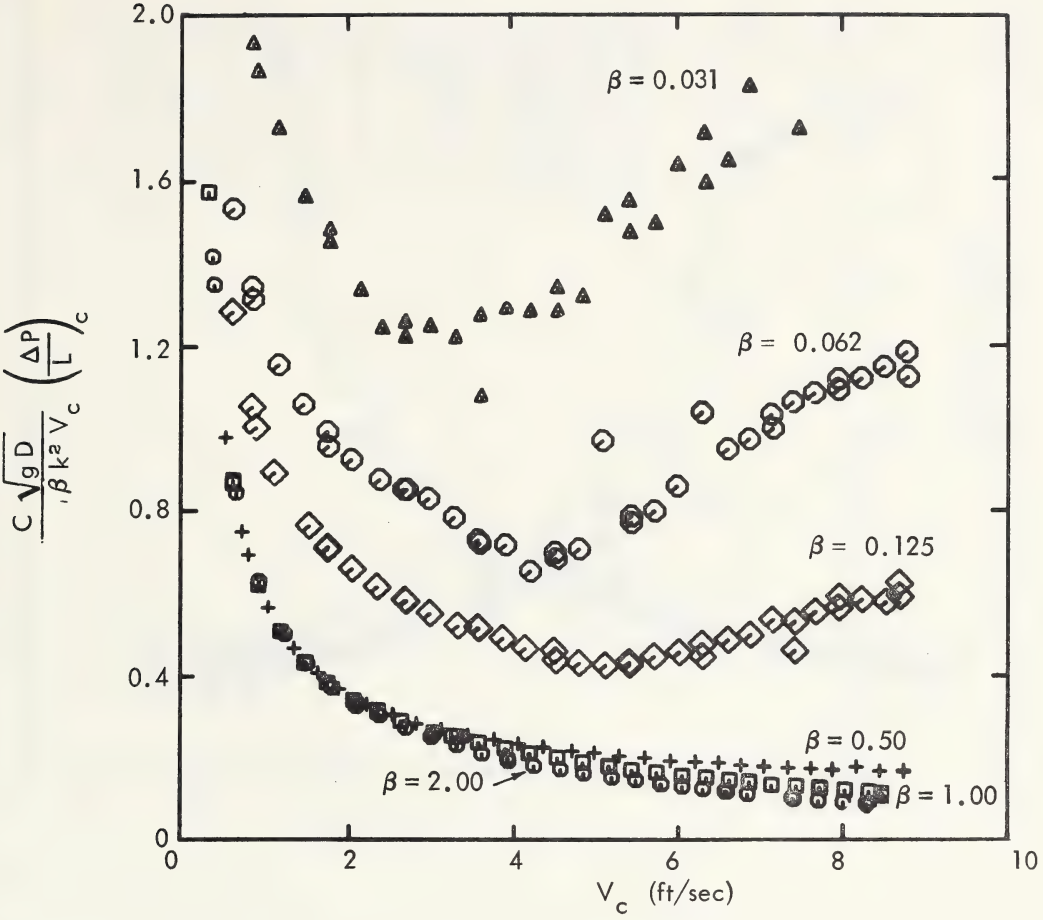

$\frac{1}{2}$ INCH PIPE WITH WATER
CORRELATION OF PRESSURE GRADIENT WITH DIAMETER RATIO, BUOYED DENSITY AND FROUDE NUMBER AS A FUNCTION OF CAPSULE VELOCITY. Data as for Figure 3-1

Figure 3-9

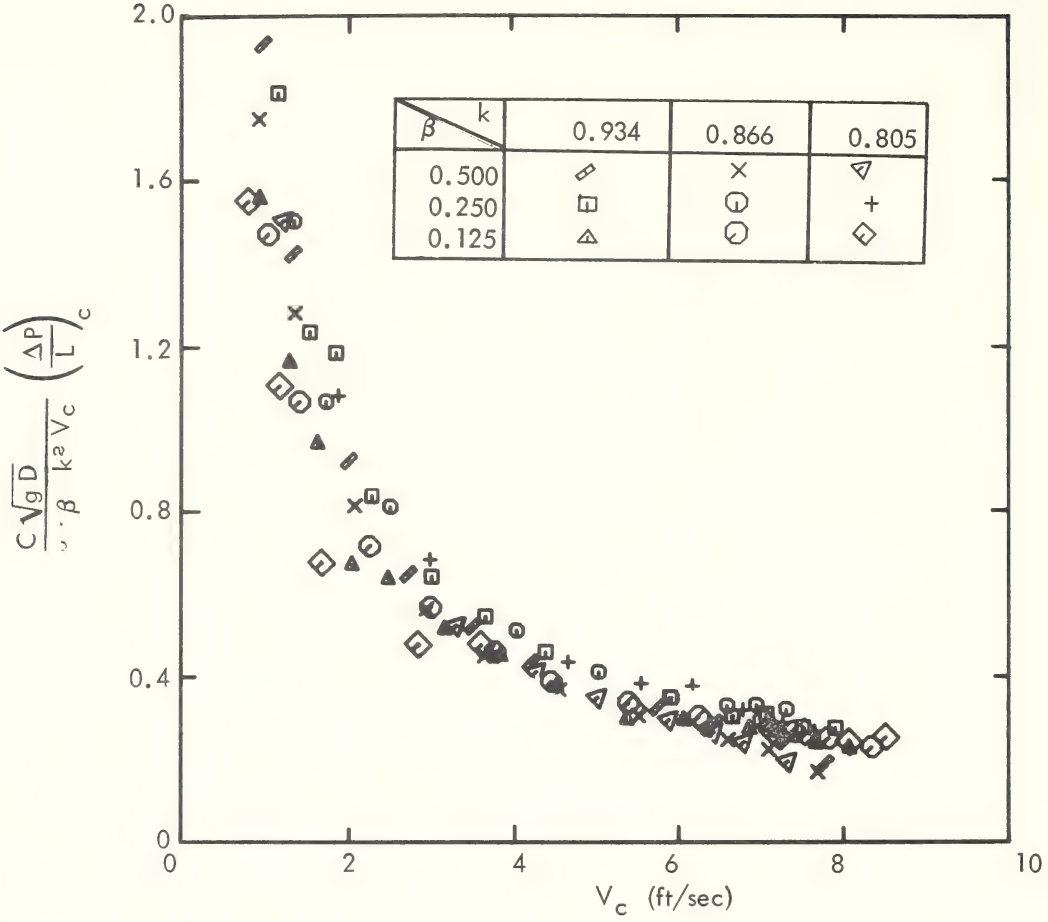

4 INCH PIPE WITH WATER
CORRELATION OF PRESSURE GRADIENT WITH DIAMETER RATIO, BUOYED DENSITY AND FROUDE NUMBER AS A FUNCTION OF CAPSULE VELOCITY
Data as for Figures 3-2, 3-4, and 3-7

Figure 3-10

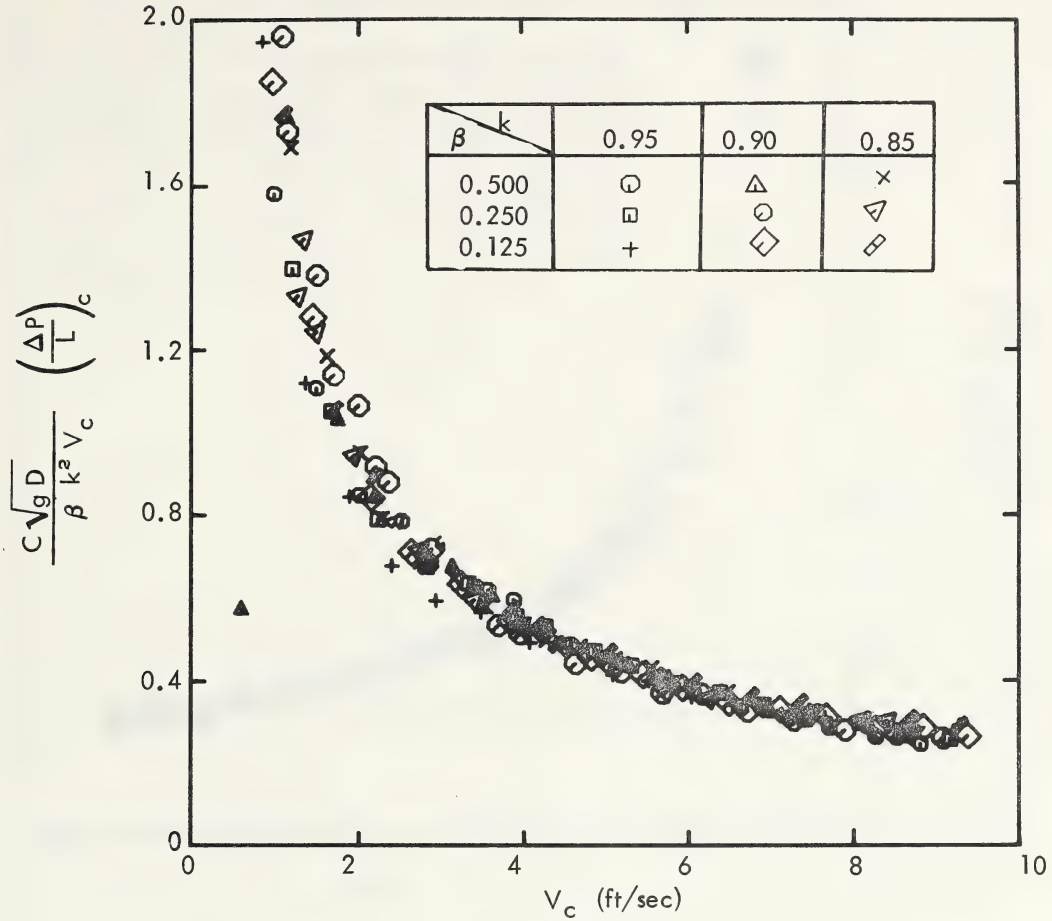

10 INCH PIPE WITH WATER
CORRELATION OF PRESSURE GRADIENT WITH DIAMETER RATIO, BUOYED DENSITY AND FROUDE NUMBER AS A FUNCTION OF CAPSULE VELOCITY.
Data as for Figures 3 -3, 3 -5 and 3 - 8.

Figure 3 -11

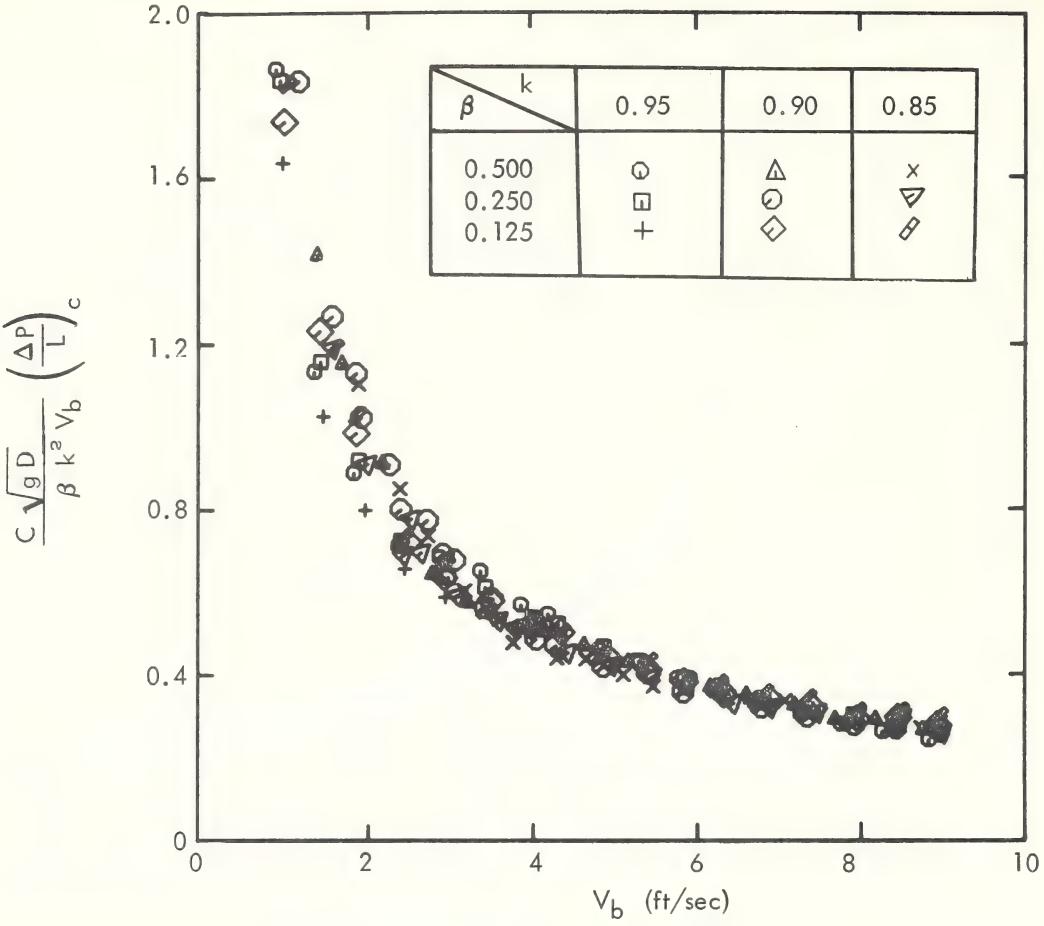

10 INCH PIPE WITH WATER
CORRELATION OF PRESSURE GRADIENT WITH DIAMETER RATIO, BUOYED DENSITY AND FROUDE NUMBER AS A FUNCTION OF BULK VELOCITY
Data as for Figure 3 -11

FIGURE 3 -12

CHAPTER IV

Hydrodynamics of Spherical Capsules

Hydrodynamics of Spherical Capsules

Summary

Pressure gradients for spherical capsules generally are smaller than for cylindrical capsules for the same mass throughput. Spheres are increasingly attractive hydrodynamically as the specific gravity of the transported material increases.

4.1 Details of Investigations of the Flow of Spheres

Trains of spheres were run in the half-inch, four-inch and ten-inch pipes. All the pipes were levelled with an instrument level to avoid measurement errors due to slope to better than $\pm$ 1/5000.

In the half-inch pipe trains of 24 stainless steel balls were used. The diameter ratio was 0.905 with tolerance less than $\pm$ 0.001. When travelling as a train the spheres spaced themselves about 1/8 inch apart. For the four-inch pipe hollow spheres were machined from PVC to a diameter ratio of 0.935 $\pm$ 0.001 inch (Fig. 4-1). Single spheres and trains of 2, 5, and 10 were loaded and run at six specific gravities from 1.55 to 4.33 (β = 0.55 to 3.33). The spheres usually appeared to have gaps of less than half a diameter between them.

In the ten-inch pipe, trains of cast aluminum and cast iron spheres were run at diameter ratios of 0.85, 0.90 and 0.95. The spheres were ground to remove high spots and the tolerances are shown in Table 3. Four to five readings were taken of the diameter of each sphere. The plus figure in the tolerances represents the mean maximum reading minus the mean measured diameter; the minus figure is the mean minimum reading minus the mean diameter.

TABLE 3

Tolerances of spheres in the 10 in. pipeline.

		ALUMINUM		IRON	
Nominal dia.(in.)	Diameter ratio	Mean measured dia. (in.)	Tolerances	Mean measured dia. (in.)	Tolerances
8.5	0.85	8.510	+0.042 -0.009	8.546	+0.032 -0.033
9.0	0.90	9.007	+0.034 -0.055	9.040	+0.039 -0.037
9.5	0.95	9.490	+0.032 -0.043	9.540	+0.049 -0.038

The stationary trains with the spheres in contact were made as nearly as possible the same lengths as those of the cylinders, viz. 4, 8, 12, 16 and 20 ft., but the spheres spread out somewhat when in movement. The gap between aluminum spheres averaged half to one diameter, while the iron spheres often appeared to be in contact, especially in the rear half of the train.

4.2 Pressure Gradients of Spheres

The half-inch and four-inch pipes.

The pressure gradient for spheres rises with an increase of bulk velocity in a similar way to that for a liquid. Fig. 4-2 illustrates this for the trains of 24 stainless steel spheres in the half-inch pipe. Fig. 4-3 is a similar plot for trains of 10 spheres in the four-inch pipe. There is little or no effect of buoyed specific gravity for the six values tested ($\beta = 0.55$ to 3.33), (S.G. = 1.55 to 4.33), as shown by the data for the highest, lowest and mean values plotted in the Figure. With accurate sphericity it appears that there is a basic pressure gradient for each volumetric throughput of spheres and the associated liquid due to distortion of the liquid velocity profile by the spheres. Rolling friction appears to be negligible for these nearly perfect spheres.

Included in the Figure for comparison are mean lines for butyrate cylinders in the same stainless steel section; these gave the lowest pressure gradients of the standard cylinders. The upper line represents cylinders of about the same buoyed specific gravity (0.50) as the lowest specific gravity spheres. The advantage of using spheres in terms of pressure gradient is very clear. The linear middle line shows that if spheres of buoyed specific gravity 0.25 fall on the same curve as the others, even at this low specific gravity it would be hydrodynamically advantageous to use spheres at bulk velocities less than $5\frac{1}{2}$ ft./sec. The wavy curve crossing both the sphere and water curves is for cylinders of $\beta = 0.063$. It shows that cylinders of this and lower specific gravities can compete hydrodynamically with spheres and even yield pressure gradients lower than that of the liquid alone. The latter phenomenon and its practical applications are discussed in Chapter VII.

The ten-inch pipe

Corresponding plots for 20 ft. trains of the three diameters of iron spheres in the ten-inch pipe are presented in Fig. 4-4. There is a modest increase of pressure gradient when the diameter ratio increases from 0.85 to 0.90 and a much larger one from 0.90 to 0.95, but the effect of diameter ratio may be modified by deviations from the spherical form. If the spheres are rolling without sliding, the velocity of the top of the spheres is twice the sphere velocity, and the distortion of the velocity profile in the annulus becomes increasingly severe as the annular width decreases. The trains of diameter ratio 0.85 seem to pass through a transition region where the pressure gradient is rather constant, after which it rises again at higher bulk velocities. The trains of diameter ratio 0.90 show a similar levelling at a rather higher velocity.

The changes of slope of the curves may indicate that the spheres were partially sliding at these higher velocities instead of only rolling. The change from pure rolling to rolling-and-sliding was noted by Ellis [1] in the course of a high-speed photographic investigation of spheres. The tendency to sliding increased with increase of bulk velocity, decrease of sphere diameter and decrease of specific gravity. In accord with those findings, the spheres of diameter ratio 0.85 show the flattening at lower velocities than those of 0.90; the curve for the spheres of diameter ratio 0.95 would probably show the same changes at still higher velocities.

Fig. 4-5 shows similar behavior for the aluminum trains, but here the trains of 0.90 diameter ratio as well as those of 0.85 show a further increase of pressure gradient after the levelling off, and the curve for the 0.85 diameter ratio trains again shows inflections at rather lower critical velocities. Again in accord with the results reported in [1], the aluminum spheres show the changes of slope at lower bulk velocities than the iron spheres of the previous Figure. A comparison of the pressure gradients of the two densities of spheres will be made later in the chapter.

It was noticed during the runs that there was a tendency at bulk velocities greater than about 8 ft./sec. for the pressure gradient not to have reached a maximum before the train began to leave the test section. The data from several such runs were discarded, but some of the lower data points may have been influenced by this effect. However, it is believed that the flattening of the curves, beginning, as it does, at

velocities of 5 or 6 ft./sec. for several trains is a genuine effect, particularly as the pressure gradient rises again at higher velocities.

The accompanying mean lines in these last two Figures for standard hollow steel cylinders of buoyed specific gravity 0.25 (S.G. = 1.25) and diameter ratio 0.90, show again that even solid iron spheres are hydrodynamically preferable to standard cylinders even at this low specific gravity. For a further comparison of spheres with cylinders reference may be made to Fig. 7-5 which shows pressure gradient curves for a cylinder of $\beta = 0.50$ (S.G. = 1.50) fitted with a polyethylene sleeve, and for a train of cylinders of the same specific gravity with pressure-reducing collars. The minimum pressure gradient for the sleeved cylinders was about 0.03 psi/ft. and for collared capsules this figure was halved. The power requirements of trains of spheres and cylinders are discussed in 4.3.

A comparison of the 0.85 and 0.95 diameter ratio iron and aluminum spheres in the ten-inch pipe is presented in Fig. 4-6. The pressure gradients of the aluminum spheres (dashed lines) are much lower than those of the iron (full lines), especially for the 0.95 diameter ratio spheres. The considerable effect of sphere specific gravity in the ten-inch pipe compared with the absence of any such effect in the four-inch pipe seems to be due to the less uniform spheres in the ten-inch pipe. Although the tolerances are good for large cast spheres, as spheres move through the pipeline any small bumps involve the expenditure of energy proportional to the height of the bump and the buoyed weight of the sphere, since work has to be done in lifting the sphere over the bump during rotation. In discussing the sphere data from the 4-inch pipe it was suggested that for accurate sphericity there is a basic pressure gradient due to the distortion of the velocity profile. To this basic pressure gradient would have to be added the pressure gradient due to the extra work caused by irregularities. No correlation between pressure gradient and specific gravity is possible since spheres of only two specific gravities have been tested, and in any case the specific gravity relationship would be obscured by the effect of sphericity and would not be universally applicable. However, the suggestion of a basic pressure gradient with an additional pressure gradient due to buoyed specific gravity may point the way to such a correlation for spheres of similar tolerance.

The effect of train length

In all the pipes there was little effect due to the number of spheres in the train

beyond the initial two or three spheres and the results may be taken to be representative of very long trains with the spheres maintained in fairly close proximity. Further spreading would, of course, reduce both the overall pressure gradient and the throughput.

Correlation of pressure gradient with diameter ratio and liquid velocity.

The pressure gradients of both the iron and aluminum spheres in the ten-inch pipeline plot linearly against the liquid pressure gradient, which is proportional to $V_b^{1.80}$. The capsule pressure gradients have therefore been correlated with the liquid pressure gradient $(\Delta P/L)_f$; the data also correlates with the function $k^2 (1 - k)$, and Figs. 4-7 and 4-8 present these correlations. The diagonal line represents a perfect correlation. The levelling of the pressure gradients of the smaller spheres and the subsequent rise of those of the aluminum spheres are evident, and this high velocity data would have to be correlated separately. In view of the effect on the pressure gradient of sphere irregularity the correlations can only be taken to apply closely to the particular trains tested.

The effect of pipe diameter.

According to the correlation for the iron spheres in the ten-inch pipe the pressure gradient for spheres of diameter ratio 0.935 (as run in the four-inch pipe) at a liquid pressure gradient of 0.002 psi/ft. say, (V_b = 4.30 ft./sec.) would be 0.021 psi/ft.; the pressure gradient for the four-inch pipe spheres is 0.0155. Corresponding figures at V_b = 7.6 ft./sec. are 0.0362 and 0.039 psi/ft. So that if iron spheres in the four-inch pipe fell on the same curve as those of the other specific gravities in the four-inch pipe the pipe diameter effect for this specific gravity would be small. On the other hand the pressure gradients for aluminum spheres of this diameter ratio in the ten-inch pipe would be about half those measured in the four-inch pipe for spheres of the same specific gravity, indicating a very significant pipe diameter effect.

The effect of pipe diameter evidently depends strongly on the buoyed specific gravity; this would be expected if, as suggested earlier, there is a basic pressure gradient due to the transport of a certain diameter of sphere plus an extra gradient, proportional to the buoyed specific gravity, due to the unevenness of the sphere surfaces and uniniformity of the sphere density. Further experimental work with spheres will be necessary before

the pressure gradient due to surface irregularities can be added to that required to transport perfect spheres in order to predict the total pressure gradient. Such a separation of the two components seems to be necessary before the effect of pipe diameter can be predicted for imperfect spheres.

It seems that it would be worthwhile to investigate further the importance of the contribution the surface irregularities of spheres make to the total pressure gradient. The difficulty is to quantify the roughness of a sphere from this point of view. One way of doing so might be to time spheres of different irregularities down a sloping water-filled pipe and relate the increases of the time of transit above that of a true sphere to the increases of pressure gradient in pipeline flow. Such experiments should lead to an answer to the question "How does the irregularity of spheres affect the power required to transport them?" They should also indicate whether such a method would be valid for predicting the performance of particular spheres being considered for commercial pipelining.

4.3 Conclusions

The low pressure gradients required by spheres compared with those needed even by smooth cylinders suggest that it would be worth facing the possibly greater manufacturing problems required in order to transport any solid with specific gravity of 1.25 or more in this form. Research on the manufacture, injection and bypassing of large cohesive spheres of beneficiated ores of good sphericity would seem to deserve high priority, as well as experiments to determine the effect of sphere un-evenness.

Reference

1. Ellis, H.S. The Pipeline Flow of Capsules, Part 5. An Experimental Investigation of the Transport of Water of Single Spherical Capsules with Density Greater than the Water. Can. J. Chem. Eng., 42, 155 (1964).

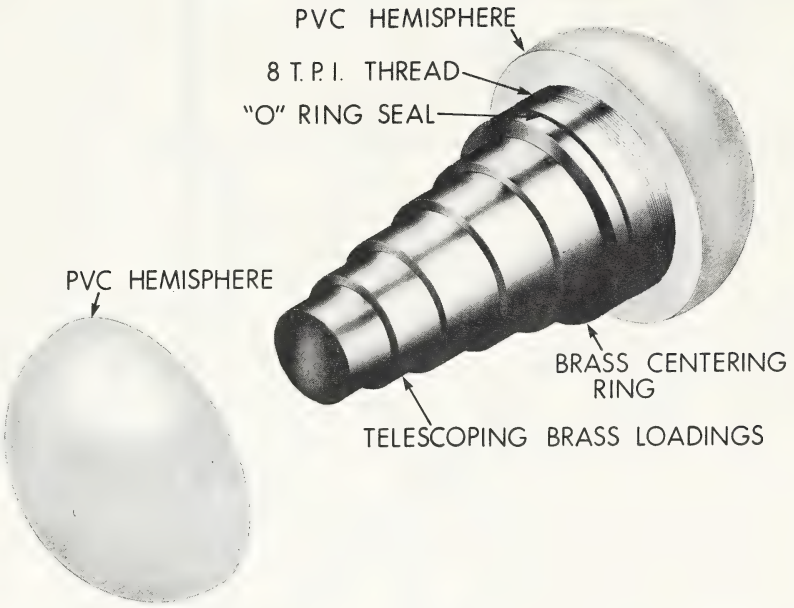

4 INCH PIPE

CONSTRUCTION OF SPHERES

FIGURE 4-1

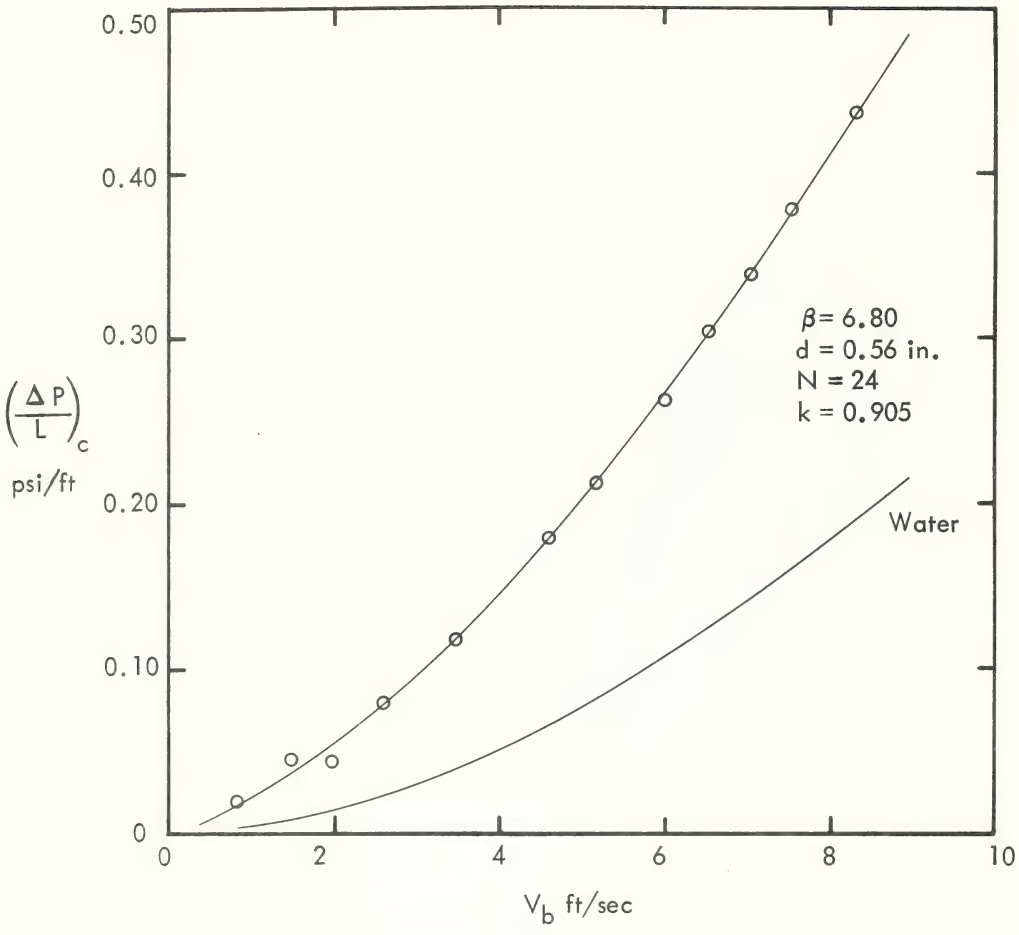

½ INCH PIPE SPHERES
VARIATION OF PRESSURE GRADIENT WITH BULK VELOCITY

FIGURE 4 -2

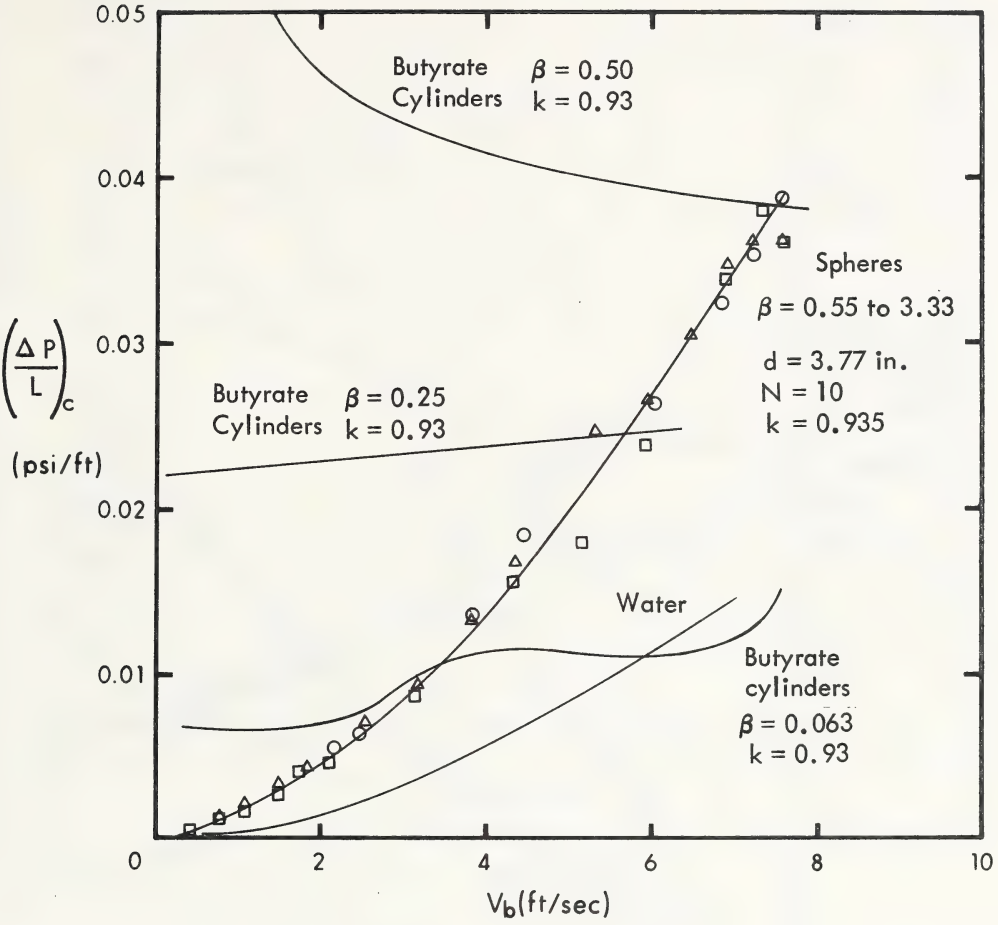

4 INCH PIPE SPHERES
VARIATION OF PRESSURE GRADIENT WITH BULK VELOCITY

FIGURE 4 -3

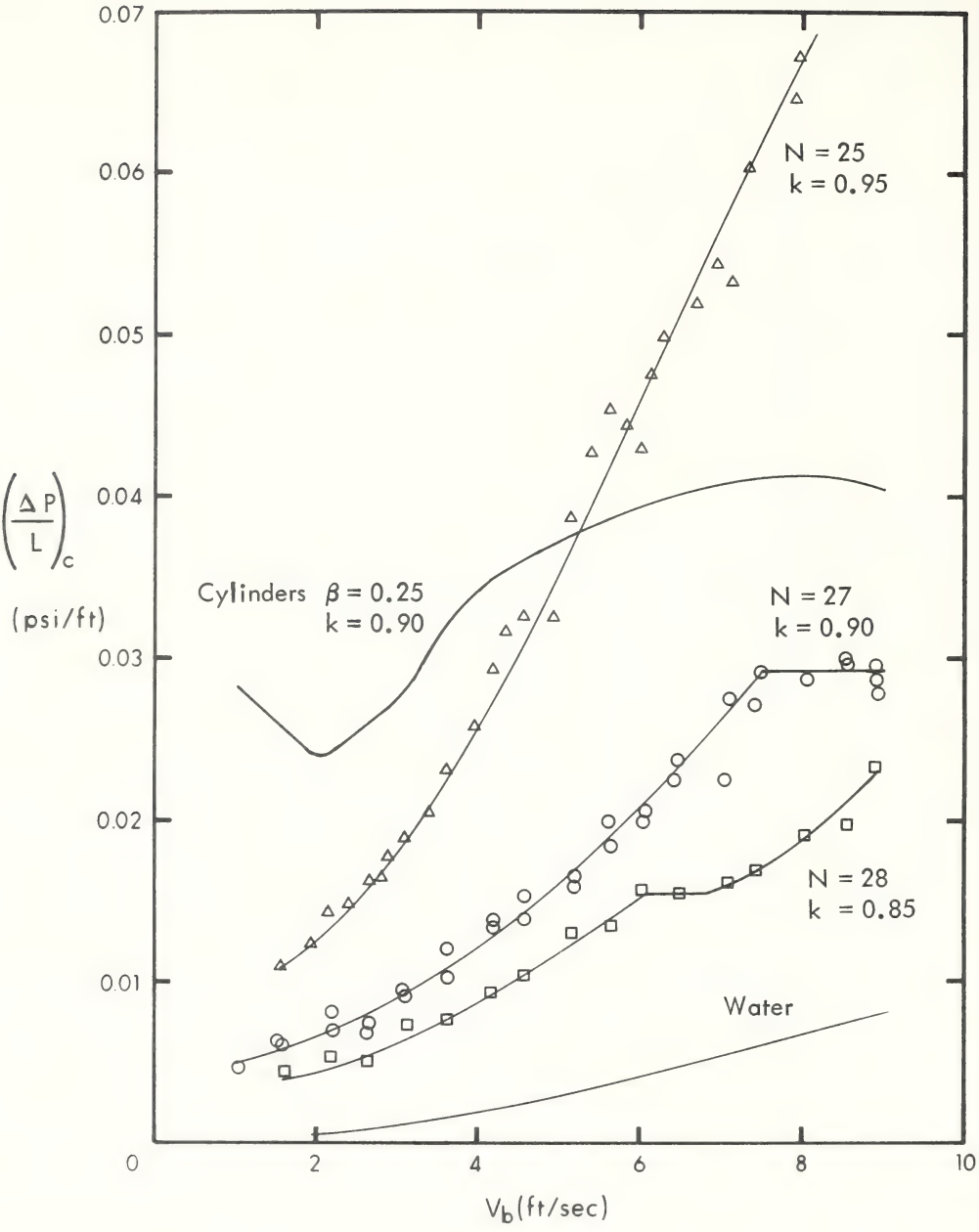

10 INCH PIPE, THREE DIAMETERS OF IRON SPHERES, $\beta = 6.20$
VARIATION OF PRESSURE GRADIENT WITH BULK VELOCITY

FIGURE 4 -4

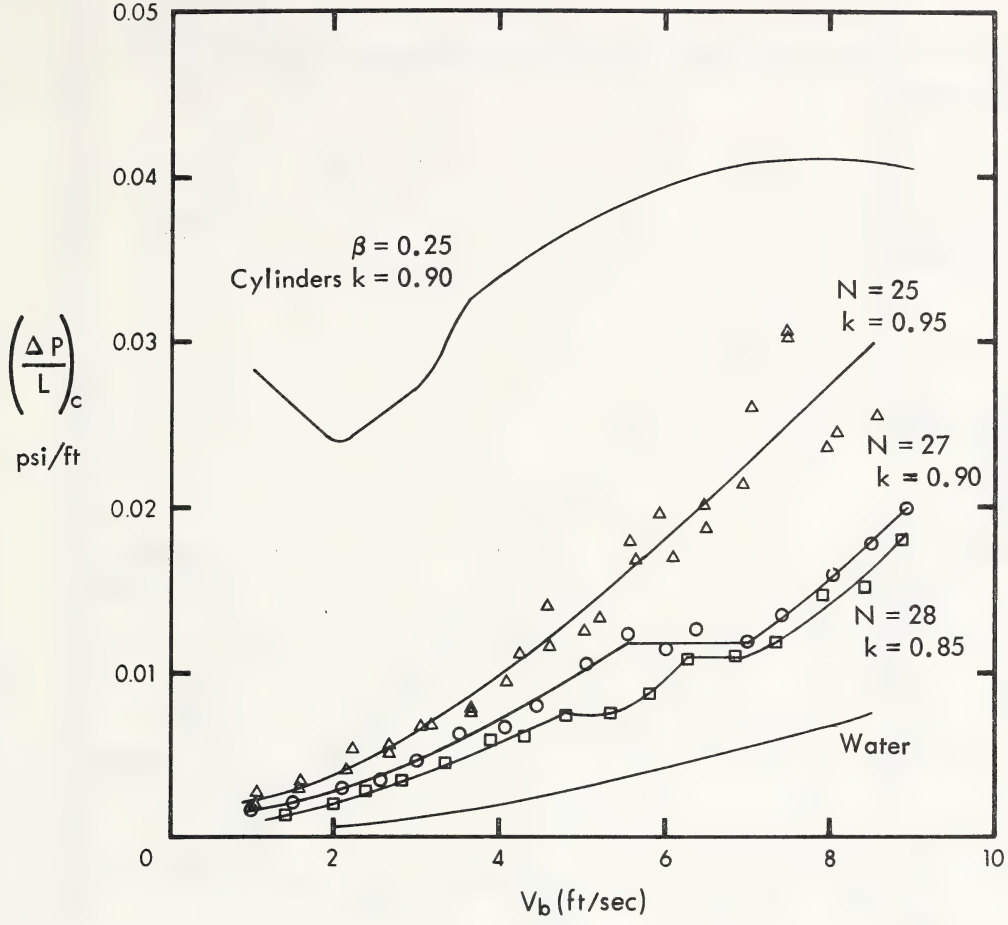

10 INCH PIPE, THREE DIAMETERS OF ALUMINUM SPHERES, $\beta = 1.70$
VARIATION OF PRESSURE GRADIENT WITH BULK VELOCITY

FIGURE 4 -5

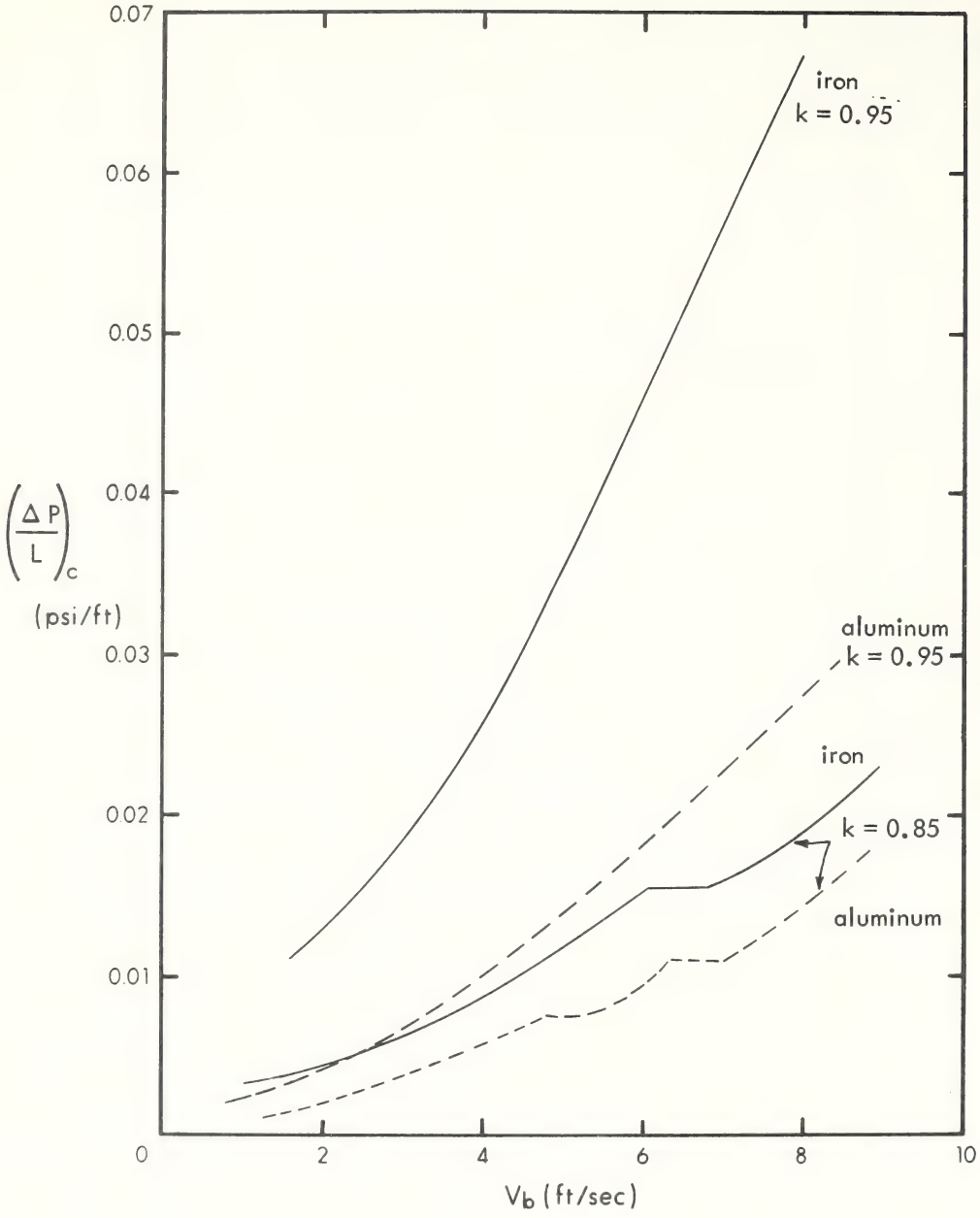

10 INCH PIPE
COMPARISON OF THE IRON AND ALUMINUM SPHERES

FIGURE 4-6

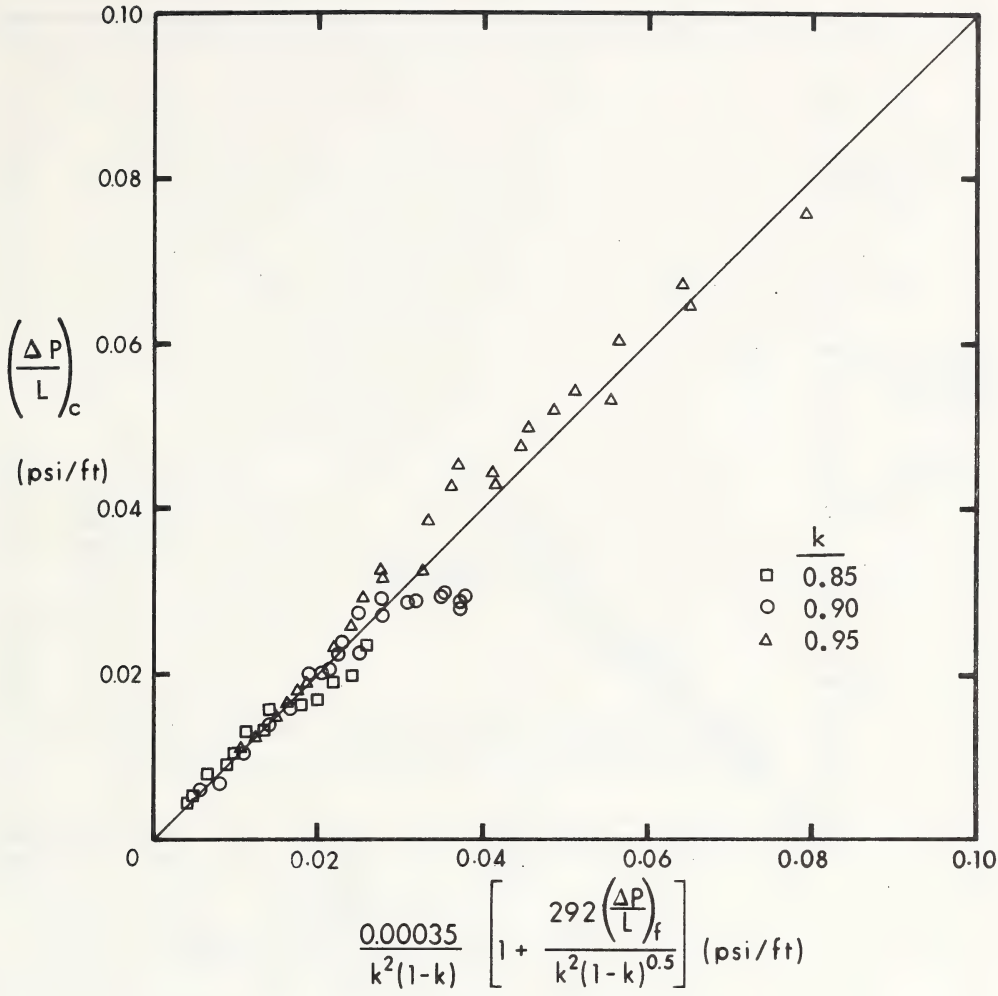

IRON SPHERES IN THE 10 INCH PIPE
CORRELATION OF PRESSURE GRADIENT

FIGURE 4 -7

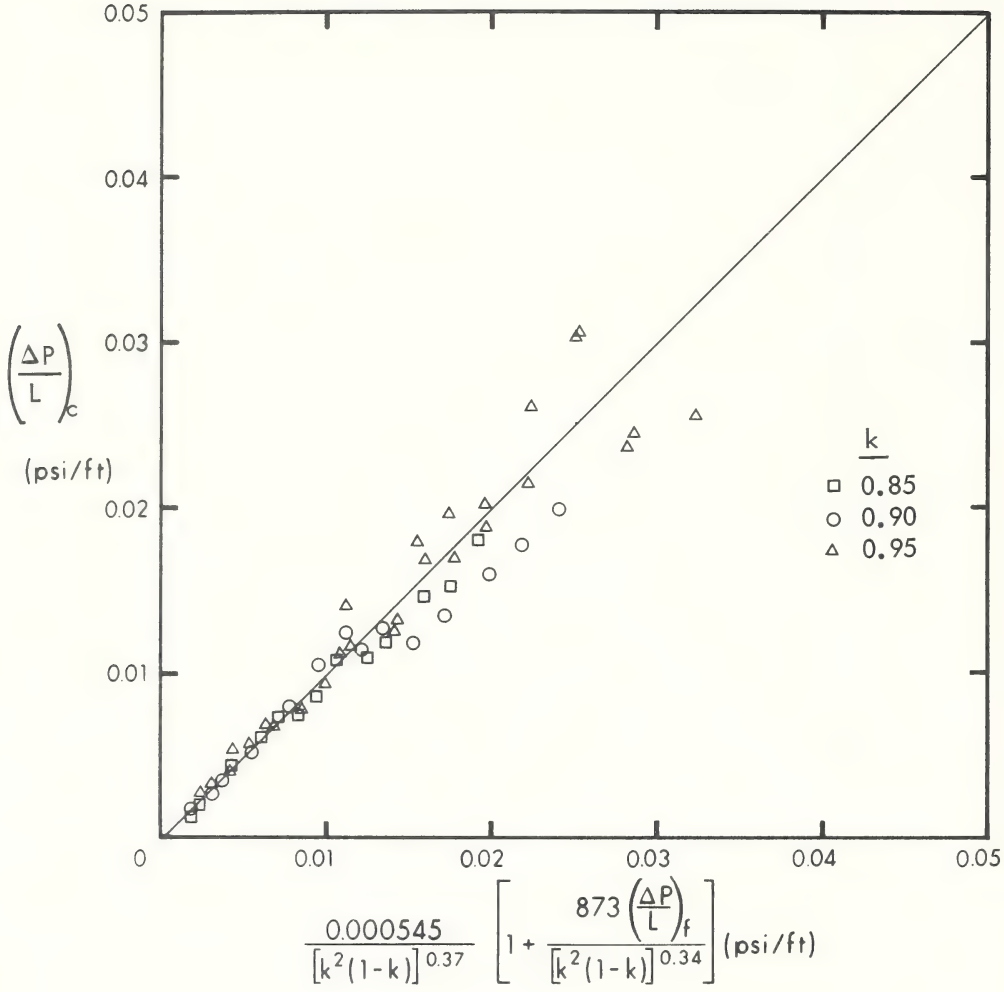

ALUMINUM SPHERES IN THE 10 INCH PIPE
CORRELATION OF PRESSURE GRADIENT

FIGURE 4 -8

CHAPTER V

A Model Which Relates the Capsule Pressure Gradient, Capsule Velocity and Liquid Velocity for Cylinders

CHAPTER V

A Model Which Relates the Capsule Pressure Gradient, Capsule Velocity and Liquid Velocity for Cylinders.

Summary

A model has been developed describing the relationship between the capsule velocity, the capsule pressure gradient and the bulk velocity. It allows the prediction of the bulk velocity when both the capsule velocity and the capsule pressure gradient are known and thus enables the calculation of the amount of liquid required to move a given quantity of solids. It also allows the prediction of the capsule pressure gradient when both the capsule velocity and the bulk velocity are known, but the measurement of these velocities must be very accurate before the capsule pressure gradient can be predicted to a reasonable accuracy. A Reynolds number developed for the model indicates whether the liquid surrounding the capsules is in laminar flow ($Re_c < 1,000$) or in turbulent flow ($Re_c > 1,000$).

5.1 Introduction

In 1970 Ellis and Kruyer [1] presented an empirical pressure and velocity correlation for cylindrical capsules conveyed in pipelines up to four inches in diameter. This correlation, which was based on a pressure-flow, or equivalent, velocity defined by $V_a - 0.35\, V_c$, was good for the data on hand at the time, but shows increased divergence for more recent data at higher Reynolds numbers.

The pressure-flow velocity is defined as the average liquid velocity in the annulus due only to the pressure force on the annulus. The present paper solves for this pressure-flow velocity by an analysis of the flow components of the liquid, providing an improved correlation.

5.2 Pressure Flow Velocity.

In the design of a commercial capsule pipeline, the capsule velocity can be determined from the required throughput of solids when the capsule diameter and the linear fill of capsules have been chosen. Two important unknowns remaining are the required liquid flow and the pressure gradient needed to overcome the friction and shear forces in the capsule pipeline at the desired capsule velocity. In this chapter an expression for the required liquid flow is derived.

All flow in a capsule pipeline is caused by a pressure gradient imposed by pumps, or by gravity, on the liquid in the pipeline. The distribution of the flow, however, is influenced by the reaction of the capsules to this imposed pressure. For this reason it is convenient in the analysis to divide the total steady volumetric flow in a typical pipe cross section into three components as illustrated by Fig. 5-1. A similar method was originally suggested by Round [2] and developed by Garg and Round [3]. The first component (1 in the Figure) is the flow of the capsule which is equal to:

$$Q_1 = \frac{\pi}{4} d^2 V_c \qquad (1)$$

This is equal to the flow of a cylinder of liquid in the spaces between capsules, with a diameter equal to that of the capsules. The remaining two flow components represent liquid flow in the annulus which is caused by two effects: liquid dragged along by the moving capsules, i.e. "Couette flow" (2 in the Figure), and flow due to the pressure force on the annular cross section from the tail to the nose of each capsule, i.e. "pressure flow" (3 in the Figure).

By definition, Couette flow exists whenever two parallel solid surfaces, separated by a liquid layer, slide past each other. When one of the surfaces is stationary and the other moving, shear forces in the liquid separating the solid surfaces cause a net liquid flow. When the solid surfaces are equal in size and large enough so that end effects may be ignored, the flow is equal to:

$$Q = \tfrac{1}{2} V_c \; w \; y \qquad (2)$$

where w is the width of the surfaces and y the distance between them. When the surfaces are curved and the liquid forms an annulus between them the annular flow rate may be approximated by:

$$Q = \tfrac{1}{2} V_c \frac{\pi}{4} (D^2 - d^2) \qquad (3)$$

A correction is required to this equation for annular flow, however, since the solid surfaces are no longer equal in size. The correction may be explained as follows: A balance of forces in an annulus with only Couette flow dictates that the total shear force on one surface must be equal to the total shear force on the other surface. Therefore the shear stresses at the two surfaces are related by:

$$\tau_p = k \tau_c$$

The resulting velocity profile for laminar flow is illustrated in Fig. 5-2 with the total flow rate represented by the area contained within A B C integrated round the annulus. When the two solid surfaces are equal in size, A C becomes a straight line and the integrated area is represented by equation 3. For a constant distance AB when the inner surface (capsule) is appreciably smaller than the outer surface (pipe), the line AC is curved and the area A B C is smaller. A relationship for Couette flow which takes into account the effect of shear stress variation with capsule diameter is:

$$Q_2 = \frac{d}{D+d} V_c \frac{\pi}{4} (D^2 - d^2) = \frac{\pi}{4} V_c (dD - d^2) \qquad (4)$$

This relationship approaches equation 2 when the diameters approach infinity, and it is equal to zero when the capsule diameter is zero; it therefore allows for the change in Couette flow with capsule diameter.

As will be shown, a previous analysis for long eccentric capsules with laminar flow in the annulus, presented by Kruyer et al [4], substantiates the validity of this correction for capsules flowing at a capsule/liquid velocity ratio near unity. Furthermore, Epstein et al [5] found this modified equation to be rigorously correct for fully eccentric capsules in laminar flow. In addition, the experimental results reported

in the present paper show that the correction applied to the Couette flow by this relationship correlates both laminar and turbulent capsule flow.

The third flow component, the pressure flow in the annulus, is obtained by subtracting the first two flow components from the total flow:

$$Q_3 = \frac{\pi}{4}\left[D^2 V_b - d^2 V_c - (dD - d^2)\ V_c\right] = \frac{\pi D^2}{4}\ (V_b - k V_c) \qquad (5)$$

The average velocity in the annulus due only to pressure-flow is obtained by dividing this flow by the cross-sectional area of the annulus:

$$V_3 = (V_b - k V_c) / (1 - k^2) \qquad (6)$$

Since this velocity is a direct response to the capsule pressure gradient it should be possible to relate the two by a friction factor, Reynolds number correlation; this has been done in the sections following. For this reason $V_3 = V_p$ is called the pressure-flow velocity since it results from the pressure force on the annular cross section.

5.3 Comparison with a Previous Analysis

In 1967 Kruyer et al [4] presented an analysis of the relationship between the capsule/liquid pressure ratio and the capsule/liquid velocity ratio for capsules flowing in liquid in laminar flow. Their predictions were based upon work done by Bentwich et al [6] for two-phase flow in pipelines. These predictions are now re-examined in the context of the pressure-flow velocity.

In laminar pipe flow the product of the Fanning friction factor and the Reynolds number is 16, while for laminar flow around long, fully eccentric, stationary cylinders in pipes, the value varies according to the diameter ratio as calculated from theory by Caldwell [7] or Tiedt [8, 9] and presented in columns 1 and 2 of Table 1. The pressure-flow as defined in this paper for a pipe with moving capsules represents the flow caused only by the direct effect of the pressure gradient on the annulus. The f (Re) product for this flow would therefore be expected to be equal to that for liquid flowing in pipes with stationary eccentric cylindrical cores under the influence of the same pressure gradient.

For fluid flow only in a pipe:

$$f_f \, Re_f = \left[\left(\frac{\Delta P}{L}\right)_f \, g_c \, D/(2 \rho V_b^2)\right] \left[V_b \, D/\nu\right] = 16 \qquad (7)$$

For capsule flow:

$$f_c \, Re_c = \left[\left(\frac{\Delta P}{L}\right)_c \, g_c \, (D-d)/(2 \rho V_p^2)\right] \left[V_p \, (D-d)/\nu\right] \qquad (8)$$

Dividing equation 8 by equation 7 yields:

$$f_c \, Re_c = \left[16 \left(\frac{\Delta P}{L}\right)_c \, (1 - k)^2 \, V_b\right] / \left(\frac{\Delta P}{L}\right)_f \, V_p \qquad (9)$$

If the pressure-flow velocity (equation 6) is generalized as

$$V_3 = (V_b - B \, V_c) / (1 - k^2) \qquad (10)$$

a test of its validity can be made by comparing the values of B , calculated from the theoretical results of [4] with those of k.

Defining, as in [4], the pressure ratio $R_p = \left(\frac{\Delta P}{L}\right)_c \Big/ \left(\frac{\Delta P}{L}\right)_f$ and the velocity ratio $R_v = V_c / V_b$ equations 9 and 10 yield:

$$B = \left[1 - \frac{16}{f_c \, Re_c} \, R_p \, (1 - k^2) \, (1 - k)^2\right] \Big/ R_v \qquad (11)$$

The values of $16/f_c \, (Re)_c$, R_p and B are given in Table 1 for calculated values of R_v near unity. This velocity ratio was selected since most potential commercial applications and most experimental results are for velocity ratios around unity.

TABLE 1

The theoretical, calculated relationship between A and k, [4], [7].

k	$f_c Re_c$	$\frac{16}{f_c Re_c}$	R_p	R_v	B	B/k
.97	9.60	1.667	369.720	0.99715	.970	1.000
.95	9.60	1.666	143.840	0.99119	.950	1.000
.93	9.61	1.665	62.108	1.00180	.930	1.000
.90	9.62	1.663	26.840	1.01730	.900	1.000
.85	9.64	1.660	15.503	0.98872	.849	.999
.80	9.67	1.654	9.586	0.96782	.797	.997
.70	9.78	1.635	4.286	0.98390	.691	.987
.60	9.97	1.604	2.728	0.94920	.581	.969
.50	10.26	1.560	1.899	0.95270	.466	.933

As shown by the column B/k in the Table, the values of B are extremely close to those of k for the practical diameter ratios of 0.8 and higher, indicating the definition of the laminar Couette flow as corrected in equation 4 is valid for capsules moving at practical velocity ratios. It will be shown from an examination of data that the definition appears to be very useful also for turbulent flow.

5.4 Accuracy of Data

Before presenting the experimental data their accuracy is discussed first. The precision of the pressure transducers on the pipelines was $\pm \frac{1}{2}\%$ of calibrated range. The capsule pressure gradients reported, however, are less precise than the instrument readings because the capsule pressure gradient was obtained by subtracting the liquid pressure drop ahead of and behind the capsules from the measured reading before dividing by the capsule length. This is illustrated in Fig. 5-3. The pressure drop

measured by each transducer consisted of three components: the liquid pressure drop over the pipe section between the first pressure tap and the tail of the capsule, the capsule pressure drop between the tail and the nose of the capsule, and the liquid pressure drop over the pipe section between the nose of the capsule and the second pressure tap. Hence the uncertainty of each capsule pressure gradient result is different, but it can be found from the relationship:

$$\text{Uncertainty} = \left[\frac{\text{Calibrated Range}}{\text{Instrument Reading}}\right]\left[\text{Instrument Precision}\right]\left[1 + \left\{\frac{\left(\frac{\Delta P}{L}\right)_f \quad (L_p - L_c)}{\left(\frac{\Delta P}{L}\right)_c \quad L_c}\right\}\right] \qquad (12)$$

Two transducers were used in the 10 inch pipeline, one calibrated to 0-5 inches of water differential and the other to 0-50 inches of water differential. The distance between pressure taps (L_p) on this pipeline was 42 ft. Two ranges of instrument calibration were also used on the laboratory lines, i.e. 0-30 and 0-120 inches of water differential and the distance between the pressure taps on these pipelines was 24 ft. In each case the lower range pressure transducer was used if the reading was below 90% of its calibrated range, otherwise the higher range pressure transducer was used.

The accuracy of the pressure-flow velocity depends on the accuracy of the measured capsule and bulk liquid velocities and the diameter ratio. The measurement of the capsule velocity was based upon the time of transit of the capsule between two light beams in the pipeline, and good accuracy was obtained by careful measurement of the distance between the light beams and by the high speed of response of the photocells. The measurement of the capsule velocity was much more accurate than the measurement of the bulk liquid velocity and for this reason any errors in the capsule velocity are neglected in the discussion. The capsule and pipe diameters were measured to within ± 0.1% or better and hence any errors in the diameter ratio are also neglected. Measurements of the liquid velocity, however, were precise to $\pm\frac{1}{2}$% of range. For most of the experimental work in the capsule pipelines the velocity range for which the flowmeters were calibrated was 0-10 ft./sec. with a resulting uncertainty of ± 0.5% x 10 ft./sec. or ± 0.05 ft./sec. for all the readings. Since the velocity term ($V_b - k V_c$) was obtained by subtracting part of the more accurate capsule velocity from the bulk

velocity, the uncertainty of ($V_b - k V_c$) was also ± 0.05 ft./sec. Dividing the velocity term by $1 - k^2$, to obtain the pressure-flow velocity (equation 6) for the various diameter ratios, tends to mask the accuracy of the measurement. For this reason $V_b - k V_c$ is plotted whenever it is important to obtain an indication of the accuracy of the measured data.

5.5 Experimental Results

A set of representative results from the four inch laboratory pipeline are presented first to show the steps in obtaining the friction factor, Reynolds number relationship of the model.

The capsule pressure gradient is reported in Fig. 5-4 as a function of the bulk velocity. Results are shown for trains of four, 2 ft. long, 0.806 diameter ratio butyrate plastic capsules loaded to various specific gravities and run in a stainless steel test section in water. Estimated lines are drawn through the results for the specific gravities of 2.0, 1.5, 1.25, 1.03 while the plusses and the triangles, representing specific gravities of 1.125 and 1.06 respectively, are left unconnected for clarity of the Figure. As shown, the pressure gradients increase markedly with specific gravity. The capsule velocity is shown as a function of the bulk velocity for the same capsule trains in Fig. 5-5. The data for most capsules show a linear relationship between the bulk velocity and the capsule velocity. The separation of the lines due to varying specific gravity is illustrated in the Figure, and, while not shown here, this separation is reduced as the diameter ratio increases. For very large diameter ratios the data for various specific gravity capsules virtually superimpose on each other. Fig. 5-6 illustrates the data of Fig. 5-4 plotted on the basis of $V_b - k V_c$, the velocity term in equation 6.

Fig. 5-7 shows the same data plotted on the basis of a friction factor, Reynolds number relationship. The definitions of the two quantities are based upon the maximum annular gap (D-d) and the pressure-flow velocity of equation 6. At zero capsule velocity the pressure-flow velocity becomes equal to the annular velocity for liquid flow past a stationary eccentric core in a pipe. Three lines defined by: $f\,(Re) = 9.6$, $f\,(Re)^{0.25} = 0.079$, and $f\,(Re)^{0.25} = 0.05$ respectively, are drawn in the Figures. The first represents the theoretical prediction of Caldwell [7] or Tiedt [8] for laminar flow of a fluid in the

annulus between a large diameter ratio, fully eccentric, stationary core and a pipe. The second is the accepted Blasius relationship for turbulent flow in a pipe and the third represents the experimental results of Tiedt [8] for turbulent flow in the annulus between a large diameter ratio, fully eccentric, stationary core and a pipe.

Figs. 5-8, 5-9, 5-10 and 5-11 show additional data on the same basis. Fig. 5-8 is a replot of the data of Figure 8 in Kruyer et al [4], representing a single 24 in. long, 0.824 diameter ratio, hollow steel cylinder loaded to three specific gravities run in light lubricating oil in a copper half-inch pipeline. Fig. 5-9 reports data from the present four-inch experimental laboratory pipeline with a stainless steel test section for a train of four 24 inch long cylindrical, hollow butyrate-plastic capsules of four diameter ratios (0.92, 0.90, 0.87 and 0.81); these were loaded to seven specific gravities between 1.0 and 3.0 and run in a mixture of polyglycol and water. Fig. 5-10 is for data from the same pipeline for the same capsule trains as Fig. 5-9, run in water. Fig. 5-11 presents data from a ten-inch steel pipeline for trains of five 48 inch long hollow steel capsules of three diameter ratios (0.85, 0.90 and 0.95) loaded to six specific gravities between 1.0 and 1.5 and run in water.

For Reynolds numbers below 1000 the Figures show very good agreement between the measurements and the predicted f (Re) = 9.6, indicating that the pressure-flow velocity is a good indicator for laminar flow in a capsule pipeline. For Reynolds numbers above 1000 the value of the experimental $f\,(Re)^{0.25}$ averages around 0.07 instead of 0.05 as might be expected for turbulent flow around fully eccentric cylinders [8]. Additional definitions of the pressure-flow velocity for turbulent flow conditions were tried to find one which would give better agreement with the results of Tiedt for stationary cylinders, but the present definition has given the least scatter in the data. Fig. 5-12, for example, shows the same experimental data of Fig. 5-10 based upon the previous definition of the pressure flow velocity by Ellis and Kruyer [1], ($V_p = V_a - 0.35\,V_c$). The present definition is shown to be superior.

5.6 Critical Reynolds Numbers

In pipe flow the critical Reynolds number at which the flow normally ceases to remain laminar is accepted as 2100. In annuli, however, it is usually somewhat less. For stationary cylinders Tiedt [8] experimentally found it to be 1200 for diameter ratios above 0.7. For capsule flow the value of the critical Reynolds number appears to average slightly lower yet, near 1000. It is difficult, however, to find a definite transition point since, unlike that in pipe flow, the data for flow in eccentric annuli generally show a gradual transition from laminar to turbulent flow.

5.7 Predicting the bulk velocity

Having thus obtained a correlation between the capsule pressure gradient, capsule velocity and bulk velocity for cylindrical capsules, over a wide range of pipe sizes, diameter ratios, capsule densities and Newtonian liquid properties, it is now possible to predict any one from the other two. In all practical capsule applications the capsule velocity will be known from the desired throughput and the delivered concentration of capsules in the pipeline. The capsule pressure gradient is a function of the capsule-pipe-liquid interaction and can not be predicted independently as yet. However, the bulk velocity may be predicted from the capsule velocity and the measured capsule pressure gradient by solving for V_b in the relationship between f and Re.

for $Re_c \leq 1000$ when $f_c\,(Re)_c = 9.6$

$$V_b \text{ predicted} = k\,V_c + (1-k^2)\left[\frac{\left(\frac{\Delta P}{L}\right)_c g_c (D-d)^2}{19.2\,\rho\,\nu}\right] \qquad (14)$$

and for $Re_c > 1000$ when $f_c\,(Re)_c = 0.07$

$$V_b \text{ predicted} = k\,V_c + (1-k^2)\left[\frac{\left(\frac{\Delta P}{L}\right)_c g_c (D-d)^{1.25}}{0.14\,\rho\,\nu^{0.25}}\right]^{0.57} \qquad (15)$$

For the purpose of predicting V_b the flow is assumed to be turbulent in the annulus and equation 15 is used. The validity of this assumption is then checked by calculating

the Reynolds number

$$Re_c = (D - d)\,(V_b - k\,V_c) \;/\; (1 - k^2)\;\nu \qquad (16)$$

If this exceeds 1000 the predicted V_b is based upon the correct equation, but if it is below 1000, V_b must be recalculated, using equation 14. Fig. 5-13 shows for the data of Figs. 5-4, 5-5, 5-6 and 5-7 the predicted bulk velocity plotted against that measured. For a perfect correlation all data would fall on the 45 degree line drawn in the Figure. As shown, the data closely follow this line.

5.8 Prediction of the Capsule Pressure Gradient

The present model is primarily intended to predict the bulk velocity from both the capsule velocity and the capsule pressure gradient, thus allowing the calculation of the amount of liquid required to move a commodity at a desired solids throughput. And as shown by Fig. 5-13 the prediction of such a velocity can be made very accurately. It is, however, also possible to use this model to predict the capsule pressure gradient from the capsule velocity and the bulk velocity. By rearranging equations 14 and 15, the capsule pressure gradient may be calculated from the following:

for $Re_c \leq 1000$

$$\left(\frac{\Delta P}{L}\right)_c = \frac{19.2\;(V_b - k\,V_c)\;\rho\;\nu}{(D - d)^2\;(1 - k^2)\;g_c} \qquad (17)$$

and for $Re > 1000$

$$\left(\frac{\Delta P}{L}\right)_c = \left[\frac{V_b - k\,V_c}{1 - k^2}\right]^{1.75} \frac{0.14\,\rho\,\nu^{0.25}}{g_c\;(D-d)^{1.25}} \qquad (18)$$

It should be stressed, however, that the measurement of the capsule and liquid velocities must be extremely accurate before a reasonable accuracy is attainable for this prediction of the capsule pressure gradient.

5.9 Calculating the liquid throughput and linear fill.

V_b represents the bulk velocity at any cross section in the capsule pipeline. When the cross section is taken in the space between the capsules the bulk velocity is the average velocity of the liquid. When the cross section is taken through a capsule it represents the average volumetric flowrate of capsule and annular liquid combined, divided by the cross sectional area of the pipe. In a potential commercial capsule pipeline the total volumetric flowrate is produced by a stream of capsules and a stream of carrier liquid. The total volumetric flowrate is equal to:

$$Q_t = \frac{\pi}{4} D^2 V_b \tag{19}$$

The time-averaged capsule flowrate is equal to:

$$Q_c = \frac{\pi}{4} d^2 V_c \lambda \tag{20}$$

where λ is the fractional linear fill.

The time-averaged liquid flowrate or the required liquid throughput is obtained by subtraction:

$$Q_f = \frac{\pi}{4} D^2 \left[V_b - k^2 V_c \lambda \right] \tag{21}$$

The steady state linear fill existing in a capsule pipeline when capsules and liquid are continuously entering the pipeline is a function of the two flowrates and is equal to:

$$\lambda = \frac{Q_c \quad V_b}{Q_t \quad V_c \, k^2} \tag{22}$$

5.10 Conclusion

In commercial work the capsule velocity will be readily calculable from the desired solids throughput and the solids concentration in the pipeline, leaving two parameters, the bulk velocity and the capsule pressure gradient to be predicted. This requires a knowledge of the effect of such factors as the capsule specific gravity and

the capsule-pipe surface interaction, which is still incomplete. The present chapter, however, has made use of the fact that for the prediction of the bulk velocity, the capsule pressure gradient is a very effective measure of the interaction of the capsule and pipe surfaces at each capsule specific gravity and velocity. It has thus been possible to predict the bulk velocity in capsule pipelines ranging from $\frac{1}{2}$ inch to 10 inches in diameter, carrier liquids with kinematic viscosities from 1 to 45 centistokes, capsule-to-pipe diameter ratios from 0.8 to 0.95, and capsule specific gravities from 1.03 to 12.

The model developed for this prediction defines a Reynolds number which indicates when the liquid in the annulus surrounding the capsules is in laminar flow ($Re < 1000$) or turbulent flow ($Re > 1000$).

References

1. Ellis, H.S. and Kruyer, J. "The Pipeline Flow of Capsules, Part 10, Empirical Pressure and Velocity Correlations for Cylindrical Capsules conveyed in Pipelines up to 4 inches in Diameter." Paper C2, Hydrotransport 1, Proceedings 1970. BHRA Fluid Engineering, Cranfield, Bedford, England.

2. Round, G.F. Private communication. 1968.

3. Garg, V.K. and Round, G.F. "Capsule Pipeline Flow - a Theoretical Study." Thermodyn. and Fluid Mech. Conv., Inst. of Mech. Eng., London, England. Proceedings 1969-70, 184, Pt. 3G (1), pp. 89-100.

4. Kruyer, Jan, Redberger, P.J., and Ellis, H.S. "The Pipeline Flow of Capsules, Part 9." J. Fluid Mech., 30, Part 3, pp. 513-31 (November 1967).

5. Epstein, N., Bianchi, R.J., Lee, V.T.Y. and Bentwich, M. "Eccentric Laminar Couette Flow of Long Cylindrical Capsules." Joint Chem. Eng. Conf. 1973, Vancouver, B.C.

6. Bentwich, M., Kelly, D.I.A., and Epstein, N. "Two Phase Eccentric Interface Laminar Pipeline Flow." ASME Transactions, J. Basic Eng., 92, Series D, No. 1, March 1970.

7. Caldwell, J. "The Hydraulic Mean Depth as a Basis for Form Comparison in the Flow of Fluids in Pipes." J. Roy. Tech. Coll., Glasgow (1930), 2, 203-20.

8. Tiedt, W. "Berechnung des Laminaren und Turbulenten Reibungswiderstandes Konzentrischer und Exzentrischer Ringspalte." Technischer Bericht Nr. 4, Institut fur Hydraulik und Hydrologie der Technischen Hochschule Darmstadt, Germany (March 1968).

9. Tiedt, W. "Review of paper by Bourne, D.E., Figueiredo, O., and Charles, M.E. Laminar Flow and Turbulent Flow in Annuli of Unit Eccentricity." App. Mech. Rev. 22, 1969.

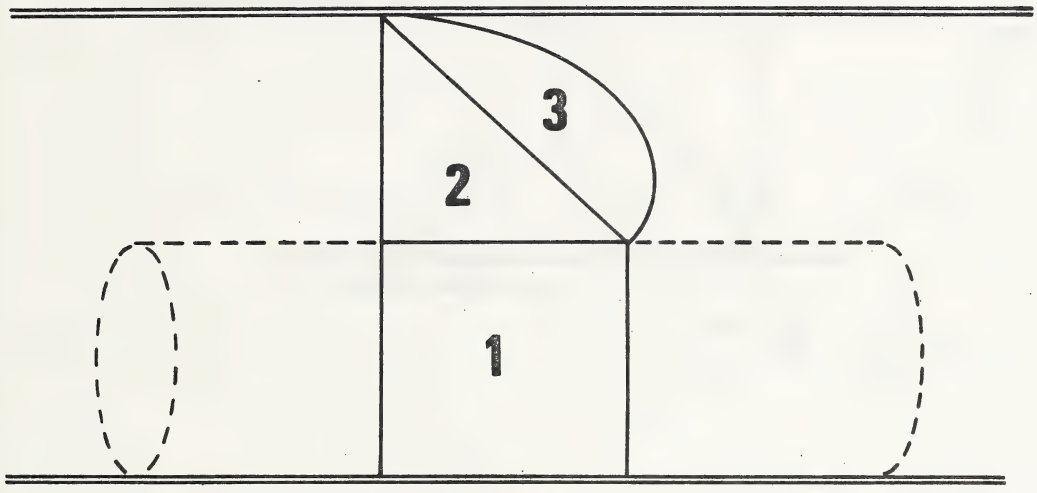

SUGGESTED FLOW COMPONENTS

FIGURE 5-1

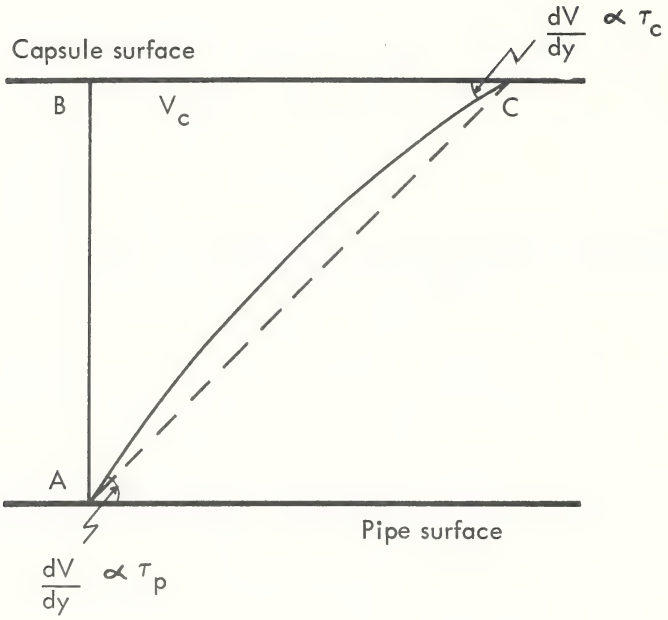

ANNULAR COUETTE FLOW

FIGURE 5-2

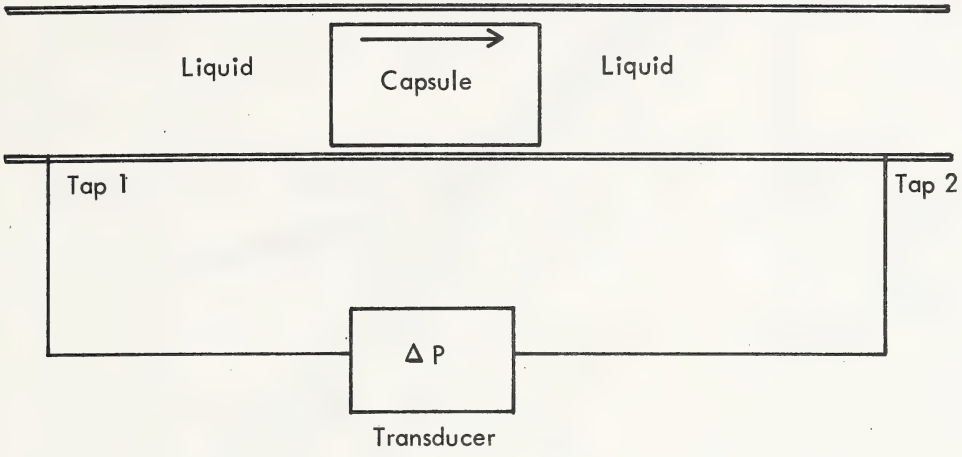

PRESSURE DROP MEASUREMENT

FIGURE 5-3

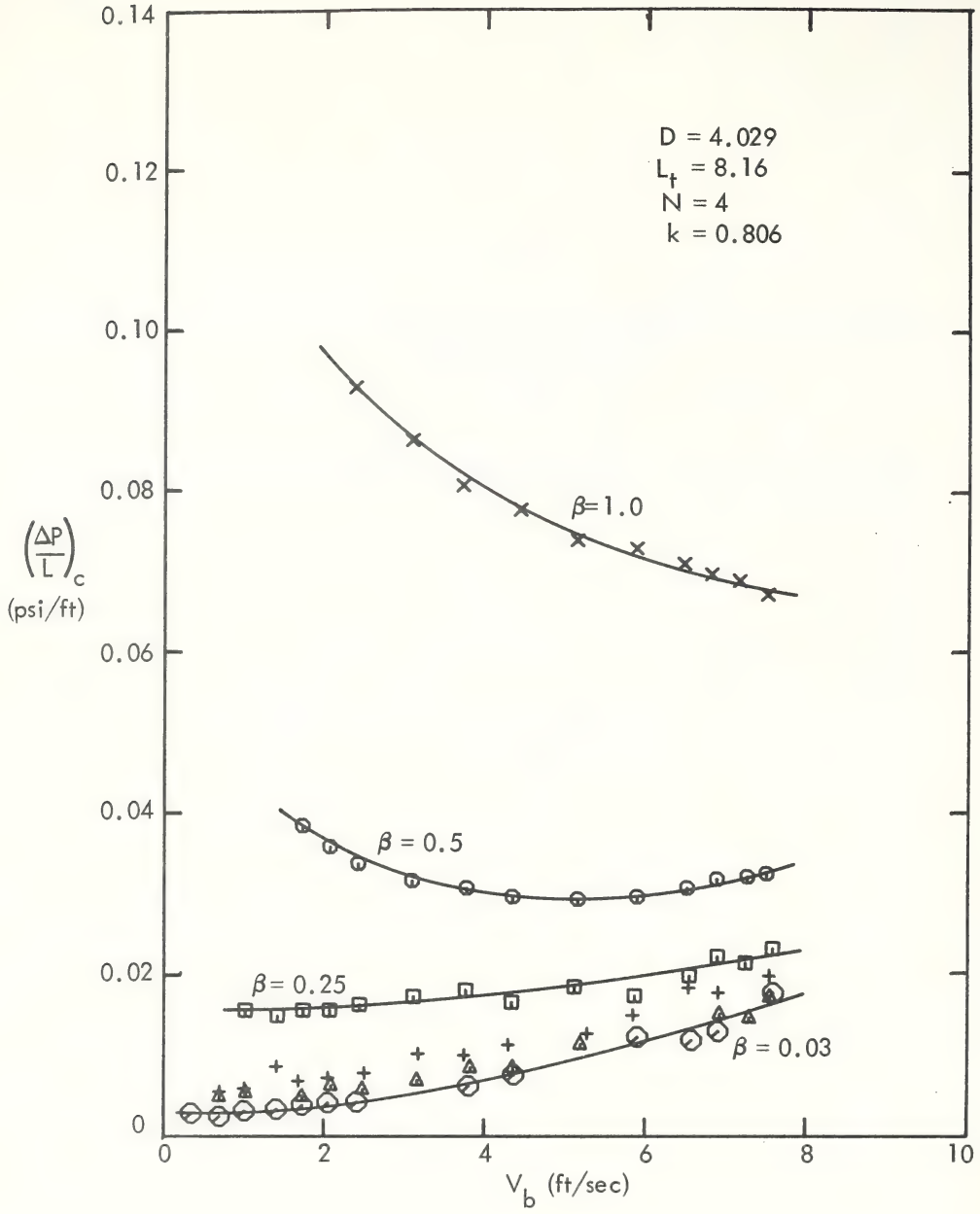

RESULTS FROM A FOUR INCH PIPELINE

FIGURE 5-4

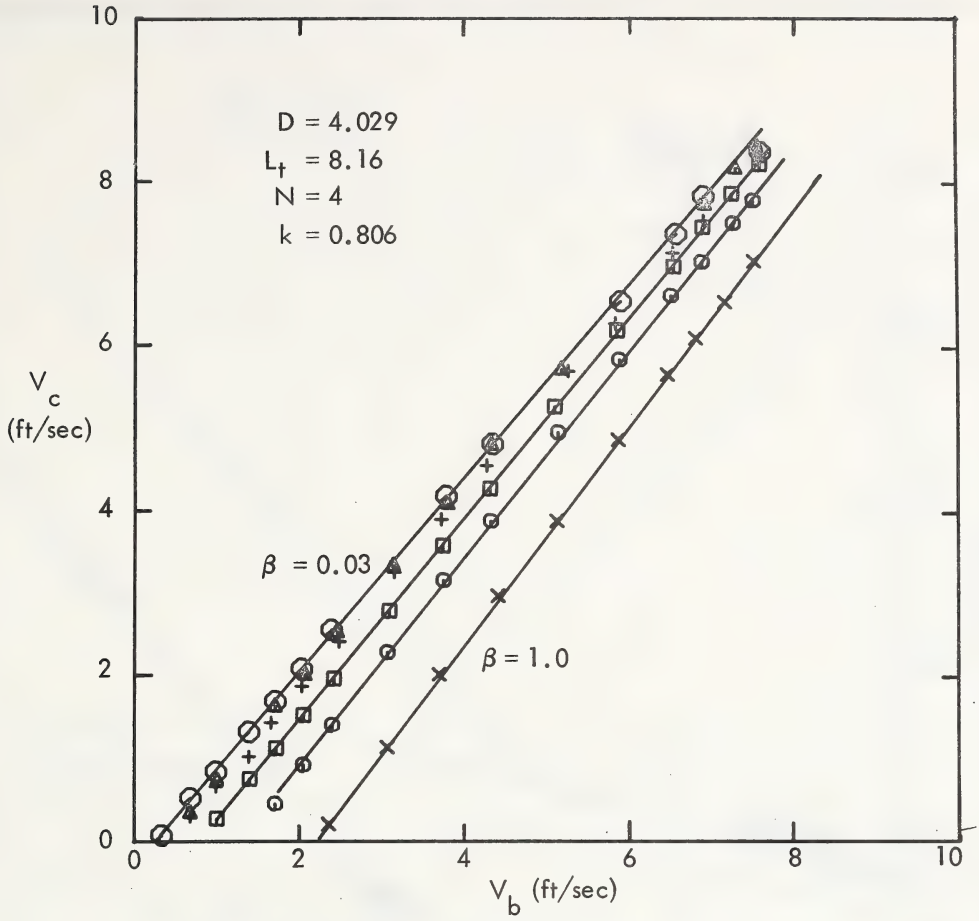

RESULTS FROM A FOUR INCH PIPELINE

FIGURE 5-5

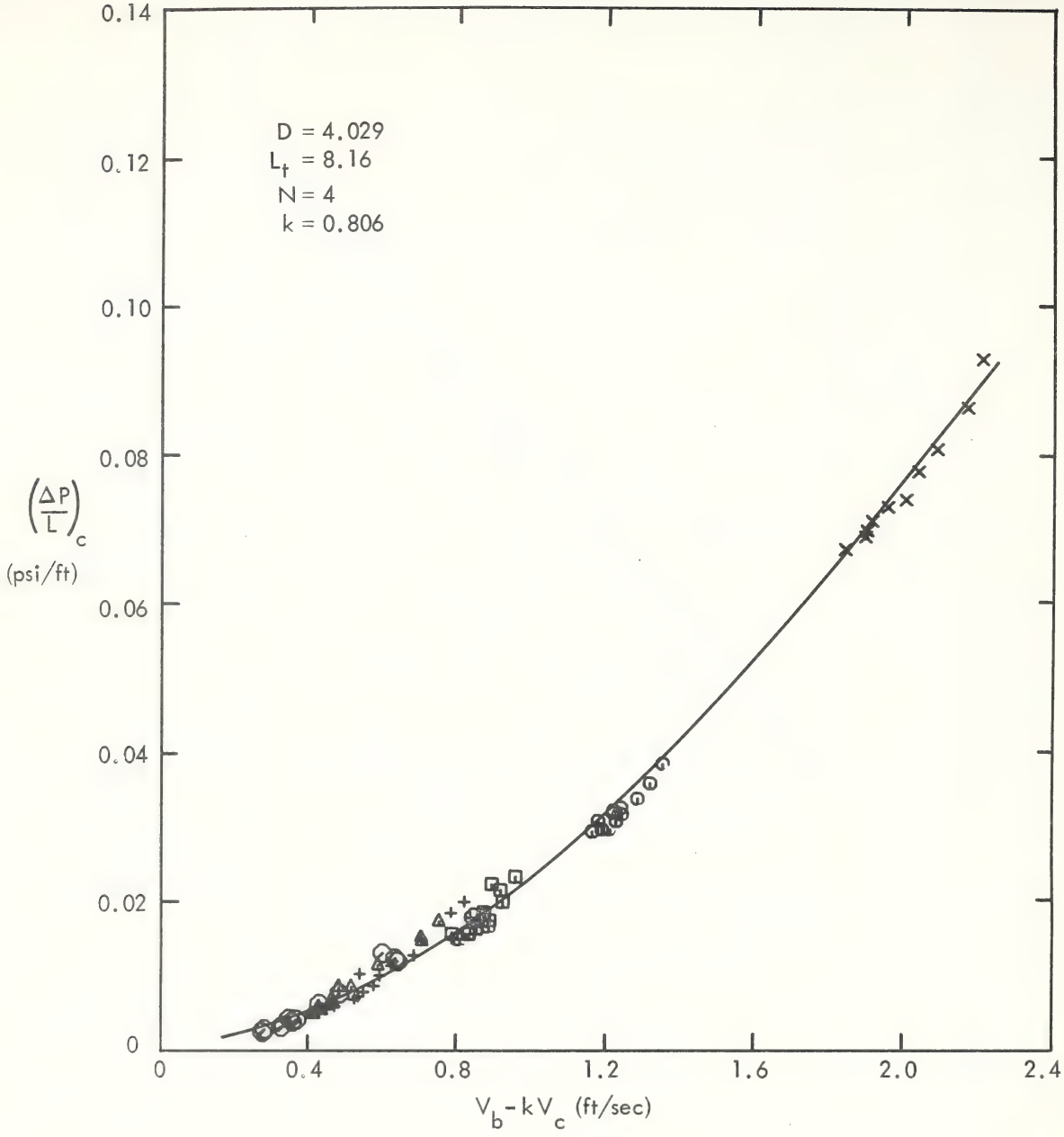

CAPSULE PRESSURE GRADIENT AS A FUNCTION OF THE VELOCITY TERM OF EQUATION 6

FIGURE 5-6

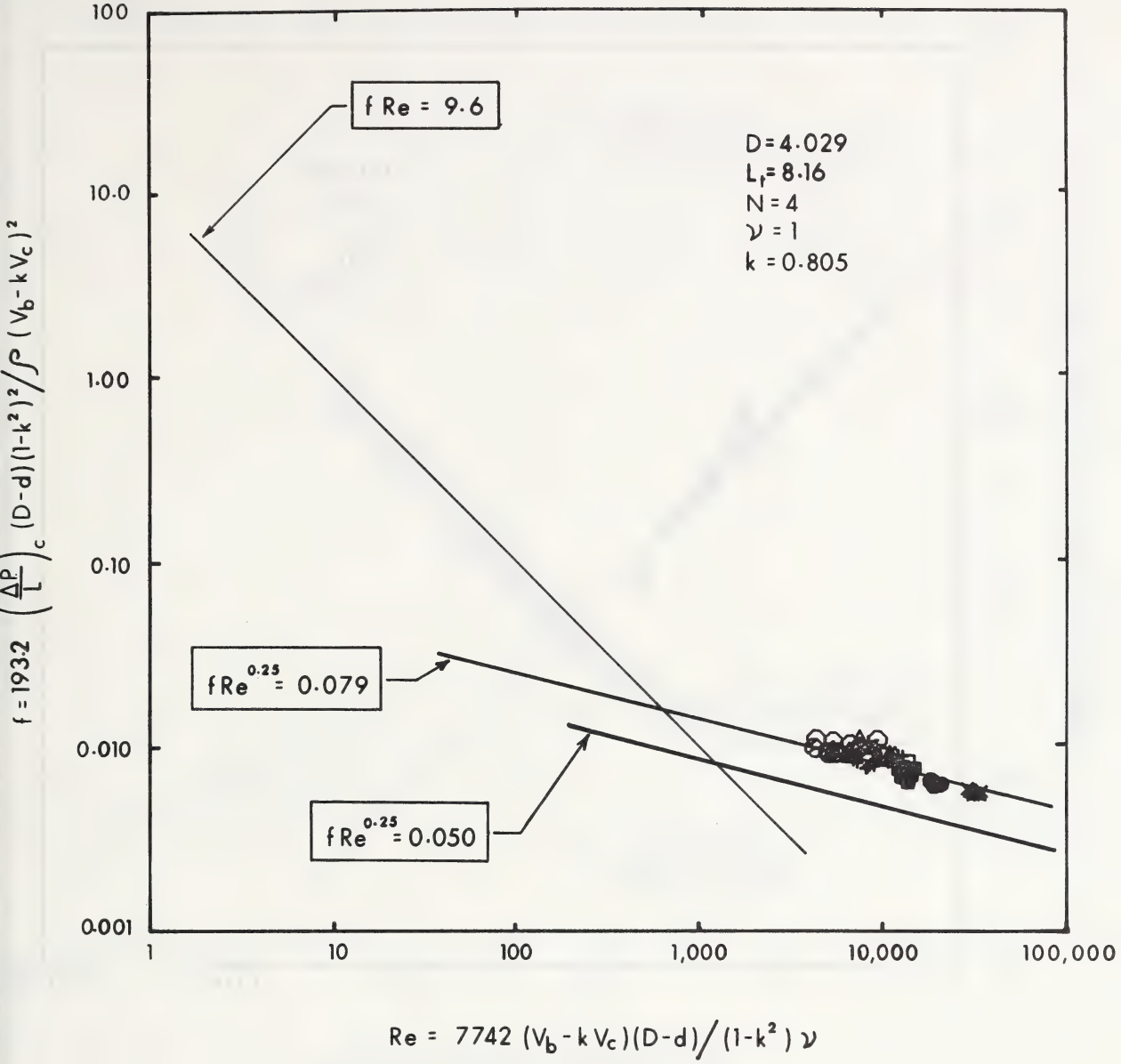

FANNING FRICTION FACTORS AND REYNOLDS NUMBERS
DATA OF FIGURES 5-4, 5-5 AND 5-6.

FIGURE 5-7

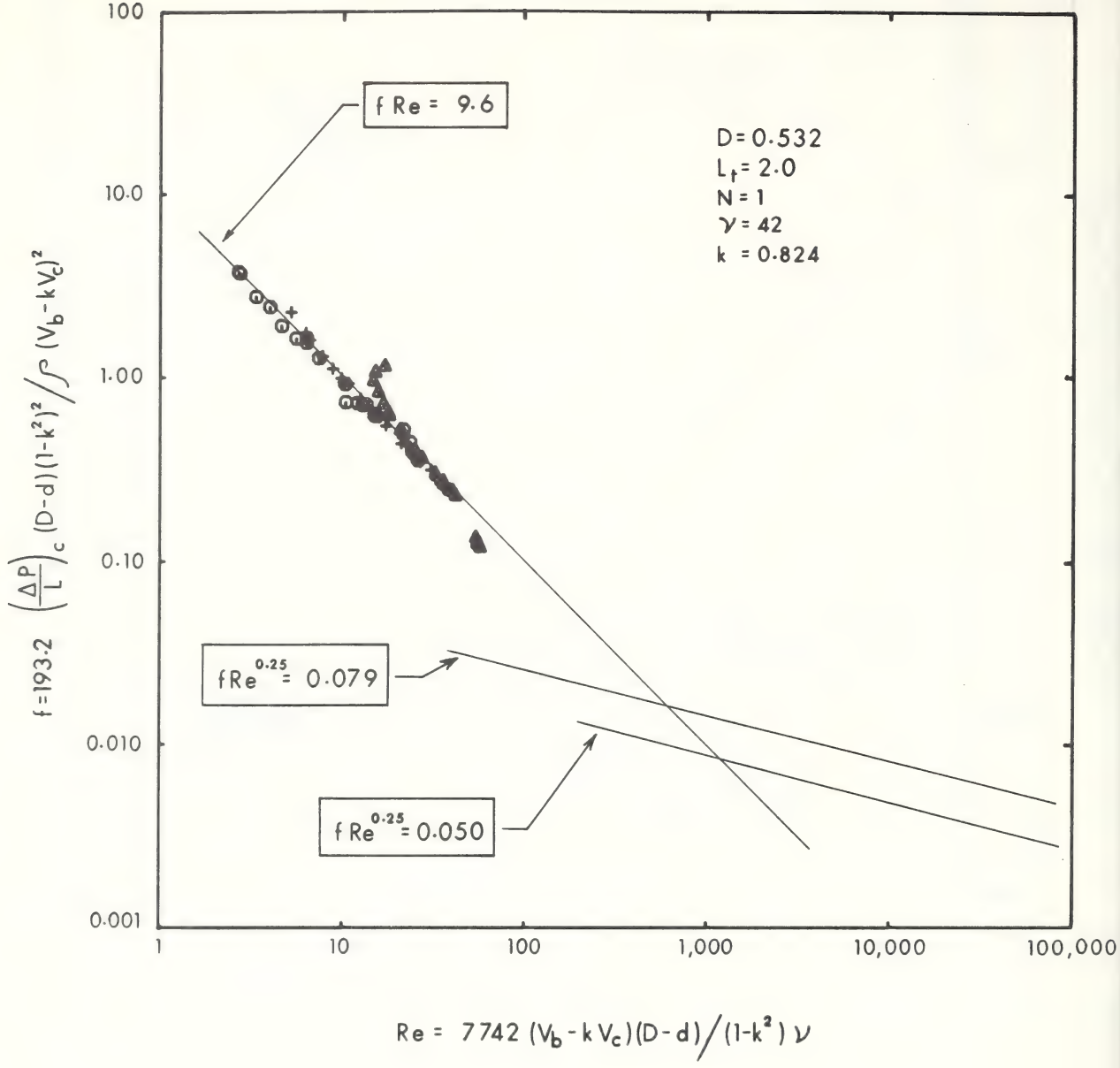

FANNING FRICTION FACTOR VERSUS REYNOLDS NUMBER FOR CAPSULE DATA IN OIL IN A $\frac{1}{2}$ INCH PIPELINE

FIGURE 5-8

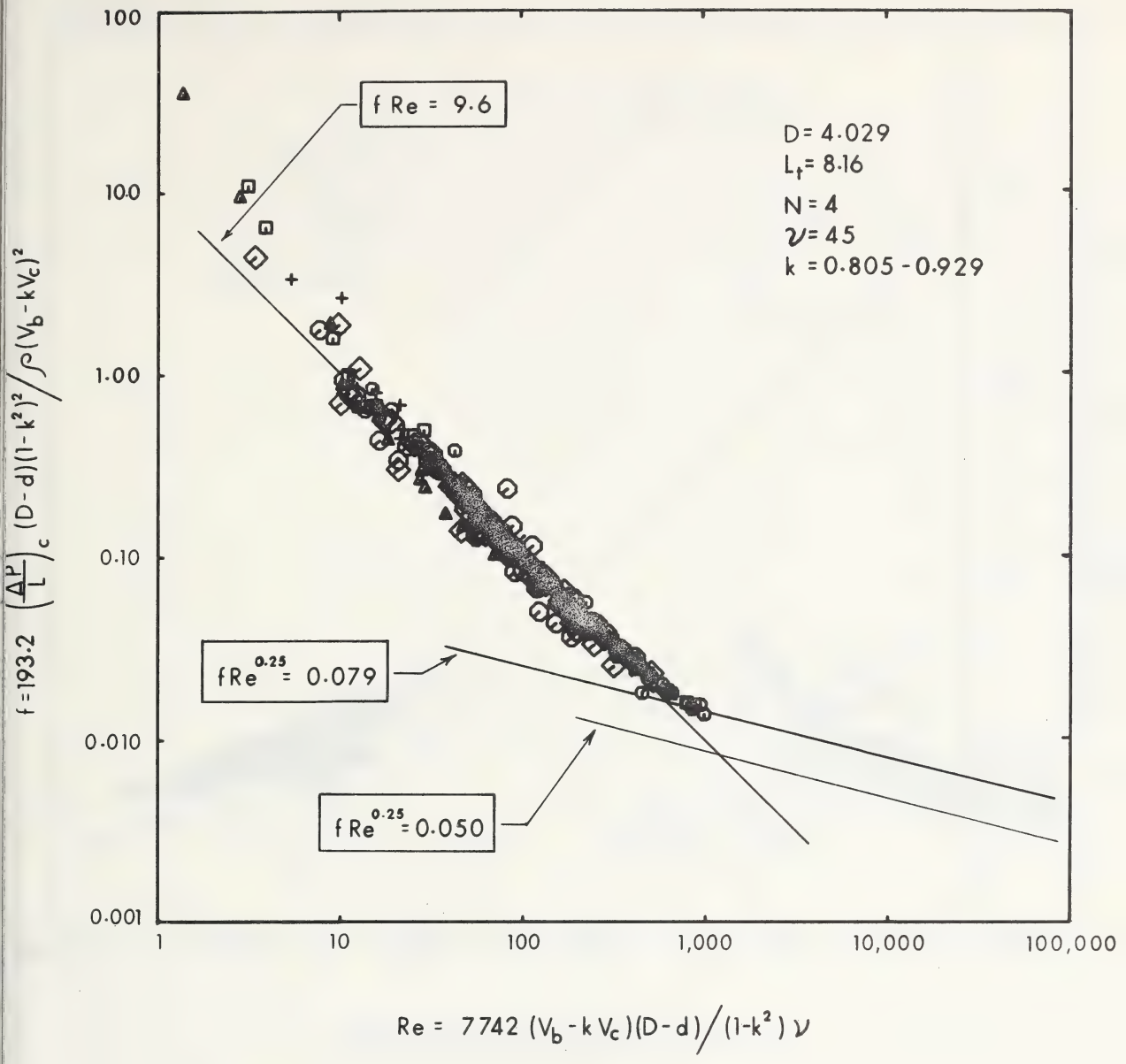

FANNING FRICTION FACTOR VERSUS REYNOLDS NUMBER FOR TRAINS OF FOUR CAPSULES IN POLY-GLYCOL AND WATER MIXTURES IN A FOUR INCH PIPELINE

FIGURE 5-9

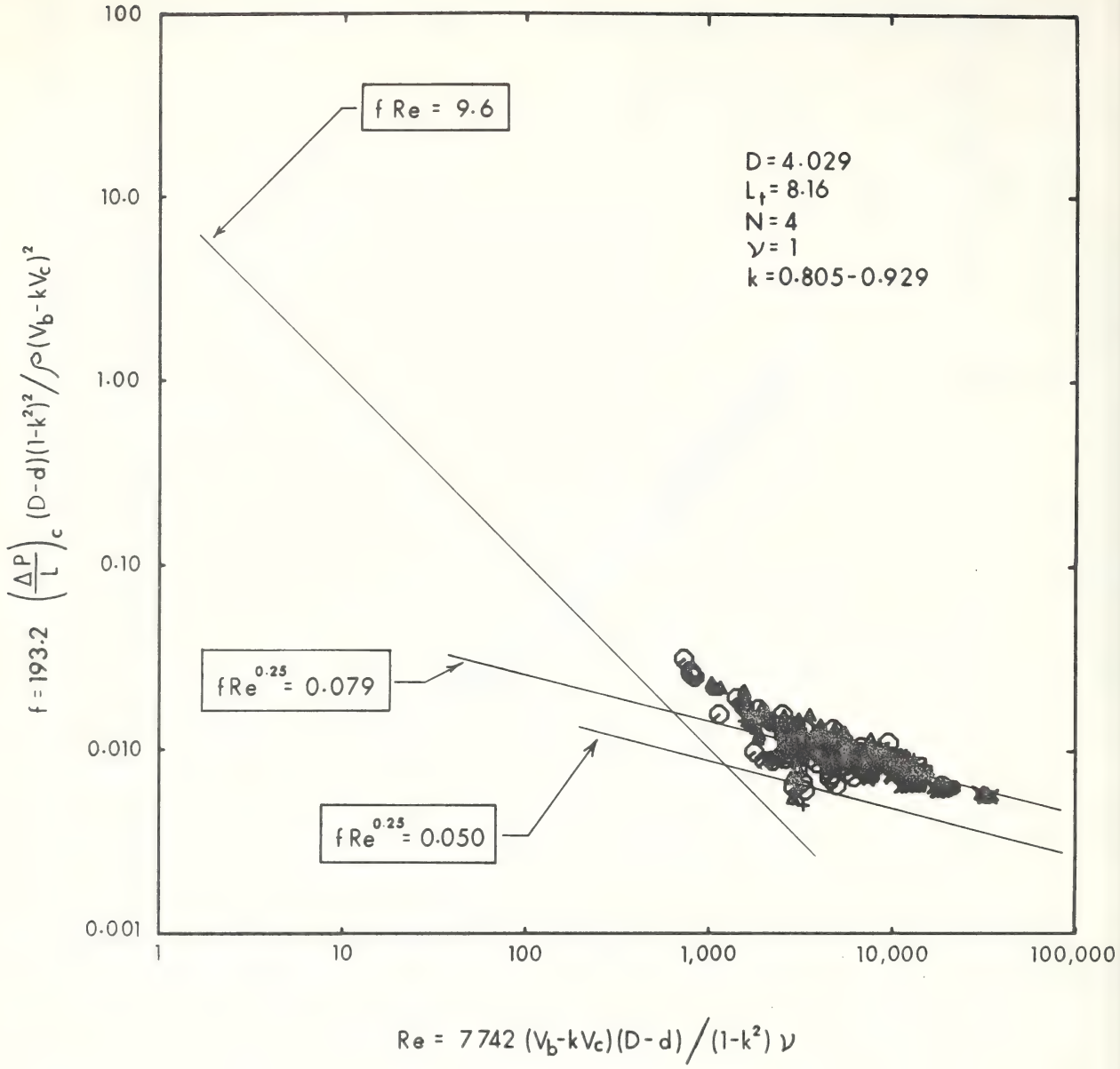

FANNING FRICTION FACTOR VERSUS REYNOLDS NUMBER FOR TRAINS OF FOUR CAPSULES IN WATER IN A FOUR INCH PIPELINE

FIGURE 5-10

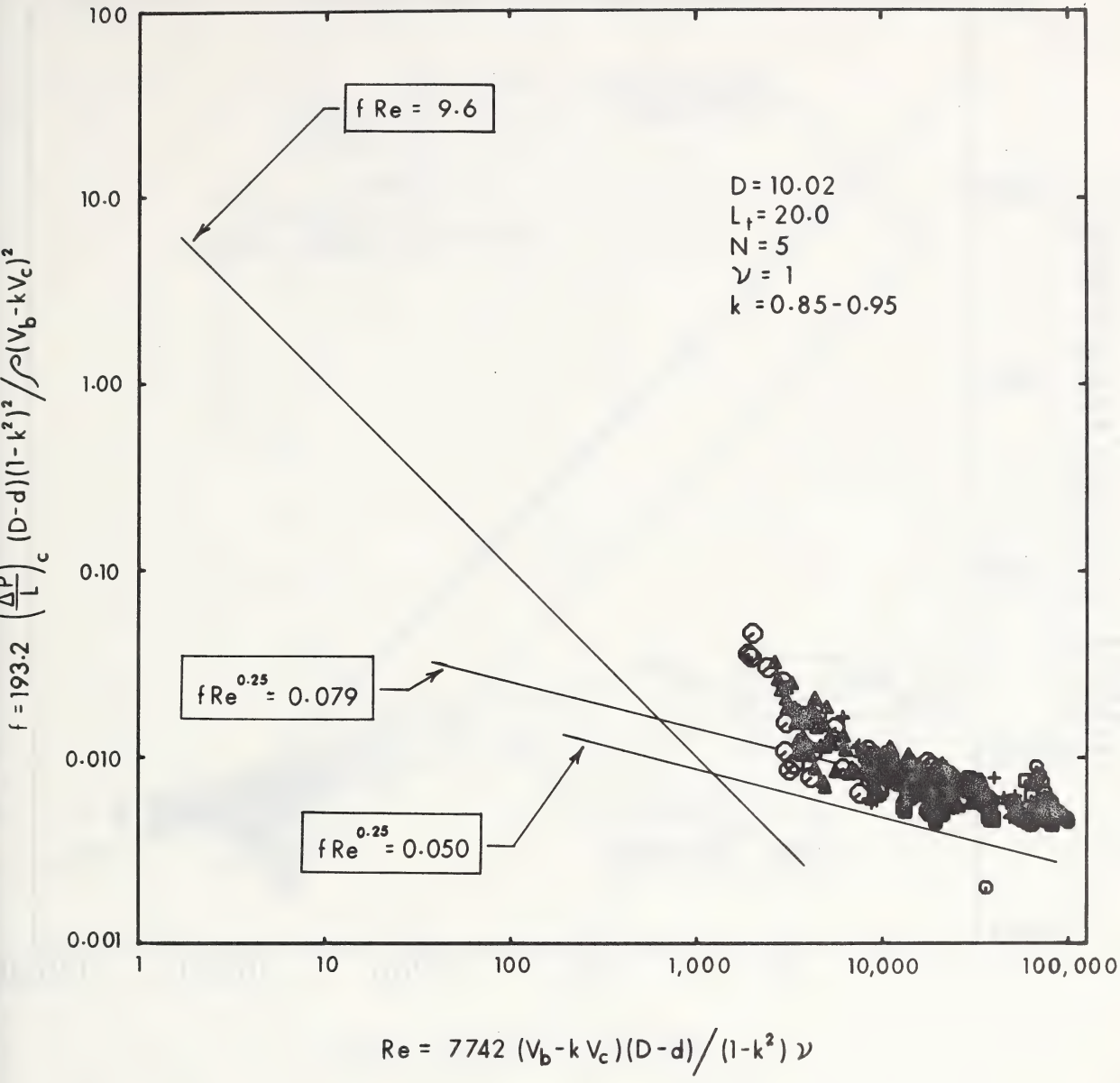

FANNING FRICTION FACTOR VERSUS REYNOLDS NUMBER FOR TRAINS OF FIVE CAPSULES IN WATER IN A TEN INCH PIPELINE

FIGURE 5-11

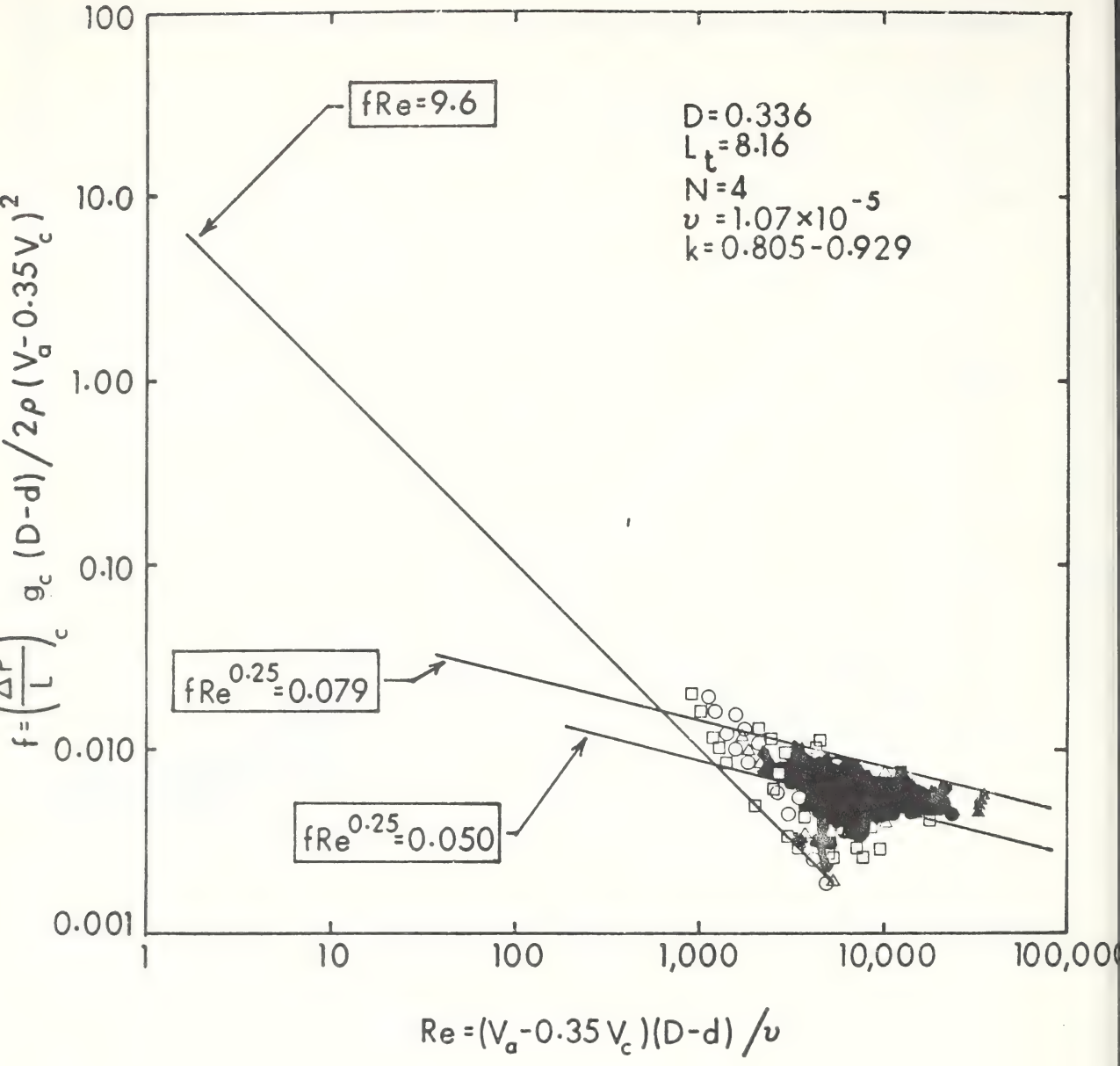

FANNING FRICTION FACTORS VERSUS REYNOLDS NUMBERS, BOTH BASED UPON AN OLDER DEFINITION OF THE EQUIVALENT VELOCITY, FOR CAPSULE TRAINS IN WATER IN A 4 INCH PIPELINE

FIGURE 5-12

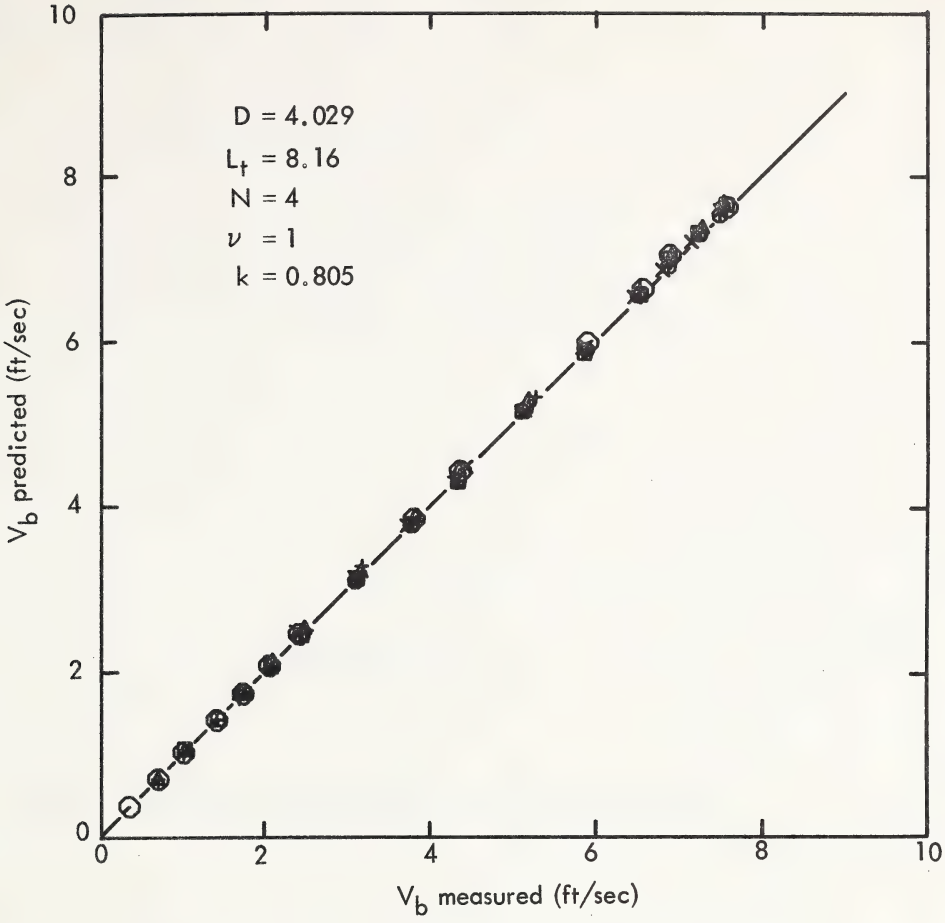

PREDICTED VERSUS MEASURED BULK LIQUID VELOCITY FOR THE DATA OF FIGURES 5-4 AND 5-5.

FIGURE 5-13

CHAPTER VI

Friction and Surface Roughness Effects in Capsule Pipelines

CHAPTER VI

Friction and Surface Roughness Effects in Capsule Pipelines

Summary

In pipeline flow the pressure gradients for cylindrical capsules differing in density from the carrier liquid are influenced by the interaction between the surfaces of the capsule and pipe walls.

It is shown that pressure gradients for capsules at the point of incipient motion can be calculated directly from the coefficient of friction. For moving capsules, however, the pressure gradients are a function of the capsule velocity, the surface roughnesses of the capsule and pipe walls and the coefficient of friction. Data are presented to show how capsule pressure gradients change with velocity for various degrees of capsule and pipe surface polish. This change is thought to be due to a gradual transition from solid-solid friction to hydrodynamic lubrication which is accelerated by polishing of the surfaces.

6.1 Introduction

When solids are transported in the form of cylinders which are denser than the carrier liquid, the interaction of the capsule and pipe surfaces influences the capsule pressure gradient to a very large degree. The effect of decreasing the capsule-to-pipe surface interaction, and hence the capsule pressure gradient, by decreasing the capsule density was discussed in Chapter III. Reduction of this interaction, however, can also be achieved at constant density by modifying the capsule and/or pipe surfaces. This chapter relates the capsule pressure gradient to the coefficient of friction and provides some preliminary results to show the effect of capsule surface at constant density.

6.2 Friction Measurements

When a cylindrical capsule is carried through the pipeline by the liquid the pressure drop between the tail and the nose of the capsule causes it to move forward. The friction force resists this forward movement while the shear forces at the capsule surface may aid or deter it, depending upon the velocity of the capsule relative to the surrounding liquid. When the capsule is stationary, at the point of incipient motion, the pressure and shear forces act to dislodge the capsule while the friction force opposes

this. A number of tests were made to measure the friction force on a train of capsules in a pipeline and to compare these with the capsule pressure gradient at the point of incipient motion. The experimental results were all obtained from the 4 in. pipeline. Details on the construction of and the data acquisition from this pipeline were discussed in the Phase I Report - and in published papers [1, 2]; the only additional equipment is a reeling device for pulling the capsule train through the pipeline at various velocities (Fig. 6-1). A cable, attached to the capsule train, passed through the end of the pipeline, over a wheel attached to a load-cell, over two alignment wheels and then was wound upon a motorized reel. For a friction measurement test the capsule train, consisting of four capsules hooked together, was pumped to the beginning of the pipeline while the cable unreeled. The reel was then engaged and the capsule train was pulled through the pipe to the end while the signal from the load-cell was measured. Previous calibrations of the load-cell and wheel arrangement allowed calculating the pulling force from the load-cell signal. These measurements were made at several velocities and the pulling force at zero velocity was obtained by extrapolation. The capsule pressure gradients for the same train were measured before and after the pulling tests without removing the capsule train from the pipeline. This procedure was followed to retain the same capsule orientation for both the pressure gradient measurements and the pulling tests.

6.3 The Pulling Force

The normal force between the capsule and the pipe wall is directly related to the buoyed capsule density and the volume of the capsule:

$$F_1 = \frac{\pi}{4} d^2 L_c (\sigma - \rho) g / 144 g_o$$

The pulling force may be expressed in terms of this normal force and the coefficient of friction:

$$F_2 = \frac{\pi}{4} d^2 L_c (\sigma - \rho) \eta g / 144 g_o \qquad (1)$$

This relationship is valid only when the capsule is moving very slowly. At the higher capsule velocities the effects of Couette shear add additional terms to the above relationship. In this chapter, however, only the pulling forces and the pressure gradients extrapolated to zero capsule velocity are compared.

6.4 The Pressure Force

Neglecting entrance and exit effects of the liquid flowing past the capsule, the pressure force on a capsule is made up of two components. The first component results from the difference in pressure between the tail and the nose of the capsule multiplied by the cross sectional area of the capsule:

$$F_3 = \frac{\pi}{4} d^2 \left(\frac{\Delta P}{L}\right)_c L_c \qquad (2)$$

This same difference in pressure causes liquid flow in the annulus and gives rise to shear stresses on the pipe and capsule walls:

$$F_4 = \frac{\pi}{4} (D^2 - d^2) \left(\frac{\Delta P}{L}\right)_c L_c = 12\tau_p \pi D L_c + 12 \tau_c \pi d L_c$$

The second component of the pressure force on the capsule,

$$F_5 = (F_4 \tau_c \pi d L_c) / (\tau_p \pi D L_c + \tau_c \pi d L_c)$$

Measurements of the wall shear stresses in concentric and eccentric annuli reported by Jonsson and Sparrow [3] for stationary cores in pipes show that τ_c is approximately equal to τ_p.

For $\tau_c = \tau_p$

$$F_5 = \left[\frac{\pi}{4} (D^2 - d^2) \left(\frac{\Delta P}{L}\right)_c L_c d\right] / (D + d) \qquad (3)$$

The total pressure force on the capsule is obtained by adding F_3 and F_5 :

$$F_6 = \frac{\pi}{4} \left(\frac{\Delta P}{L}\right)_c L_c \left[d^2 + d (D^2 - d^2) / (D + d)\right]$$

$$= \frac{\pi}{4} \left(\frac{\Delta P}{L}\right)_c L_c D d \qquad (4)$$

6.5 Equating the Forces

Equating the pulling force to the pressure force and assuming that lift forces on the capsule can be neglected provides a simple method for predicting the capsule pressure gradient at incipient motion from the coefficient of friction:

$$F_2 = \frac{\pi}{4} \; d^2 \; L_c \; (\sigma - \rho) \, \eta \, g/144 \, g_o = F_6 = \frac{\pi}{4} \left(\frac{\Delta P}{L}\right)_c \; L_c \; D \, d$$

or

$$\left(\frac{\Delta P}{L}\right)_c = k \; (\sigma - \rho) \; \eta \; g/144 \; g_o \qquad (5)$$

Table 1 shows representative results of pulling tests and pressure gradient measurements for cylindrical capsules in the 4 in. pipeline. The pulling forces were measured at several capsule velocities and extrapolated to zero. Similarly, the capsule pressure gradients were measured at several velocities and also extrapolated to zero capsule velocity. The four lowest capsule densities represent trains of four butyrate plastic cylinders in a stainless steel pipe while the highest density represents a single stainless steel cylinder in a butyrate plastic pipe.

As shown by the Table the capsule pressure gradient at incipient motion as measured and as predicted from the coefficient of friction obtained by a pulling test show good agreement. The pressure gradient at incipient motion is useful for predicting the capsule pressure gradient required to start stalled capsules in a pipeline. For a stationary capsule, however, the coefficient of static friction applies,while the coefficients measured in these tests were for sliding friction. In most cases the coefficients of static or sliding friction do not differ greatly. The pressure gradient at incipience also relates to the pressure gradient for moving capsules as will be discussed subsequently.

Lazarus and Kilner [4] also discussed incipient pressure gradients but their work included both entrance and exit effects and lift forces. The results presented here suggest that the effect of these is only minor.

TABLE 1

Predicted and Measured Capsule Pressure Gradients Extrapolated to $V_c = 0$

Pipe Surface *	S.S.	S.S.	S.S.	S.S.	But.
Capsule Surface *	But.	But.	But.	But.	S.S.
Capsule Buoyed Specific Gravity	0.125	0.250	0.500	1.00	2.00
Diameter ratio	0.87	0.87	0.87	0.87	0.87
Coefficient of friction	0.25	0.30	0.22	0.28	0.40
Predicted pressure gradient extrapolated to $V_c = 0$ lb/in^2 ft	0.012	0.028	0.042	0.106	0.30
Measured pressure gradient extrapolated to $V_c = 0$ lb/in^2 ft	0.013	0.028	0.050	0.102	0.30

* S.S. = Stainless Steel; But. = Cellulose Acetate Butyrate.

6.6 Capsules in Motion

As shown, the capsule pressure gradient at incipient motion can be predicted fairly accurately from the coefficient of friction. Pressure gradients for moving capsules, however, are not equal to the pressure gradient at incipience but vary with capsule velocity. In addition, as the capsules are run in the pipeline, the surface in contact with the pipe wall can change in roughness, causing a change in the measured capsule pressure gradients. Fig. 6-2 is a plot of results obtained in the butyrate test section. A single smooth, stainless steel capsule loaded to a buoyed specific gravity of 2.00 was inserted into the pipeline, after which the capsule pressure gradient was measured as a function of the capsule velocity. These data are represented by the symbols of the upper curve in the Figure (Run 1143). Upon completion of these measurements the capsule was shuttled back and forth through the pipeline

at a velocity of about 3 ft./sec. for a total of 76 hours after which, without removing the capsule from the pipeline or disturbing its orientation, the capsule pressure gradients were once more measured as a function of the capsule velocity (Run 1159). The capsule was then removed to allow for recalibration of the instruments. The capsule did not rotate in the pipeline during the tests since the centre of gravity was below its centreline. The bottom surface of the capsule closest to the pipe wall during the tests had become somewhat polished. The capsule was reinserted with the polished surface at the bottom and then shuttled back and forth through the pipeline for an additional 147 hours. Similarly, without removing the capsule from the pipeline, the capsule pressure gradient was measured again as a function of capsule velocity. The data from this last test are shown by the symbols of the bottom curve in the Figure (Run 1168). The pressure gradient measurements were repeated and then the capsule was removed from the pipeline. The surface of the capsule closest to the pipe wall during these tests had become highly polished and the width of the polished area was about $\frac{1}{2}$ inch. After recalibration of the instruments the capsule was reinserted into the pipeline, but with an unpolished part of the capsule surface nearest to the pipe wall. The capsule pressure gradients were measured as a function of the capsule velocity, and without removing the capsule these measurements were repeated. The data are shown in Fig. 6-3 where the bottom curve represents the highly polished capsule surface and the upper curve represents the capsule after it was reinserted into the pipeline at the new orientation. Both repeat tests are plotted in this Figure. The repeatability of the measurements with the highly polished surface close to the pipe wall was good, but for the tests with the polished surface away from the pipe wall, the repeat measurements (open squares) were lower, showing the effect of polishing after only an hour of capsule movement. (c.f. Runs 1170 and 1171.)

During the experiments the capsule surface was examined each time the capsule was removed from the pipeline and a qualitative correlation was found between the pressure gradients measured and the degree of polishing of the capsule surface in contact with the pipe wall. During these tests the smoothness of the pipe surface was not examined, but it stands to reason that it also became polished with time. Before the tests started the capsule surface was uniformly smooth around its periphery and only one segment $\frac{1}{2}$ in. wide became polished during the tests. The top curve of Fig. 6-2 and the top curve of Fig. 6-3 both

represent unpolished, smooth capsule surfaces near the pipe wall. A comparison of these data shows that the polishing of the butyrate pipe surface for approximately 230 hours of running between the first (Run 1143) and last (Run 1170) experiments which represent similar capsule surfaces has indeed given rise to a lower capsule pressure gradient.

6.7 Lubricated Capsules

The results reported above are for single capsules run in clean water. Fig. 6-4, however, shows results from a carrier liquid which had become contaminated with fungi. The upper curve represents the capsule pressure gradients for a train of four 0.87 diameter ratio stainless steel capsules loaded to a buoyed specific gravity of 2.00 and run in the 4 in. butyrate test section in clean water. The bottom curve is for data from the same capsule train but run in contaminated water. During these tests the pipe surface had become covered with a thin coat of slippery fungi similar to that found on rocks along lakes of stagnant water. As shown by the Figure the effect of a slippery coating is to reduce the capsule pressure gradient very significantly both at incipience and over the whole range of capsule velocities tested.

6.8 Coated Capsules

Reductions in the capsule pressure gradients are also evident when cylindrical steel capsules are wrapped with a plastic tape as shown by Fig. 6-5 (4 in. stainless steel pipeline). The upper curve represents a train of metal cylinders flowing in a metal pipeline, while the bottom curve represents the same capsule train wrapped with plastic tape. Fig. 6-6 (10 in. pipeline) shows the reduction achieved when a single steel capsule (upper curve) was encased in a plastic sleeve (lower curve).

6.9 Discussion

The data show that the coefficient of friction has a pronounced effect on the capsule pressure gradient. The pressure gradients for the stainless steel capsules which were loaded to a buoyed specific gravity of 2.00 and run in clean water, all extrapolate to approximately 0.30 lb./in^2 ft. at zero capsule velocity, in spite of the wide divergence at the higher capsule velocities due to the effect of polishing. This was the value of the capsule pressure gradient at incipient capsule motion predicted from the friction measurements of these capsules as shown in Table 1.

The pressure gradients for the capsules lubricated by the fungi, however, extrapolated to 0.10 lb./in^2 ft. at zero velocity. While the coefficient of friction was not measured for these capsules, the pressure gradient data indicate a change in this coefficient from 0.40 to 0.13 due to the lubricating layer.

The pressure gradients for moving capsules, which vary widely with capsule density, velocity, surface roughness and coefficient of friction, may be regarded as embracing a spectrum of interactions between the pipe surface, the capsule surface and the liquid.

At the one extreme, when the capsule is stationary, at the point of incipient motion, there is solid-solid contact between the capsule and the pipe walls and the theory of friction [5] applies in which the friction force is:

1. equal to the coefficient of friction multiplied by the load perpendicular to the surfaces,
2. independent of the apparent area of contact,
3. generally independent of the roughness of the two surfaces,
4. influenced by the lubricating quality of any oxide coating or contaminating film on the solid surfaces.

At the other extreme, the theory of hydrodynamic lubrication applies when a capsule with a density close to that of the carrier liquid is moving fast through the pipeline and the solid surfaces do not contact but are separated by a thin layer of liquid. The force required to sustain this movement is:

1. directly proportional to the viscosity of the liquid,
2. directly proportional to the velocity of the capsule,
3. inversely proportional to the thickness of the liquid layer,
4. generally independent of the roughness of the pipe or capsule surfaces.

Between these two extremes of complete solid-solid contact and complete hydrodynamic lubrication there is a spectrum of mixed lubrication where both types exist simultaneously. When asperities on the solid surfaces break through the lubricating layer of liquid and rub against each other, the attendant drag due to the local coefficient of friction is very much higher than that due to the shear in hydrodynamic lubrication. As the roughnesses of the

solid surfaces increase, the concentration of local areas of solid-solid friction also increases, raising the overall drag on the capsule and hence the pressure gradient. However, increasing the sliding velocity or decreasing the normal load (capsule density) or the surface roughnesses promotes transition from solid-solid friction to shear and hence lowers the capsule pressure gradient. Therefore any change of the coefficient of friction or the capsule density has a direct bearing upon the capsule pressure gradient at incipience and over the whole range of capsule velocities tested. Generally the surface roughness effect is significant only when the capsule is moving.

6.10 Conclusion

It has been shown that for cylindrical capsules the pressure gradient required to start capsules can be calculated directly from the coefficient of friction. This coefficient may be obtained by measuring the force required to pull the capsules through the liquid-filled pipe. The capsule pressure gradient for moving capsules, however, in addition to being a function of the coefficient of friction is also a function of the capsule velocity and the surface roughnesses of the capsule and pipe walls. A lubricating layer between the capsule and pipe walls reduces the capsule pressure gradient.

References

1. Kruyer, Jan. "Low Pressure Gradients in Capsule Pipelines." Paper F2, Proceedings Hydrotransport 2, BHRA, Coventry, England 1972.

2. Kruyer, Jan. "Capsule Pipelining - Data Acquisition and Control of an Experimental Four-Inch Pipeline." Computers, Electronics Control Show & Symposium, Calgary, Canada 1973.

3. Jonsson, V.K. and Sparrow, E.M. "Experiments on Turbulent-Flow Phenomena in Eccentric Annular Ducts." J. Fluid Mech. (1966), Vol. 25, Part 1, pp. 65-86.

4. Lazarus, J.H. and Kilner, F.A. "Incipient Motion of Solid Capsules in Pipelines." Paper C3 Proceedings Hydrotransport 1, BHRA, Coventry, England, 1970.

5. Rabinowicz, Ernest. "Friction and Wear of Materials." Chapter 4, "Friction". John Wiley & Sons, Inc. New York, 1966.

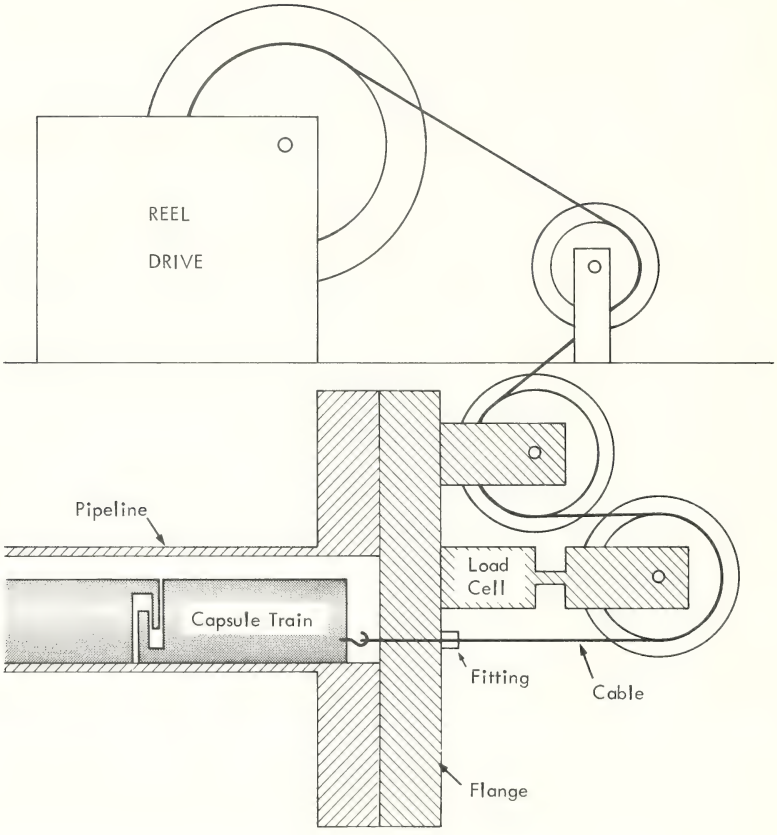

4 INCH PIPELINE

DEVICE FOR PULLING CAPSULES FIG. 6-1

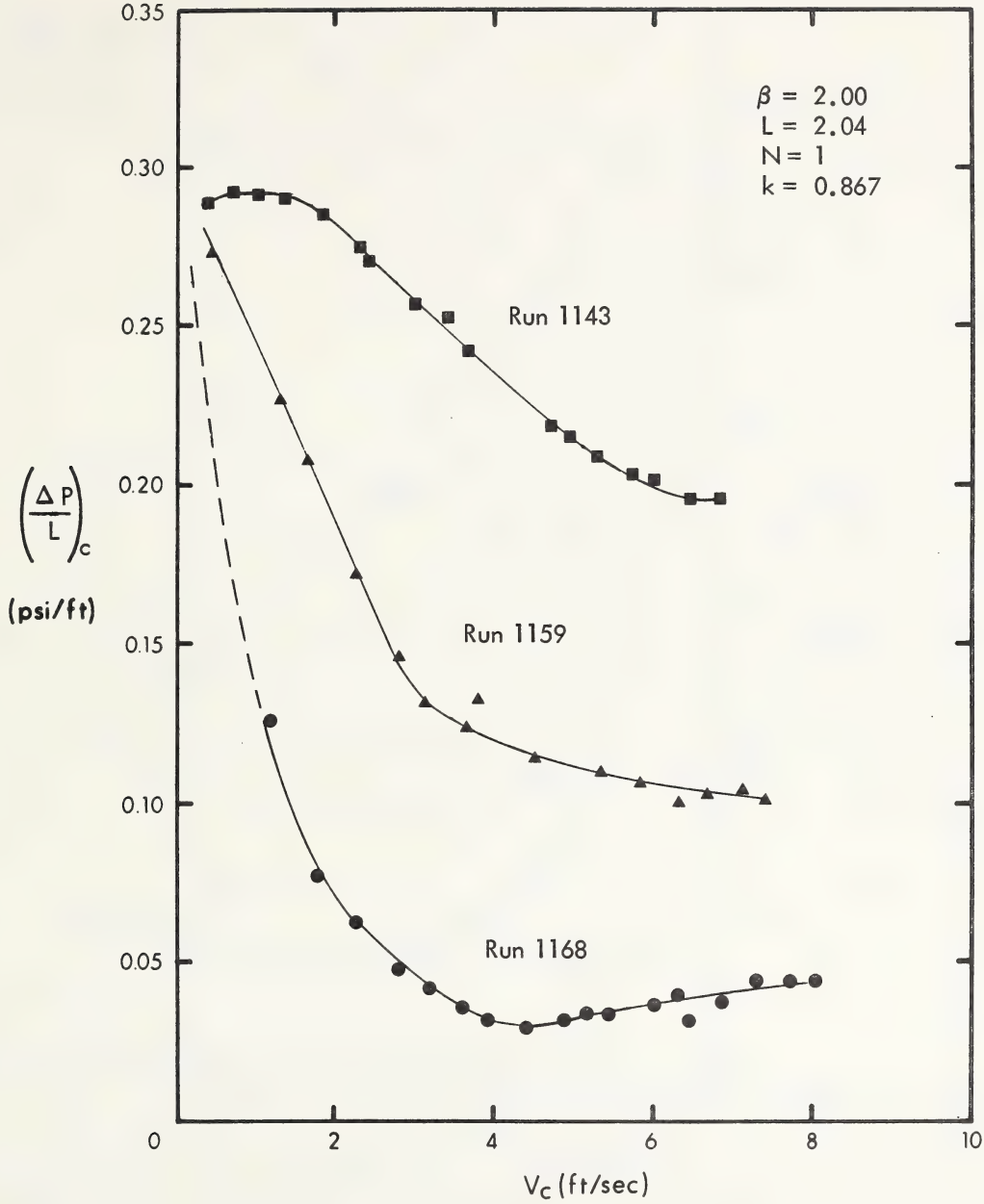

4 INCH BUTYRATE PIPE

PRESSURE GRADIENTS AS THE STEEL CAPSULE WAS RUN FOR EXTENDED PERIODS OF TIME

FIG. 6-2

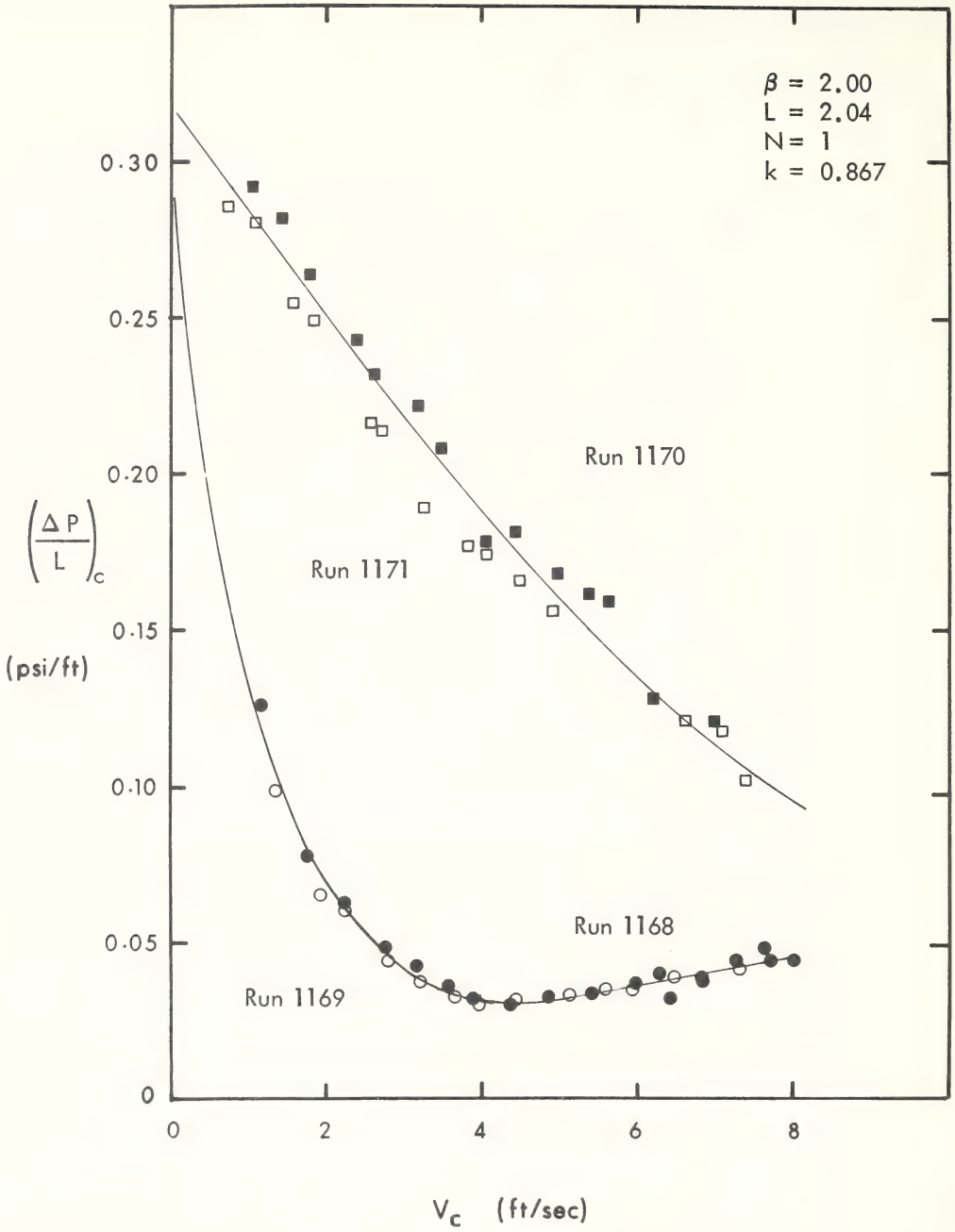

4 INCH BUTYRATE PIPE

PRESSURE GRADIENTS BEFORE AND AFTER ROTATION OF A STEEL CAPSULE (AN EXTENDED PERIOD OF RUNNING PRECEDED RUN 1168)

FIG. 6-3

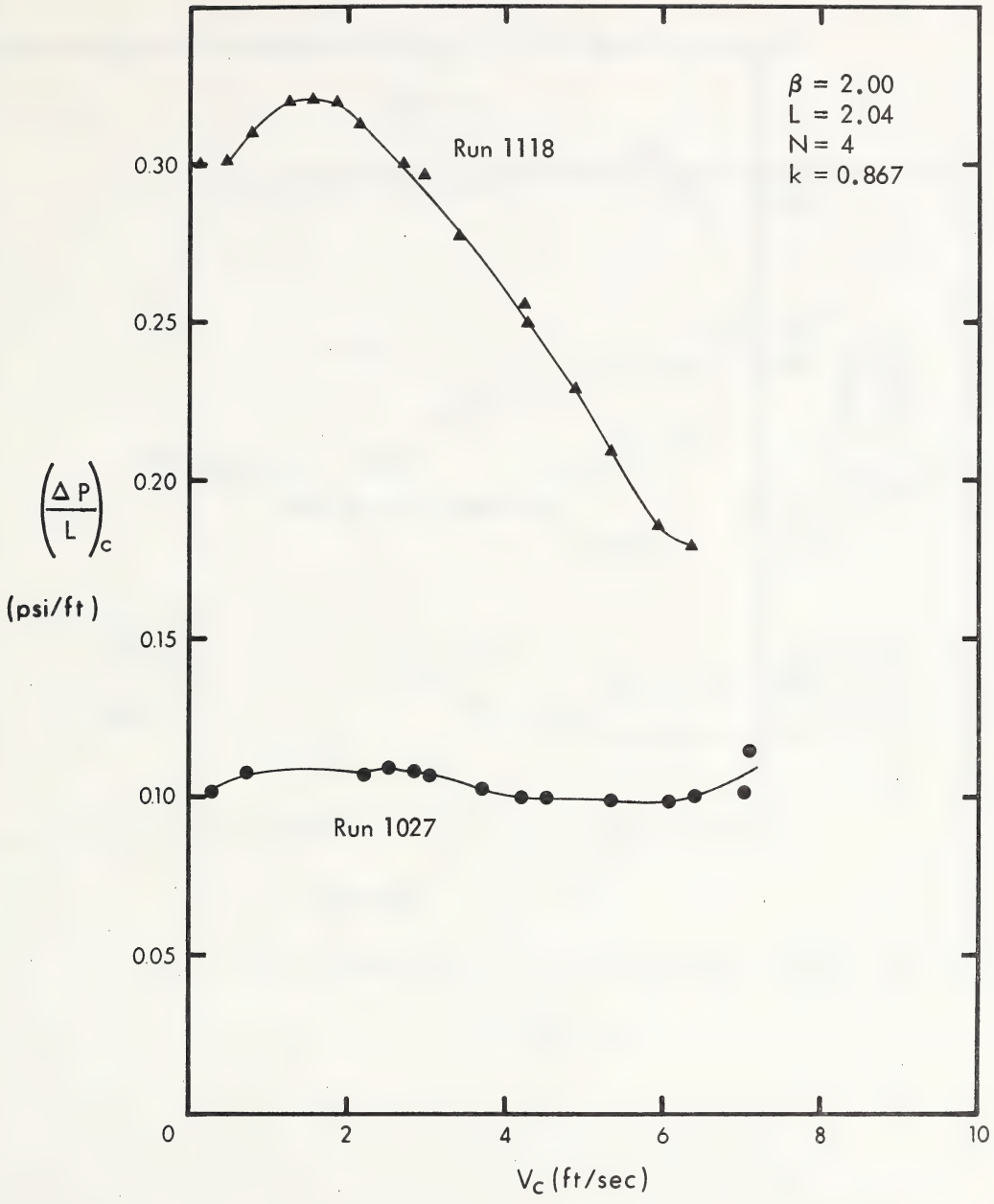

4 INCH BUTYRATE PIPE

PRESSURE GRADIENTS FOR STAINLESS STEEL CAPSULES WITH AND WITHOUT A SLIPPERY COATING

FIG. 6-4

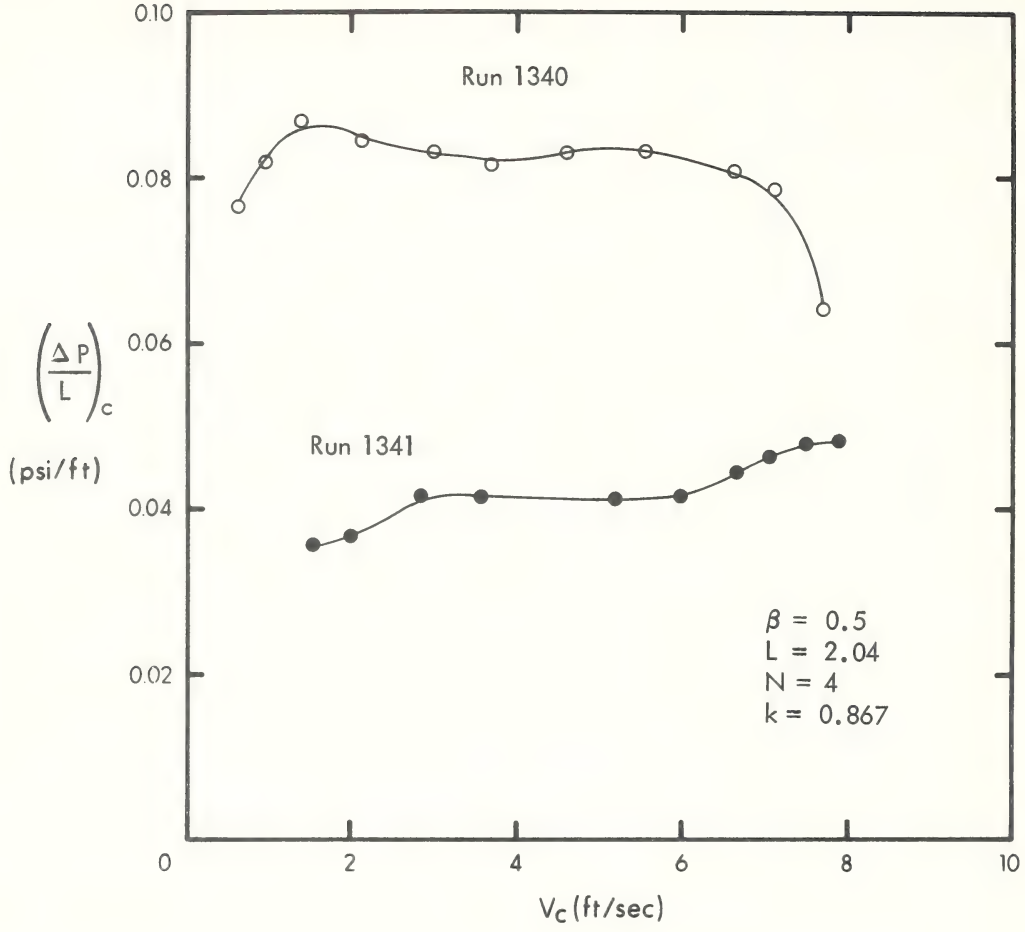

4 INCH STAINLESS STEEL PIPE

PRESSURE GRADIENTS FOR A STEEL CAPSULE WITH AND WITHOUT A COATING OF POLYKEN TAPE

FIG. 6-5

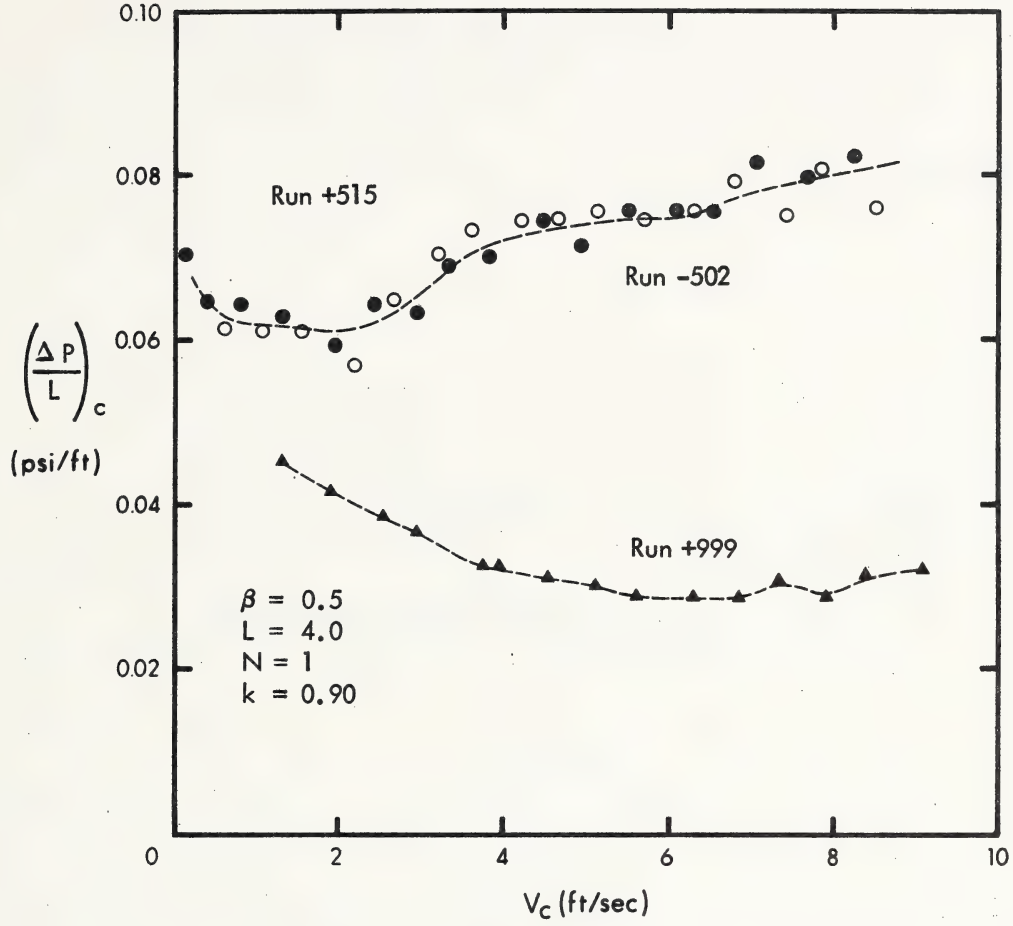

10 INCH PIPELINE

PRESSURE GRADIENTS FOR STEEL CAPSULES WITH AND WITHOUT A COATING OF POLYETHYLENE

FIG. 6-6

CHAPTER VII

Methods of Minimizing Pressure Gradients

CHAPTER VII

Methods of Minimizing Pressure Gradients

Summary

Low pressure gradients are a necessity for viable capsule pipelining. In this chapter some means of achieving this end are discussed. By careful selection from different pressure-reducing methods it is possible to minimize the power requirements of capsules. Lowering the specific gravity of cylinders by creating sealed voids would yield pressure gradients only slightly above, or even below, those of the transporting liquid alone.

7.1 Friction reduction

Figure 6-4 (reproduced as Fig. 7-1) illustrated the reduction of pressure gradient due to a lubricating layer between the capsules and pipe, and Figs. 6-5 and 6-6 (Figs. 7-2 and 7-3) showed the effect of a coating of plastic applied to the capsules in the 4 inch and 10-inch pipelines respectively. The substantial reductions of pressure gradient indicate the need for further experimentation on means to reduce friction between the capsules and the pipe.

7.2 Spherical Capsules

Chapter 4 showed that the pressure gradients for spherical capsules are very much lower than for cylindrical capsules at specific gravities over about 1.25. In addition, spheres are easier to insert into the pipeline and to recover from it, and the bypassing of pumps is also easier. Experimentation to determine the effect of out-of-roundness and surface irregularities on the pressure gradient is needed, as is development work on the manufacture, injection and bypassing of large cohesive spheres.

7.3 Collared Capsules

A method of pressure reduction for cylinders which has been used with excellent results [1] is the fitting of a band or collar located slightly forward of the centre of the capsule. It has been shown [2] that for laminar flow in the capsule-pipe annulus the clearance between the capsule and the bottom of the pipe is one of the

major parameters influencing the capsule velocity and pressure gradient, and there is little doubt that this is also true for turbulent flow. The most effective way of increasing the clearance so far tested is the fitting of a collar. If this is fitted to the leading half of the capsule it holds the capsule at a minimum angle to the pipe and increases the buoyant force by increasing the pressure of the liquid under the capsule and by providing an upward shear on the leading half.

Figure 7-4 allows comparison of the pressure gradients in the four-inch stainless steel pipe due to stainless steel capsules, butyrate capsules and capsules with a collar. The curve of Fig. 4-3 for spheres is shown dashed. All the pressure gradients have been related to the pipe diameter and the diameter ratio as in Chapter IV to allow comparison of data from different diameter ratios and from the four-inch and ten-inch pipes. The upper two curves (runs 1218 and 1340) refer to trains of stainless steel capsules. The reduction in pressure gradient in run 1340 compared with run 1218 is due to the polishing of the pipe and capsules during the intervening 121 runs. Run 1484 is a train of butyrate capsules in the same stainless steel pipe; the pressure gradients are very similar to those of the taped capsules, run 1341, of Fig. 7-2. The lowest curve, run 1469, is for a train of capsules provided with collars by wrapping them with vinyl tape, 0.015 inches thick, 4 inches wide. One wrap was made at the back of the capsules and seven with the back edge of the tape 8 inches from the front of the $24\frac{1}{2}$ inch capsules. In this way a collar about 0.105 inches thick X 4 inches wide was formed, and the back of the capsule also rested on a vinyl surface. Several thicknesses of collar were tested and the best results were obtained from this collar with the greatest number of wraps. The pressure gradients required by this train of capsules are remarkably low when compared with those of the other trains.

Figure 7-5 compares the pressure gradients measured in the ten-inch pipe for a train of loaded steel cylinders, for the single cylinder with a polyethylene sleeve of Fig. 7-3 and for a train of capsules with collars. The data for the sleeve refer to a single capsule, but the effect on the pressure gradient of the number of capsules in a train was always very small. The collars were formed in the same way as for the four-inch pipe cylinders by wrapping them with several layers of vinyl tape. Different widths and numbers of wraps were applied at varying distances from the front of the 9-inch diameter capsules. The thickness, width and location of the collar were not at all critical, but the 1/8 inch thick X 4 inch wide

collars with their rear edges 16 inches from the front of the 48 inch capsules gave the best results; the data for these are plotted in the Figure.

Comparison of Figs. 7-4 and 7-5 shows that the collared capsules in the four-inch and ten-inch lines gave similar pressure gradients when related to the pipe diameter, and those for the butyrate and taped capsules in the four-inch pipe, e.g. run 1484, are similar to those for the vinyl-sleeved capsule in the ten-inch pipe, again related to the pipe diameter.

The results of the tests of collared capsules in both the four-inch and ten-inch pipes reinforce previous findings that pressure gradients can be reduced by up to 80% by the use of collars.

7.4 Capsules Containing Voids

It has been noted in earlier chapters that the pressure gradients of capsules of low buoyed specific gravity are often less than those of the conveying liquid alone; this is due to at least some suppression of turbulence in the capsule-pipe annulus. Figs. 7-6 and 7-7 illustrate the phenomenon for trains of cylinders of $\beta = 0.031$ in the half-inch and four-inch pipes. In the ten-inch pipe no trains of capsules gave pressure gradients less than those of the water, but data for a single capsule of the same specific gravity as the water is illustrated in Fig. 7-8.

Friction-reducing surfaces in the ten-inch line would probably allow trains of low specific gravity to be transported at or below the pressure gradient of the liquid, since turbulence is greater than in a smaller pipe and partial suppression of turbulence should be more effective in reducing the pressure gradient.

The low pressure gradients of capsules of low specific gravity suggest manufacturing capsules with voids (air pockets). For example, Fig. 7-9 is a plot of horsepower per mile versus solid throughput in millions of tons per year. The following expressions were used for the Figure:

$$\left(\begin{array}{c}\text{Horsepower/mile of capsules}\\ \text{and annular liquid}\end{array}\right) = \frac{(\Delta P/L)_c \times 5280\,(\pi D^2/4)\,V_b}{550}$$

$$= \underline{7.54\,(\Delta P/L)_c\,D^2\,V_b}$$

$$\text{Solid throughput (millions of tons/year)} = \frac{(\pi d^2/4)\, V_c\, \sigma \times 3600 \times 24 \times 365}{144 \times 2000 \times 10^6}$$

$$= 8.60 \times 10^{-5}\, d^2\, V_c\, \sigma$$

The data of the upper curve show the performance of a train of loaded steel capsules of specific gravity 1.50 in the ten-inch pipe. The data may be considered representative of capsules with a steel surface enclosing material of specific gravity 1.50 and transported through a ten-inch steel pipe.

If a third of the hypothetical material were extracted from each capsule the specific gravity would be reduced to 1.00, neglecting the weight of the shells. Such capsules would have a performance curve like the lower curve of Fig. 7-9. This is in fact a plot of data from a train of specific gravity 1.031, and capsules of specific gravity 0.98 gave very similar results. It would be difficult to manufacture capsules of exactly the specific gravity of the liquid so that a range of capsule densities from about 61 to 64 lb./ft.^{3} has been included in the example. The curve for water is also shown. Though the capsules require about twice the power of water alone it will be remembered that they were steel-shelled in a steel pipe. In view of the pressure gradient reductions achieved with smooth capsule and pipe coatings there is little doubt that the power requirements could be still further reduced by the use of smooth capsule and/or pipe coatings.

The very great power saving indicated for the same throughput of solid material suggests that this technique must be carefully considered in suitable cases. For example, it seems particularly applicable to materials which could be cast into cylinders, such as sulphur (e.g. by foaming the liquified material). Containerization (a large shell packed with smaller containers) suggests another type of application.

7.5 Conclusions

If material with a specific gravity greater than 1.25 can be readily formed into strong cohesive spheres rather than cylinders a great saving of power will result from their use (see Chapter 4). If it is decided to use cylindrical forms, substantial pressure gradient reduction is possible by one or a combination of the following methods:

(1) Reduction of the coefficient of friction by applying a low-friction coating to the capsule and/or pipe, or by cultivation of a biological slime.

(2) The use of smooth capsule and pipe surfaces.

(3) Fitting the capsules with collars. This is the most effective way of reducing the power required for the transport of cylinders other than method (4).

(4) Manufacturing the capsules with voids. This can reduce the power requirements by an order of magnitude.

References

1. Ellis, H.S. and Kruyer, J. "Some Effects of Fitting Cylindrical Pipeline Capsules with Collars or Runners." Hydrotransport 2, BHRA Fluid Eng., Cranfield, Bedford, England (1972).

2. Kruyer, J., Redberger, P.J. and Ellis, H.S. The Pipeline Flow of Capsules, Part 9. J. Fluid Mech. 30, 3, 513-531 (1967).

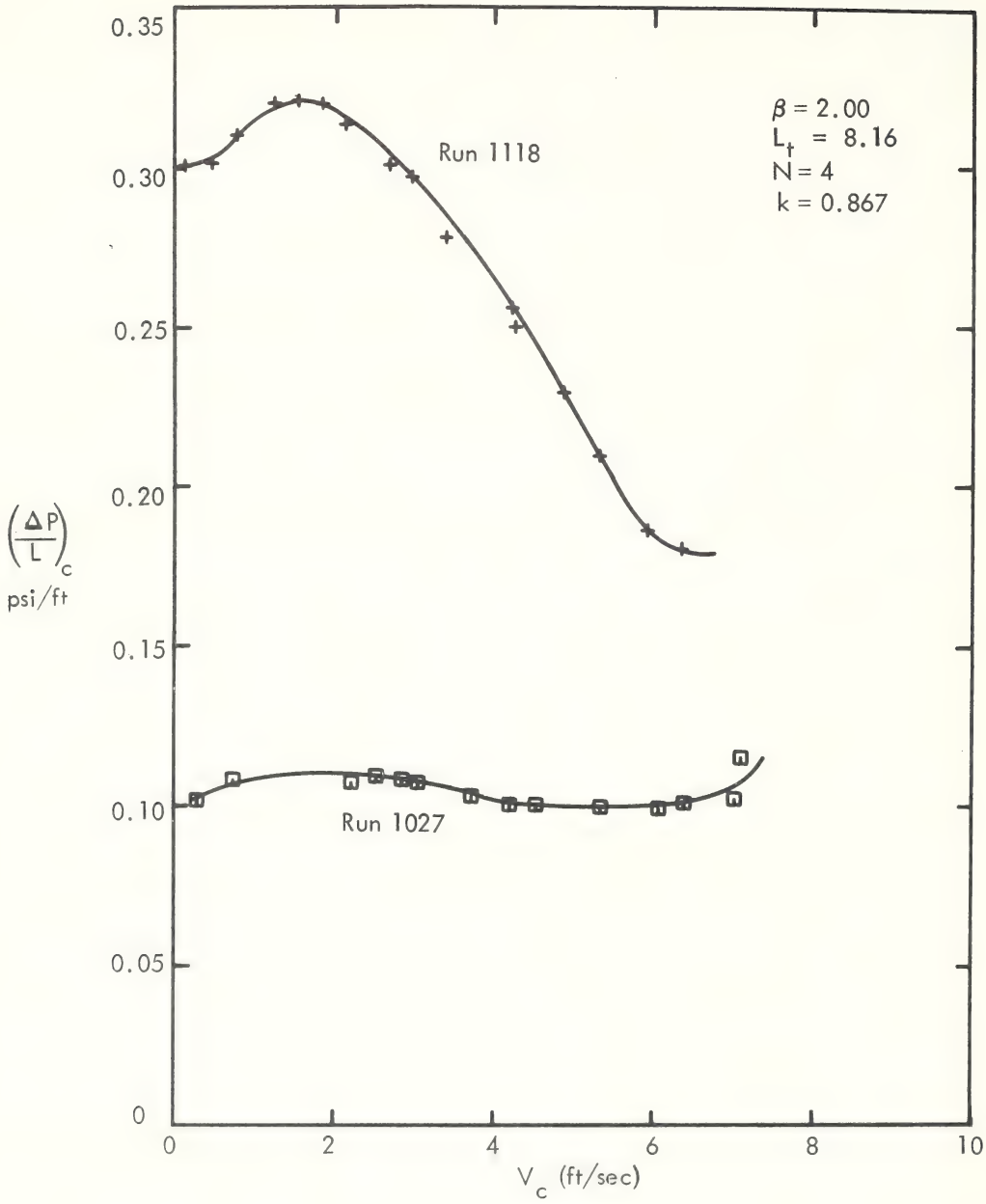

4 INCH PIPE
PRESSURE GRADIENTS FOR SOLID SURFACES WITH AND WITHOUT A SLIPPERY COATING

FIGURE 7-1

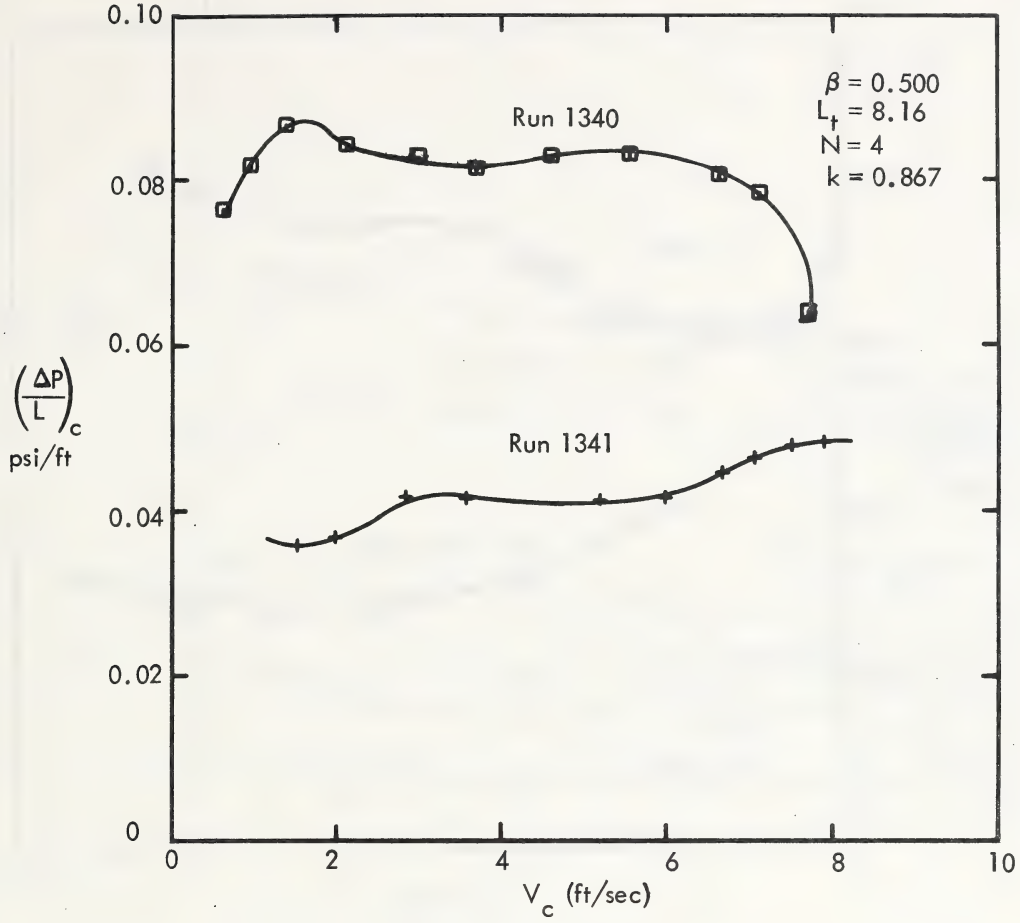

4 INCH PIPE
PRESSURE GRADIENTS FOR CAPSULES WITH AND WITHOUT A COATING OF POLYKEN TAPE

FIGURE 7 - 2

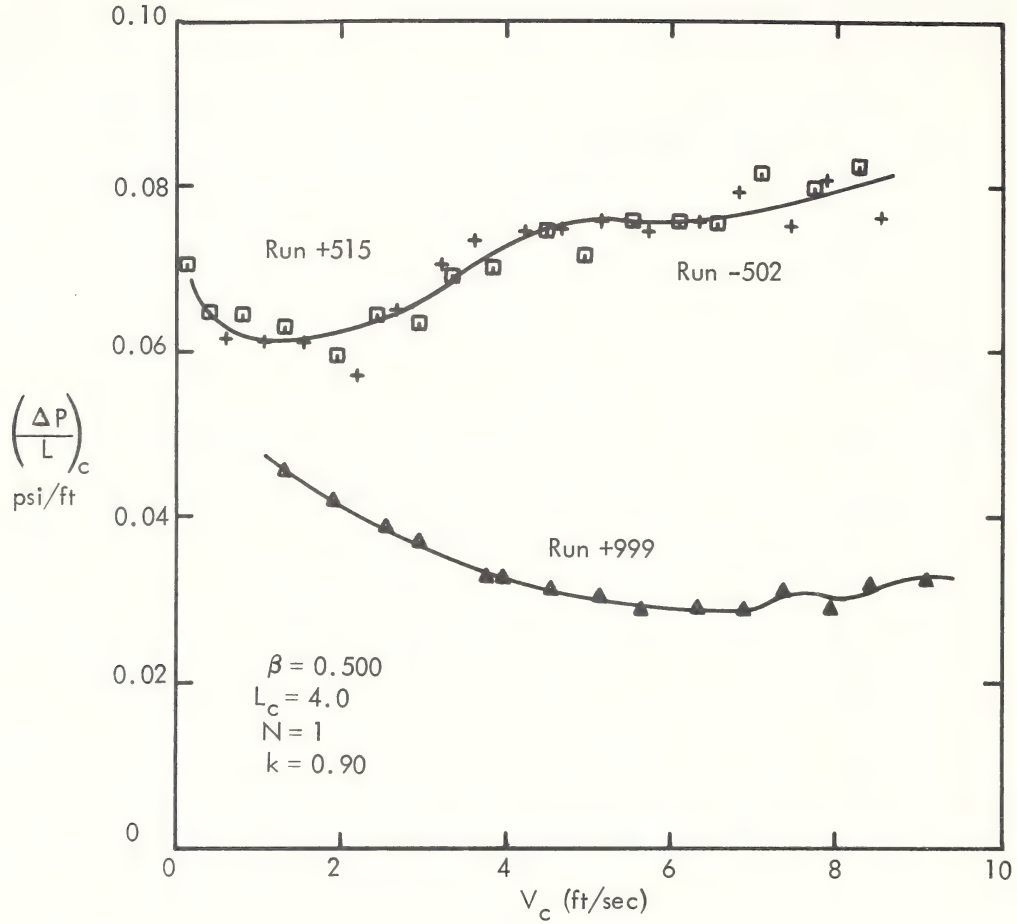

10 INCH PIPE
PRESSURE GRADIENTS FOR CAPSULES WITH AND WITHOUT A COATING OF POLYETHELENE

FIGURE 7-3

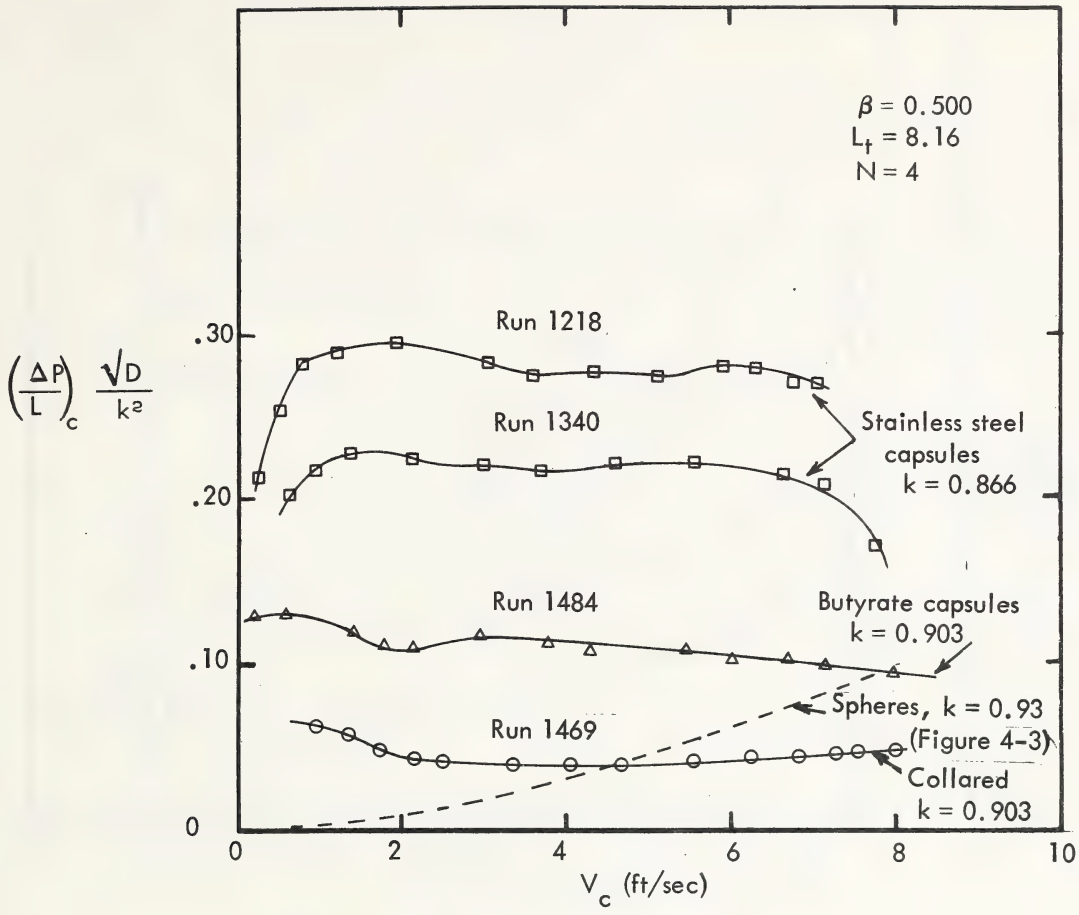

4 INCH PIPE
PRESSURE REDUCTION BY SMOOTH SURFACES AND BY COLLARS

FIGURE 7-4

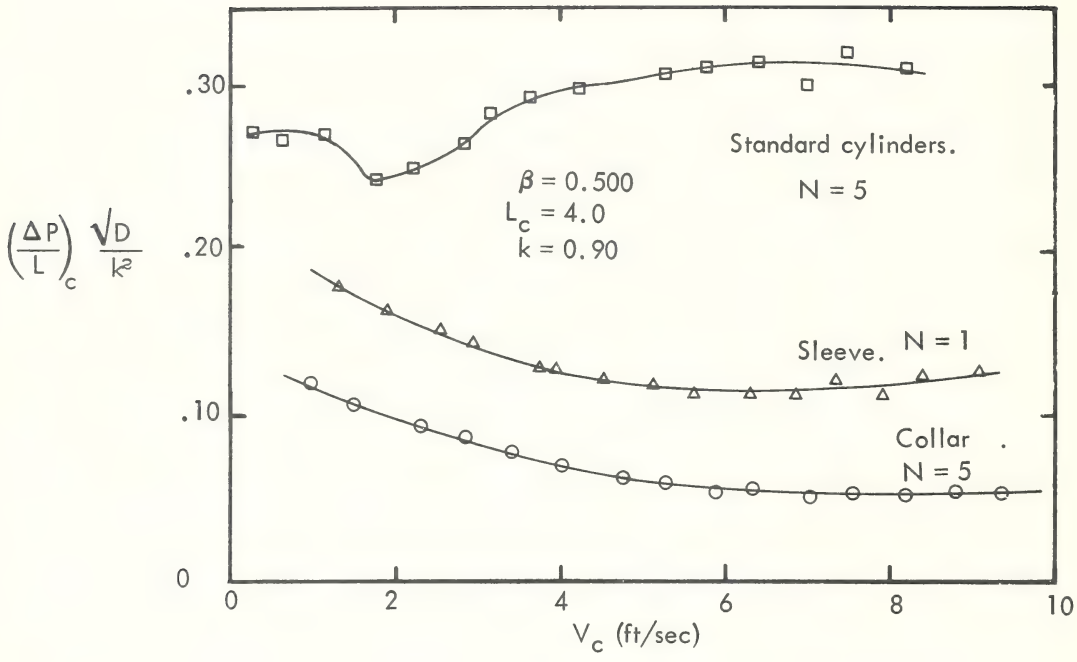

10 INCH PIPE
PRESSURE REDUCTION BY A POLYETHELENE SLEEVE AND BY COLLARS

FIGURE 7-5

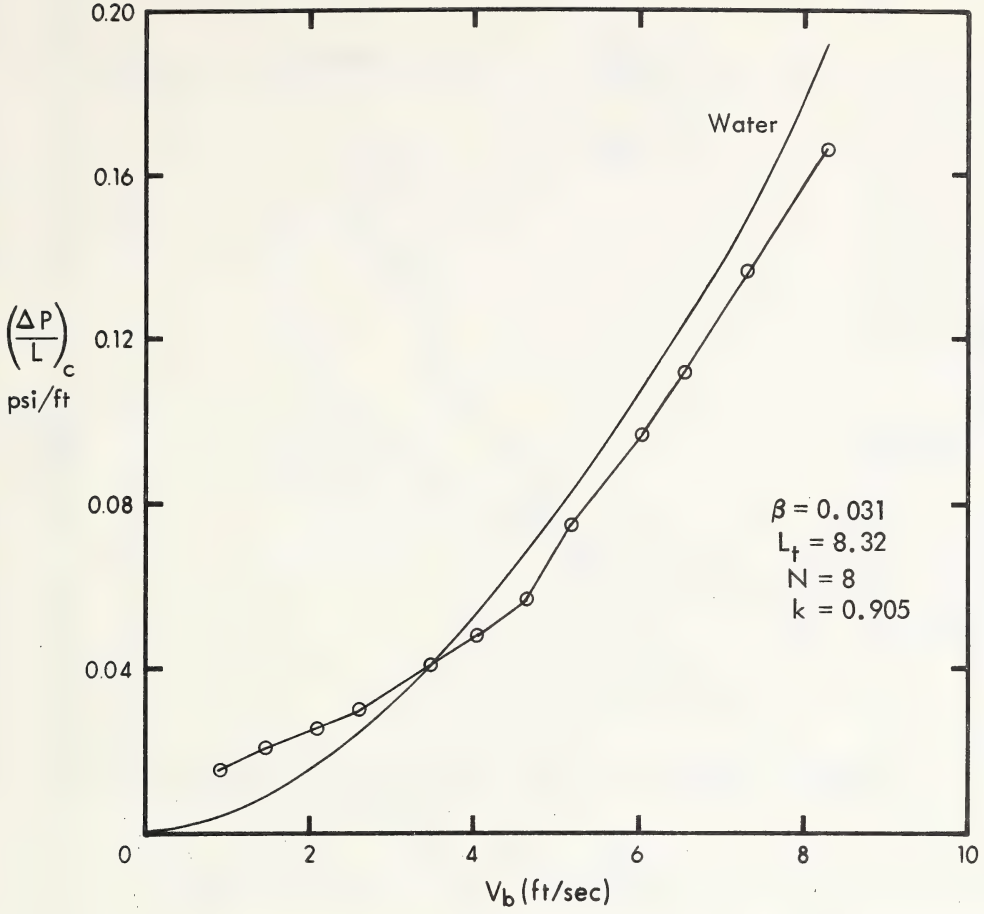

$\frac{1}{2}$ INCH PIPE
SUPPRESSION OF TURBULENCE RESULTING IN PRESSURE GRADIENTS BELOW THOSE OF THE LIQUID

FIGURE 7-6

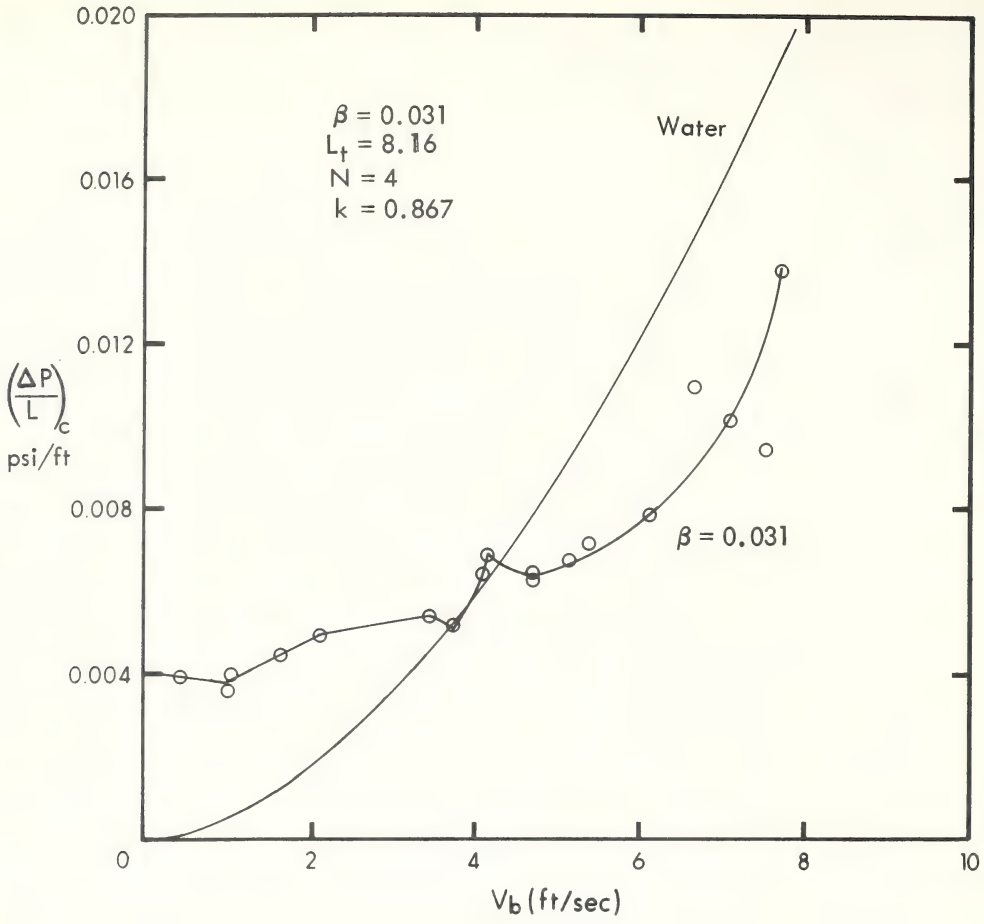

4 INCH PIPE
SUPPRESSION OF TURBULENCE RESULTING IN PRESSURE GRADIENTS BELOW THOSE OF THE LIQUID

FIGURE 7-7

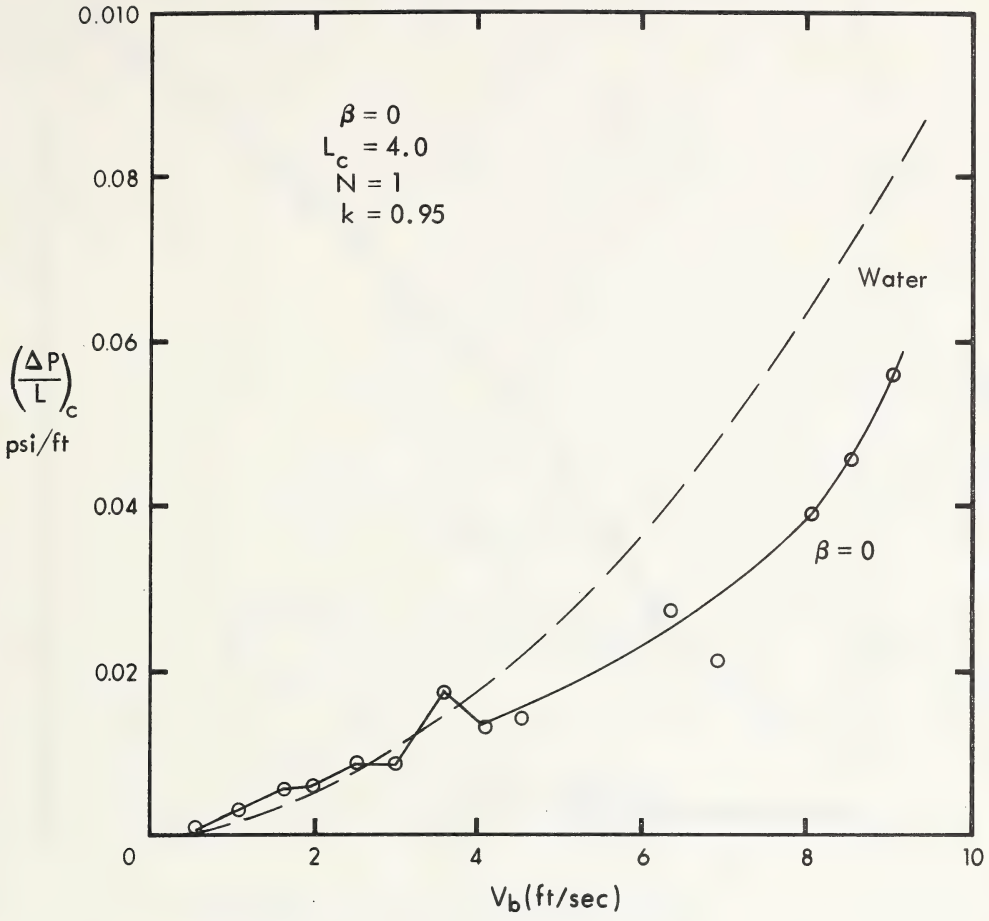

10 INCH PIPE
SUPPRESSION OF TURBULENCE RESULTING IN PRESSURE GRADIENTS BELOW THOSE OF THE LIQUID

FIGURE 7-8

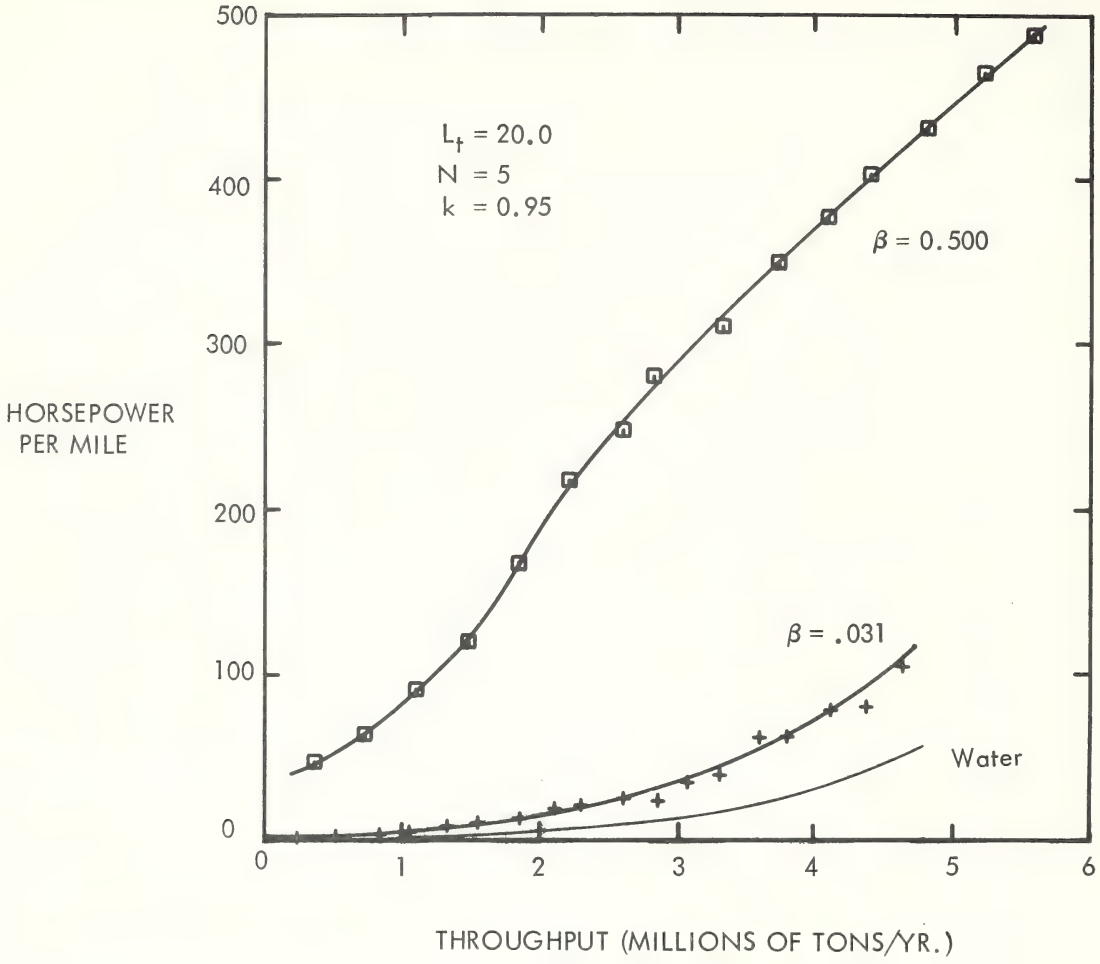

10 INCH PIPE
POWER SAVED BY THE USE OF VOIDS

FIGURE 7-9

CHAPTER VIII

Further Work Required

CHAPTER VIII

Further Work Required

Summary

The work is divided into that planned for the remainder of the project and that which it is already clear will be needed in certain vital areas after the completion of the project.

8.1 Work planned for the remainder of the project.

It has now been shown that there is a very definite relationship between the capsule pressure gradient, capsule velocity and liquid velocity from which one of these can be predicted from the other two. Work is planned in a two inch pipeline to further confirm the validity of the relationship. Work with liquids of various viscosities will be continued in the four-inch pipeline with the same object and to pinpoint more precisely the critical Reynolds number where the flow in the annulus changes from laminar to turbulent. Additional measurements will also be made in the ten-inch pipeline at an elevated temperature in order to confirm the above model at lower viscosities in this pipeline.

It has been shown that for cylinders, the capsule pressure gradient is affected by three definite influences: the roughness of the surfaces, the coefficient of friction between the surfaces and the distortion of the velocity profile of the liquid. Experimental and theoretical work will be done to probe deeper into the effect of each. For example, different capsule surfaces will be tested. The study of the relationship between capsule density and pressure gradient is also part of this effort.

The goal of the project is the prediction of the power requirements, the pressure gradients and the velocities in capsule pipelines. Much of the remaining time will be spent on correlating the experimental data with a view to meeting this requirement and to developing simple methods of determining the hydrodynamics of commercial capsule pipelines. It has already been shown that the results are very dependent upon the types of materials and pipe used and the verified correlation will thus be limited to those materials that have been tested.

Looking ahead and comparing the work which Phase II has shown to be necessary with that scheduled for the remainder of the project, it is clear already that certain vital areas will need further work after the completion of the present project.

8.2 Friction testing and reduction

The relationship between friction, capsule pressure gradient and annular velocity developed in Chapter VI points to the need for quantitative measurements of friction in pipes of various surfaces for commercial commodities. The testing of surface coatings for encapsulated cylinders with various pipe surfaces will also be required. Surface roughness reduction has been shown to be a most important tool in minimizing pressure gradients; a detailed survey of the cost of smoothing pipe and capsule surfaces is therefore required.

8.3 Spherical Capsules

In view of the low power requirements of spheres compared with those of the smoothest cylinders (see Chapter IV), spherical capsules would have to receive the first consideration for transporting all but the lightest materials. Research on the manufacture, injection and by-passing of large strong spheres deserves high priority. Serious efforts should be made to design a "straight through" pump for spheres, and attention should be given to determining the effect on the power requirements of surface irregularities.

8.4 Cylindrical Capsules containing voids.

The remarkable reduction of power requirements made possible by the use of voids (Chapter VII) calls for investigation of the manufacturing possibilities for voided cylindrical capsules of sufficient mechanical strength and pressure resistance. This is a facet of the general need to undertake research on the rapid production of capsules. It seems likely that it would only be economical to transport large capsules, for example, of beneficiated ores if they could be produced in spherical or voided cylindrical forms.

8.5 Injection and bypassing of capsules

The success or failure of capsule pipelining, in the last analysis, will depend upon the ability to inject and - in the case of long distance transportation - bypass both cylindrical and spherical capsules in a commercial setting. Considerable development work still has to be done in these areas.

CAPSULE PIPELINING -

Data Acquisition and Control of an Experimental Four-Inch Pipeline

VII–4

Jan Kruyer
Research Council of Alberta
Contribution No. 606

ABSTRACT

In 1971 a contract was signed between the Canadian Federal Ministry of Transport and the Research Council of Alberta, covering a three-year period beginning January 1, 1971, and stipulating a hydrodynamic study of capsule pipelining to provide reliable information for assessing the economics of commercially sized capsule pipelines. Since the experimental program associated with this study requires the collection and processing of a large amount of experimental data, the decision was made at the outset to use computers, where possible, for data acquisition and control.

The present paper describes a 4-inch I.D. automated experimental pipeline used in the study. A small computer was used for acquisition of the experimental data and for control of the pipeline. For data acquisition, the analog signals from transducers on the pipeline were converted to frequencies which were read by the computer program. This method, which used voltage to frequency converters, enabled highly accurate measurements to be taken. Control of the electrically operated pipeline valves and pumps was maintained by the computer program using registers in the computer interface.

The pipeline has yielded a vast amount of accurate experimental data, and the time and expense involved to set up this fully automated system is felt to be well justified.

INTRODUCTION

Capsule pipelining is a potential method for the long-distance movement of solids whereby the solids are carried in the pipeline in the form of a long train of cylinders or spheres with diameters approaching that of the pipeline. Increasing demands for economical freight transport have led to tests of the pipeline flow of such trains of capsules which may consist of rigid slugs, flexible bodies of coherent paste, or enclosed commodities, and are carried along by the flowing liquid. The concept was introduced by Hodgson and Charles [1961, ref. 1] and many other papers concerning capsule pipelining have subsequently appeared in the literature [e.g. ref. 2 to 13].

In 1971 a contract was signed between the Canadian Federal Ministry of Transport through the Transportation Development Agency and the Research Council of Alberta. It covers a three-year period beginning January 1, 1971, and stipulates a hydrodynamic study of capsule pipelining to produce information whereby reliable judgment can be made of the economics of capsule pipelining in commercial sized pipelines.

Since the experimental program associated with the study required the collection and assimilation of a great amount of experimental data, the decision was made at the outset to use computers, where possible, for acquisition of the experimental data and for control of the pipelines. This provided a means of obtaining the most reliable data in the shortest possible time, and thus it was anticipated that a large number of experimental measurements could be accommodated economically within the required three years of the contract.

The present paper describes the methods used to measure capsule flow variables and to control a 4-inch experimental pipeline.

PARAMETERS AND VARIABLES

The parameters selected in the experimental capsule pipeline study were:

1. Pipe diameter
2. Capsule diameter
3. Length of the individual capsules
4. Number of capsules in a train
5. Capsule specific gravity
6. Capsule shape (sphere, cylinder, etc.)
7. Viscosity and specific gravity of the carrier liquid as a function of temperature (liquid properties)
8. Flow valve adjustment.

The variables measured during the study were:

1. Bulk velocity of the carrier liquid
2. Capsule velocity

3. Pipeline pressure gradient for liquid only (liquid pressure gradient)
4. Pipeline pressure gradient for capsules and liquid
5. Inlet and outlet temperature of the pipeline liquid.

The pressure gradient for capsules only (capsule pressure gradient) was calculated from both the pressure gradient for capsules plus liquid and the pressure gradient for liquid only. [Ref. 11 gives details for this calculation.] The liquid viscosity and specific gravity were calculated from the liquid properties and the average pipeline liquid temperature. Figures 1 to 3 show some typical results for a train of four 3-5/8 inch diameter 1.25 specific gravity capsules flowing in water in a 4.016-inch pipeline. Figure 1 shows the capsule velocity as a function of the bulk velocity of the carrier liquid.

The threshold liquid velocity, which all capsules require before they start to move, is a function of the buoyed capsule density. When moving slowly the capsules flow at a lower velocity than the bulk velocity of the carrier liquid, but the capsule velocity increases faster than the bulk velocity so that at the high velocities the capsules move faster than the carrier liquid.

Figure 2 shows the liquid pressure gradient (0) and the capsule pressure gradient (Δ) both as a function of the bulk velocity.

All capsules require a threshold pressure gradient before they start to move. When moving at low velocities the capsule pressure gradient is higher than the liquid pressure gradient. The capsule pressure gradient, however, does not increase nearly as quickly with higher bulk velocities as does the liquid pressure gradient. Instead, as the bulk velocity increases the capsule pressure gradient may decrease before starting to slowly increase. In some cases the capsule pressure gradient may even be less than the corresponding liquid pressure gradient at the same bulk velocity. A more detailed discussion of this phenomenon is presented in reference 11.

Figure 3 shows the liquid viscosity. Since in the experimental runs the bulk velocity was varied gradually from high to low, this last Figure gives an indication of the variation of the liquid viscosity due to changes in the liquid temperature as the experiment progressed.

The above results are representative of the more than 52,000 lines of experimental data obtained so far from the 4-inch laboratory capsule pipeline.

THE PIPELINE

Figure 4 is a schematic representation of the laboratory shuttle pipeline which was straight and level and allowed the shuttling back and forth of long, large-diameter ratio capsules.

The pipeline consisted of four lengths of pipe, each approximately 20 ft. long, joined by flanges. A brass ring, inserted in each flange concentric with the bore of the pipe, eliminated step changes in the internal diameter of the pipe at the joints (Figure 5). Smooth transparent cellulose acetate butyrate (C.A.B.) pipe of schedule 40 size was used because of its high impact strength and since it was the only pipe of standard size readily available which allowed the observation of capsule behavior. Schedule 40 was selected to facilitate the manufacture of test sections of other materials in this standard size without changing appreciably the internal pipe diameter. The C.A.B. pipeline was laid on a continuous mahogany cradle, supported linearly every two feet by an angle iron frame (Figure 6). A walk, supported by the structural columns of the pilot plant building, was built along the pipeline for ease of servicing. Fibreglass fittings and pipe were used for the return lines. Three centrifugal pumps, each producing a flow of 100 USGPM at 55 psi, were connected in parallel to provide a maximum flow of 300 USGPM representing a liquid velocity of about 8 ft./sec. in the pipeline. Lower velocities were obtained by throttling the flow with valves V_6 and V_7 and by turning off one or two of the pumps when the throttling caused pressures in the pipeline in excess of 55 psi. A four-way valve (V_1) determined the direction of liquid flow. A removable C.A.B. or stainless steel test section, 20 ft. long and with an internal diameter which varied from 4.02 to 4.03 inches, was mounted in the pipeline.

A tank, attached to the pipe at one end, allowed for the opening of the pipeline by removing the end cap, and for the inserting of capsules into the pipe section between the liquid inlets from valves 2 and 3. After replacing the end cap and turning on the pumps, with valve 2 closed and valve 3 open, the capsules remained stationary while the liquid reached its steady state velocity as it flowed into the pipeline through valve 3. By closing valve 3 and opening valve 2, the capsules were injected into the flowing liquid and very quickly gathered momentum. Only a short distance of travel was needed for acceleration, so that when measurements were taken as the capsules travelled through the test section in the forward direction, the system was operating under steady state conditions. The liquid temperature was maintained at 60°F by the use of a $7\frac{1}{2}$ ton cooling unit connected to a heat exchanger in the capsule insertion tank. A portion of the pipeline liquid stream circulated from the pumps through this tank and thus controlled the temperature of the liquid in the pipeline to within 2°F. Pressure-sensitivity safety switches mounted at several points in the pipeline turned off all the pumps when pressures exceeded 60 psi. Two safety photocells (S in Figure 4) also turned off all the pumps before capsules approached the pipe ends too closely and thus prevented pressure shock waves and possible pipe rupture.

THE CAPSULES

Stainless steel and C.A.B. tubes, provided with endcaps of polyvinyl chloride and sealed with O-rings, were used as

the cylindrical capsules (Figure 7). Their specific gravities were varied by loading them with steel rods which fitted tightly between the endcaps. Capsule lengths were kept constant to within 0.05 inch, and maximum variation in diameter was less than 0.03 inch. Capsules volumes were determined from the capsule weight in air and in water to an accuracy of 0.2 percent, while the capsule weights were adjusted to the selected specific gravities to within 0.5 percent. After loading, a vacuum was applied momentarily to the capsules through a special fitting in order to keep the caps on the tubes while in the pipeline.

Specially machined PVC spheres (Figure 8), consisting of PVC hemispheres which fitted together and could be loaded uniformly to various specific gravities, were used for the spherical capsules.

VARIABLES MEASURED

A PDP-8-S [ref. 13] mini-computer was used for acquisition and partial processing of the data and for control of the pipeline.

Figure 9 is a flow diagram showing how the measured variables entered the computer, how the pipeline pumps and valves were controlled, and how the data were recorded. The numbers near the top of the figure indicate how many channels were used to record each of the variables.

Temperatures were measured at the pipe inlet and outlet by two linear thermistors [ref. 16], (Figure 4, T_i, T_o), each excited by a regulated 1.500 volt supply and providing D.C. voltages proportional to the liquid temperatures. These voltages were converted to proportional frequencies for reading by the computer.

Pressure differentials along the pipeline were measured between taps I and IV with transducers of two ranges, one calibrated from 0 to 25 inches of water differential and the other from 0 to 100 inches. The pressure taps in the C.A.B. pipe wall (Figure 10) were made by glueing C.A.B. blocks to the outside of the pipe and drilling these to provide 1/16 inch holes through the pipe wall. These holes were carefully deburred at the inner pipe wall and small vessels were attached to the blocks to remove entrapped air and to make pressure connections with the transducers. Similar taps of a somewhat modified design were used for the stainless steel test section. The transducers, which were excited by a regulated 5.000 volt D.C. supply, provided output voltages directly proportional to the pressure differentials imposed on them. The voltages from the transducers were also converted to proportional frequencies for reading by the computer. In addition, the voltage from the high range transducer was displayed on an oscilloscope with a long retention phosphor screen to allow monitoring of the pressure differential. Both transducers were used simultaneously and, since they covered different pressure ranges, this allowed the selection of the most accurate reading after the data were collected.

A crystal oscillator was used for recording time, and photocells [ref. 17, 18, 19] were used to detect the capsule train. As illustrated in Figure 11, laser beams passing through the C.A.B. pipe wall illuminated each photocell. Lights and optical glass windows were used for the stainless steel test section. When a light beam was interrupted by the capsule train moving in the pipeline, an electrical pulse issued from the disturbed photocell. The photocell pulses were used by the computer for timing of the capsule movement and control of the pipeline.

A 3-inch I.D. magnetic flowmeter was used for measuring liquid flow into the pipeline. This device, being insensitive to changes in liquid viscosity, generated a frequency which was proportional to the liquid bulk velocity.

DATA ACQUISITION

The computer interface consisted of eight 12-bit binary counters, a 9-bit photocell sensing register, and a 24-bit set-reset register [ref. 15] for control of the pipeline valves and pumps.

The experimental variables such as the liquid temperatures and the pressure gradients were each converted to proportional frequencies by means of voltage to frequency converters [ref. 20], and these frequency pulses were accumulated by the binary counters. The photocell pulses were recognized by the sensing register so that under program control the counters were read when the photocells pulsed. Micro-instructions assigned to stop (IOT 1), read (IOT 2), and start the counters (IOT 4) facilitated reading them at any instant without having to synchronize the counter pulses with the computer. This was done by combining all three micro-instructions into one (IOT 7) instruction. A computer with 1 μ second between micro-instructions, sampling a 10,000-Hz signal this way ten times per second, loses on the average 0.02 count pulses per reading, which is negligible in this case. An overflow indicator (flag) in each counter interface permitted the use of the computer memory to expand the capacity of each counter.

The use of voltage to frequency converters connected to binary counters in the computer interface provided an effective method of data acquisition. Compared with a multiplexer and analog-to-digital converter, the voltage to frequency converters more readily allowed accurately averaged low level signal measurements without congesting the input-output channel of the computer. For relatively slow mini-computers, like the PDP-8-S, this is an important consideration. Figure 12, which shows a typical trace of the pressure drop between the pipe taps as a capsule train moves through the pipeline, serves to illustrate the method of data acquisition. The fluctuating line represents the differential pressure between the two pressure taps in the pipeline and, since this was converted

to a frequency in the data acquisition process, it also represents the analog frequency. In a typical experiment the capsules initially move in the pipeline towards the first pressure tap so that the pressure differential, which is shown between B and C, is caused by the flowing liquid only - the liquid pressure drop. The trace of the pressure differential in Figure 12 increases between C and D when the capsule train passes the first pressure tap, only to become approximately constant again when all the capsules have passed this tap; consequently, the trace shown between D and H represents the pressure differential as capsules move between the taps. While in this Figure it is shown as being higher than the differential for flowing liquid only, in practice it is sometimes lower. The pressure differential remains constant until the capsules reach the second pressure tap, after which it reverts to the pressure differential for liquid only.

In the data acquisition process, the liquid pressure differential was measured by reading the counter at B, again reading it at C, and dividing the difference by the time interval measured as the capsules moved between B and C. The resulting quotient represents the average liquid differential pressure measured as the capsule train moved between the photocells at B and C with flowing liquid only between the pressure taps. It may be expressed as:

$$\text{Average } \Delta P = \frac{\int_B^C \Delta P \, dt}{\int_B^C dt}$$

where ΔP is the instantaneous pressure differential between pressure taps and t is time. Similar integrations were also performed simultaneously for all the other variables, the integration limits in each case being the time of transit of the capsule train between the two consecutive photocells. This method has the advantage of improving the accuracy of the low-range signals at low capsule velocities, since the readings were averaged over the long transit time of the slowly moving capsules. The integrations were also executed as the capsule train passed between photocells at D and E, E and F, F and H, providing an additional three average readings for all the variables, but for these the capsule train was moving between the pressure taps.

COMPUTER PIPELINE CONTROLS

The pumps were controlled either manually, using start-stop stations, or automatically by computer control of the starter solenoids. A simple SCR control matched the 24-volt DC control signal from the computer interface with the 220 AC of the starter solenoids. All the pipeline valves were provided with electric 24-volt DC operators. These valves were controlled by a three position switch with open, close, and automatic positions. Automatic control of the pumps and valves in the pipeline was governed by a control register interfaced with the computer with each of the valves and pumps assigned to a specific bit in the control register. Setting of a particular register bit by the computer resulted in the automatic opening of the assigned valve or starting of the assigned pump, while clearing of a particular bit had the opposite effect. The flow throttle valves were controlled by two bits in the same register such that one bit controlled the opening of the valves while the other bit controlled their closing. This was necessary in order to adjust the control valves and then hold them at a selected setting; the other valves being either fully open or shut.

EXPERIMENTAL PROCEDURE

Figure 13 shows a typical computer print-out of an experimental run. At the beginning of the run the operator loaded the capsules to the desired specific gravity, inserted the capsules into the pipeline, and then checked that the liquid was at the desired temperature. The valve and pump switches were then set from manual to automatic and the computer program started. A few feet of paper leader tape were first punched, and then the heading was typed for the capsule train inserted in the pipeline. The heading was in the form of a conversation called up by typing an H. The computer program typed out "RUN NUMBER" to which the operator replied with the number (1123 in this case). Several other lines of information were then requested by the computer program to which the operator responded. The typing of a carriage return closed each line of conversation and automatically called up the next request.

Since the same capsules were loaded to various specific gravities and run at each specific gravity, information regarding capsule diameter and length was repeated many times during the experimental program for the headings of the various runs. For this reason a table of capsule code numbers, diameter ratios, and lengths was stored in the computer memory which was called up by the program whenever a particular capsule code number was typed in.

From Figure 13 the first capsule number typed in was 050, which was immediately followed by a print-out of 0935 indicating a capsule to pipe diameter ratio for capsule 50 of 0.935. This was followed immediately by a print-out of 2450, indicating a capsule length of 24.50 inches. The remaining capsule numbers were typed in to provide information on the complete train after which a carriage return closed the conversation.

The next program step in Figure 13, called up by a type-in of C2, was a short calibration procedure whereby the frequencies of each of the variables were sampled consecutively, four times for one second. Some of this information was used as the data were processed at a later stage. The first column, while not used in further processing, shows the frequency of the crystal oscillator; the remaining six columns show, respectively, the frequency of the flowmeter at zero flow, the frequencies of the 100-inch and the 30-inch differential pressure transducers at zero pressure differential, the frequency of the

D.C. excitation voltage for the pressure transducers, and the frequencies of the inlet and the outlet temperature thermistors.

An S typed in commenced the actual experimental run. As a result the computer program turned on the pumps, adjusted the valves for flow in the forward direction with valve 2 closed and valve 3 open, and controlled the flow. The flow was controlled while the capsules were between valves 2 and 3, by comparing the flow frequency measured by the computer with a preselected set point and then adjusting the throttle valve setting to give the selected flow. A table of 10 to 60 flow set points stored as part of the computer program provided for automatic selection of flow and pump setting for each sequential capsule pass during the test run. The flow settings for each run represented a range of descending liquid velocities in the pipeline from 8 to 0.2 ft./sec. The program thus selected the first flow set point and adjusted the flow. When the desired liquid flow rate was reached, the capsules were released into the flowing stream by the computer program as it closed valve 3 and opened valve 2. The program then moved to a subroutine to service the counter overflow flags and to sense photocell pulses. When a counter overflow flag was detected the appropriate memory location assigned as the overflow buffer for that particular counter was incremented, and when a photocell pulse was detected all the counters were read along with the content of their overflow buffers. The resulting readings were stored as a block in an area in the memory assigned to that particular photocell which had pulsed. The completion of a capsule pass was indicated by the pulse from photocell 9. After reading the counters, the program turned off the pumps, adjusted the valves for flow in the reverse direction, turned on a pump, and brought the capsule train back to the inlet of the pipeline. A delay was programmed between each of the above steps of valve adjustment, and stopping and starting of the pump, in order to operate the pipeline without causing pressure waves in the liquid. One line of data was typed out as the capsules returned, giving the measurements as the capsule train moved between photocells 4 and 5. Three further lines were typed out when the capsules had returned and while the pumps stopped and the valves readjusted for flow in a forward direction, giving measurements as the capsule train moved between photocells 6 and 7, 7 and 8, 8 and 9, respectively. Each line of data represented a capsule velocity, flow frequency, two pressure differential frequencies, an excitation frequency, and two temperature frequencies in columns similar to the type-out for the C2 calibration. Before typing out, the data for columns 2 to 7 were partially processed by subtracting the consecutive data blocks and dividing the resulting differences by the capsule transit time intervals, so that the average frequency of each of the variables between successive photocell pulses was determined and punched and typed out. The paper tape thus produced was used for further processing to obtain the actual liquid velocities, pressure gradients, and temperatures. This method of processing of the data in two stages compensated for instrument drift, and, resulted in greater accuracy of the measurements since the averages of instrument calibrations before and after a series of experiments were used in the calculations. The data for column 1, however, was divided into the respective distances between the photocells so that each printout represented the actual capsule velocity. In Figure 13, therefore, the first capsule velocity was 8.009 ft./second.

After typing out the four lines of data, the computer program selected the next flow set point and, after adjusting the flow, initiated the next capsule pass. This was repeated until the measurements at the desired flow settings were completed or until the liquid flow was insufficient to cause capsule movement. Lack of capsule movement was detected by the program when the capsule train took more than 4 minutes to leave the lock and pulse photocell 4. When the test was completed, the program typed a -1 to indicate the end of the paper tape and then punched out a foot of trailer tape. Figure 13 shows only the first few lines of data for run 1123 and for that reason the -1 is not shown.

The time required for each experimental test varied from 1 to 3 hours, depending upon the length of and the values in the flow set point table. Since the pipeline was fully automated, this provided time for the operator to load the next train of capsules to the required specific gravity and prepare the paper tapes for further processing on a PDP-9 computer.

DISCUSSION

There are several stages of sophistication in data acquisition and control of an experiment. Each needs to be considered as a possible method when setting up an experimental facility. Highly sophisticated methods of acquisition and control require a long time to set up before useful results are produced, while with simple systems the time between construction of the experimental facility and obtaining the first experimental data is much shorter. Stages of sophistication and their accuracy and rate of data acquisition may be grouped under three broad headings:

1. Strip chart recording of the analog voltages, clock reading of the time intervals, and manual control. - Medium accuracy, slow.
2. Direct digitizing of all the data for visual read-out from displays or from a printer, and manual control. - Good accuracy, slow.
3. Direct digitizing of all the data, punching a paper tape for processing at a later date by a computer, and semi-automatic control of the facility by the use of separate controllers. - Good accuracy, medium speed.
4. Data acquisition and control of the experimental facility by computer. - Good accuracy, fast.

It is difficult to make a direct comparison between the various methods of data acquisition for experimental facilities solely on the basis of results obtained. Several factors have bearing on the considerations, each of which may be difficult to relate to the others. Of these factors,

the amount of data required and the accuracy of the final results are predetermined by the objectives of the experimental program, while a selection of the degree of sophistication will depend on the relative importance of cost per data line collected and time required for each data line collected.

The importance of each of these factors has to be evaluated before an experimental facility is designed. For a facility of the size and scope of the capsule pipeline described in the present paper, the time and expense involved to set up a fully automatic system have proven to be well justified. Construction of the pipeline and instrumentation commenced some months before the starting date of the contract (January 1, 1971) and was completed on May 1st. Writing and debugging the computer program was completed by August 1st. Preliminary runs with capsule trains were made and the instruments were calibrated until October 1st when the experimental program commenced. Between October 1971 and February 1973 a total of 650 experimental runs were made, each comprising about 20 liquid velocities which represented 80 lines of data. As a result 52,000 lines of data were collected during a period of 17 months. Measurements had previously been obtained from a similar pipeline but of the type where the data were digitized and read off visual counter displays. The data were manually punched on paper tape for processing on a computer. Results obtained from this pipeline amounted to 10,500 lines of data during a period of 33 months. Measurements obtained from a smaller pipeline (3/8 inch I.D.) by means of strip charts and a clock yielded 2600 lines of data during a period of 12 months. On comparing these results the strip chart approach to data acquisition yielded an average of 216 lines of data per month, the manual reading from displays approach yielded an average of 318 lines of data per month and the fully automatic method yielded an average of 3058 lines of data per month. The construction and set-up times for these facilities were not included in the above comparisons and neither was the total construction cost of each. In general, it may be stated that for short term experiments the simplest methods of data acquisition should be chosen, provided they meet the required accuracy of measurement. For projects that are to last several years, however, the additional expense and set-up time of a fully automated system may be expected to more than pay for itself.

CONCLUSION

A fully automatic method of data acquisition and control of an experimental 4-inch capsule pipeline has yielded a vast amount of accurate experimental data. These data are to be used in the design of potential commercial capsule pipelines.

ACKNOWLEDGMENTS

The author hereby expresses his appreciation to Mr. E.J. Parranto for the construction and operation of the experimental pipeline and to Mr. P.T. Afaganis for operating the experimental pipelines, and assisting with the construction of the computer interface, and with the writing of the computer program. Appreciation is also expressed to Miss B. Barrigan for further processing the data on the PDP-9 computer.

REFERENCES

[1] Hodgson, G.W. and Charles, M.E. "The Pipeline Flow of Capsules, Part 1: The Concept of Capsule Pipelining." Can. J. Chem. Eng. 39, 27-36, 1961.

[2] Charles, M.E. "The Pipeline Flow of Capsules, Part 2: Theoretical Analysis of the Concentric Flow of Cylindrical Forms." Can. J. Chem. Eng. 41, 2, 46-51, 1963.

[3] Berkowitz, N. and Jensen, E.J. "The Pipeline Flow of Paste Slugs, 1. Concepts and General Flow Behavior." Can. J. Chem. Eng. 43, 6, 280-85, 1965.

[4] Ellis, H.S. "The Pipeline Flow of Capsules, Part 4: An Experimental Investigation of the Transport in Water of Single Cylindrical Capsules with Density Greater than that of the Water. Can. J. Chem. Eng. 42, 2, 69-76, 1964.

[5] Kruyer, Jan, Redberger, P.J., and Ellis, H.S. "The Pipeline Flow of Capsules, Part 9: Analytical and Experimental Correlation of the Velocity, Pressure Gradient and Eccentricity of a Cylinder Carried Along a Pipe by a Liquid in Laminar Flow." J. Fluid Mech. 30, 3, 513-531, 1967.

[6] Ellis, H.S. and Kruyer, Jan. "The Pipeline Flow of Capsules, Part 10: Empirical Pressure and Velocity Correlations for Cylindrical Capsules Conveyed in Pipelines up to 4 inches in diameter." Paper C2. Hydrotransport 1 (1970). Research Council of Alberta Contrib. No. 485.

[7] Jensen, E.J. and Bruce, J.G. "Capsule Pipelining, a Feasibility Assessment." Paper C1, Hydrotransport 1 (1970). Research Council of Alberta Contrib. No. 493.

[8] Kruyer, Jan. "Method of Transporting a Substance along a Pipeline." U.S. Patent Spec. 3,633,976 (February 1972); Canadian Patent Spec. 881,986 (Sept. 28, 1971).

[9] Ellis, H.S. and Kruyer, Jan. "Some Effects of Fitting Cylindrical Pipeline Capsules with Collars or Runners." Paper F4, Hydrotransport 2 (1972). Research Council of Alberta Contrib. No. 565.

[10] Kruyer, Jan, and Garg, V.K. "Pressure and Couette Flow in a Capsule-Pipe System: Experimental Verification." Paper F3, Hydrotransport 2 (1972). Research Council of Alberta Contrib. No. 564.

[11] Kruyer, Jan. "Low Pressure Gradients in Capsule Pipelines." Paper F2, Hydrotransport 2 (1972). Research Council of Alberta Contrib. No. 566.

[12] Jensen, E.J. and White, L.M. "Capsule Pipelining - Solid Waste Disposal," in press. Research Council of Alberta Contrib. No. 597.

[13] Digital Equipment Corporation. Small Computer Handbook, 1967. 146 Main Street, Maynard, Mass Mass.

[14] Digital Equipment Corporation. Logic Handbook, 1967.

[15] Digital Equipment Corporation. Introduction to Programming, 1968.

[16] YSI Components Division. YSI Thermilinear Components, October, 1965. Yellow Springs, Ohio.

[17] Hewlett Packard. Pin Photodiode HP 5082-4200 Series, October, 1968. 620 Page Mill Road, Palo Alto, Calif. 94304

[18] Hewlett Packard. Application Note 915, January, 1967.

[19] Hewlett Packard. Application Note 917, March, 1967.

[20] Hewlett Packard. Voltage to Frequency Converter Model 2212A, 1968.

FIGURE 1. Capsule velocity as a function of bulk velocity for a train of four 24.55 inch long 3 5/8 inch diameter cylindrical capsules loaded to specific gravity of 1.25 and run in water in the 4.029 inch I.D. stainless steel test section.

FIGURE 2. Pressure gradients as a function of bulk velocity for the same experimental run as Figure 1. (Δ) = capsule pressure gradient, (0) = liquid pressure gradient.

FIGURE 3. Liquid viscosity for the same experimental run as Figure 1.

FIGURE 4. Schematic illustration of the 4-inch laboratory pipeline.

FIGURE 5. Typical pipe joint.

FIGURE 6. Pipeline support.

FIGURE 7. Typical cylindrical capsule.

FIGURE 8. Typical spherical capsule.

FIGURE 9. Data flow diagram.

FIGURE 10. Typical pressure tap.

FIGURE 11. Typical lightbeam-photocell assembly.

FIGURE 12. Trace of a typical pressure differential between taps in a pipeline containing capsules.

FIGURE 13. Copy of part of a typical computer print-out for an experimental run.

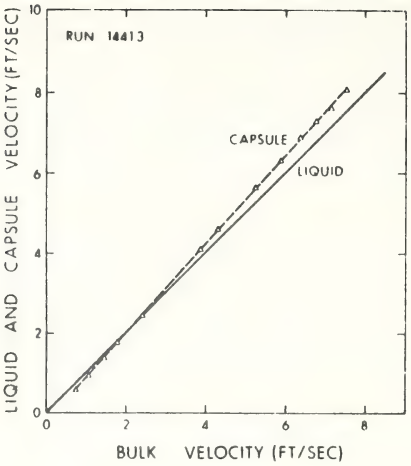

FIGURE 1. Capsule velocity as a function of bulk velocity for a train of four 24.55 inch long 3 5/8 inch diameter cylindrical capsules loaded to specific gravity of 1.25 and run in water in the 4.029 inch I.D. stainless steel test section.

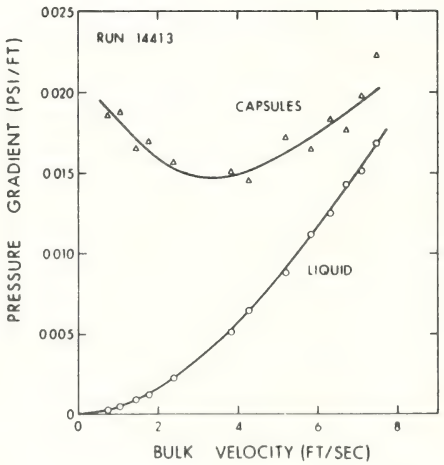

FIGURE 2. Pressure gradients as a function of bulk velocity for the same experimental run as Figure 1. (Δ) = capsule pressure gradient, (0) = liquid pressure gradient.

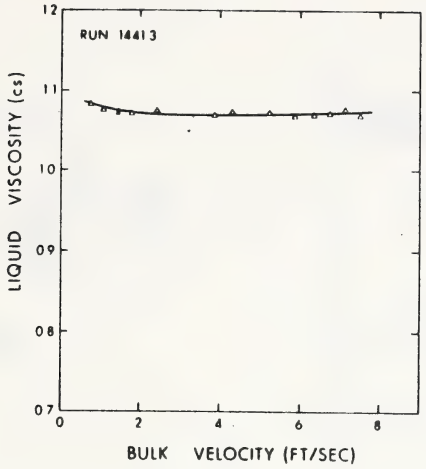

FIGURE 3. Liquid viscosity for the same experimental run as Figure 1.

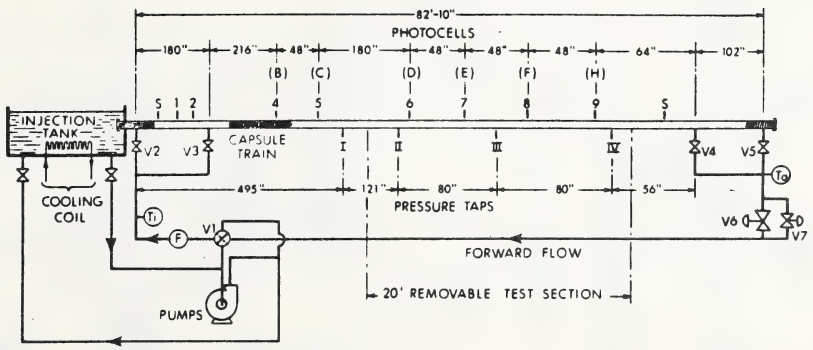

FIGURE 4. Schematic illustration of the 4-inch laboratory pipeline.

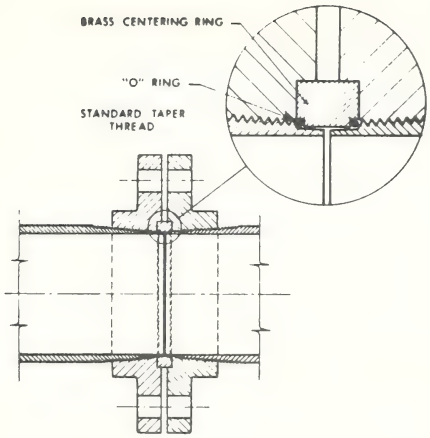

FIGURE 5. Typical pipe joint.

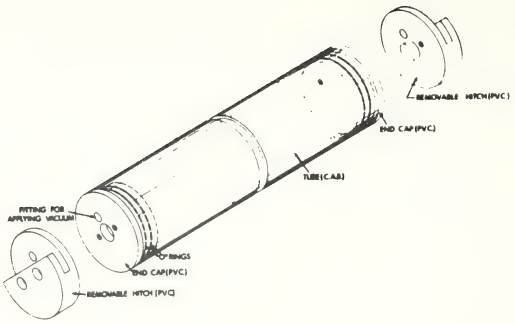

FIGURE 7. Typical cylindrical capsule.

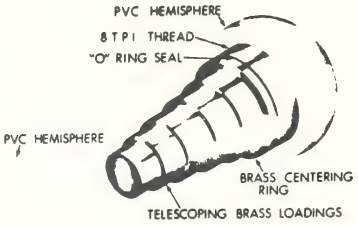

FIGURE 8. Typical spherical capsule.

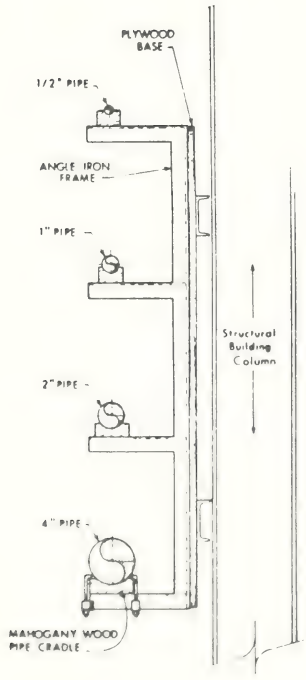

FIGURE 6. Pipeline support.

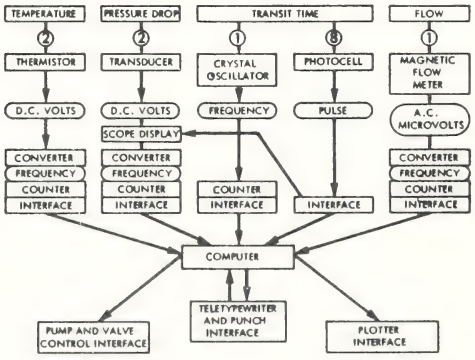

FIGURE 9. Data flow diagram.

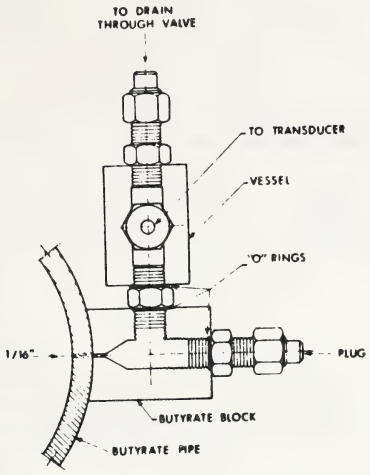

FIGURE 10. Typical pressure tap.

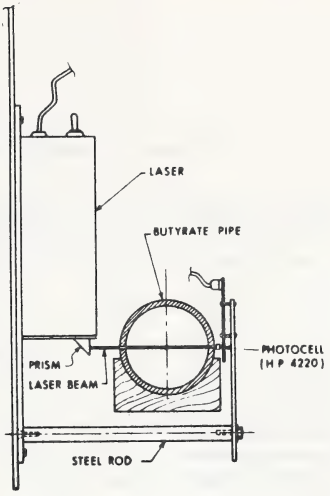

FIGURE 11. Typical lightbeam–photocell assembly.

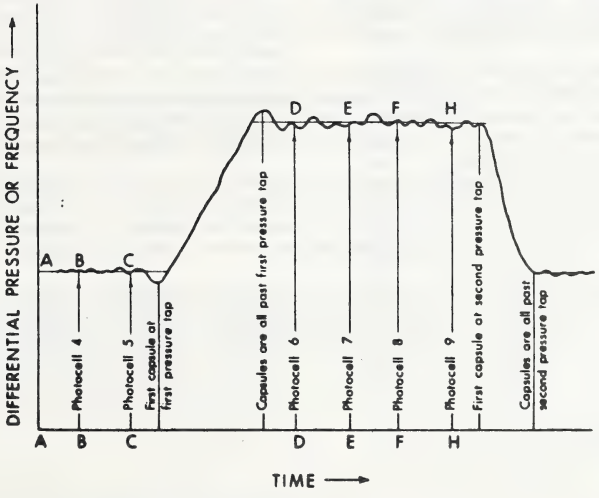

FIGURE 12. Trace of a typical pressure differential between taps in a pipeline containing capsules.

```
H RUN NUMBER:              1123

PIPE/LIQUID CODE:          411

TOTAL CAPSULE WEIGHT:  016730.0

CAPSULE DENSITY:           0.938

CAPSULE NUMBERS:
0 5009352450
0 5209352450
0 5409352450
0 5609352450
C 2
00065553 00000477 00000642 00000414 00009104 00004554 00004564
00065552 00000475 00000643 00000413 00009103 00004555 00004564
00065553 00000480 00000642 00000414 00009103 00004556 00004565
00065552 00000479 00000643 00000414 00009103 00004557 00004565
S
00800968 00008911 00003701 00000686 00009102 00004562 00004576
00793104 00008924 00003896 00000738 00009103 00004561 00004577
00791646 00008894 00003896 00000765 00009102 00004559 00004581
00793164 00008917 00004072 00000866 00009101 00004560 00004580

00767601 00008563 00003504 00000605 00009103 00004560 00004579
00759017 00008550 00003795 00000746 00009101 00004559 00004578
00758707 00008547 00003907 00000751 00009102 00004559 00004580
00762653 00008570 00003908 00000780 00009102 00004561 00004578

00727924 00008137 00003287 00000543 00009101 00004558 00004579
00724798 00008132 00003234 00000468 00009103 00004559 00004577
00720691 00008149 00003153 00000498 00009103 00004558 00004578
00721740 00008120 00003267 00000540 00009099 00004559 00004577

00693284 00007779 00003026 00000458 00009102 00004554 00004582
00690183 00007761 00003029 00000452 00009102 00004555 00004578
00685548 00007764 00003180 00000515 00009102 00004554 00004577
00688306 00007766 00003405 00000604 00009104 00004557 00004576

00675057 00007573 00002979 00000414 00009103 00004556 00004571
00667120 00007553 00003073 00000444 00009104 00004558 00004572
00664368 00007577 00003028 00000427 00009103 00004557 00004570
00666913 00007536 00003140 00000496 00009103 00004558 00004571
```

FIGURE 13. Copy of part of a typical computer print-out for an experimental run.

CAPSULE PIPELINING

Operation and Data Acquisition of a Ten Inch Experimental Pipeline

VII–2

A. A. Roehl
Alberta Research

G. C. Michaels
Green, Michaels and Associates Ltd.

Edmonton, Alberta

ABSTRACT

A four hundred foot long, ten inch diameter experimental pipeline was constructed to study the hydrodynamics of capsules in large diameter pipes.

A PDP8/S computer with 4K storage was used to relieve the operator from routine operating procedures, provide immediate "print-out" in engineering terms, plot a graph of the data measured after each pass of the capsule train and record the results on paper tape for permanent records.

The software program provided a unique calibration system of the primary sensing devices, followed by verification of the new calibration constants by calculating and plotting pressure gradient behavior against velocity.

The software consisted of three sets of programs: an operating data collection system, a calibration system, and a static data system, loaded as program overlays on a background program. Required additions to the program have been accomplished with overlays and without rewriting the original program. This system has given consistent, repeatable and accurate results.

INTRODUCTION

Capsule pipelining is a method of solids transportation where large solid bodies of various shapes and sizes are transported in a carrier liquid. The "state of the art" of the concept was derived from small diameter pipelines, and as the technology evolved it became increasingly clear that data from larger diameter pipelines were required.

Data on capsule behavior and energy requirements for the movement of a capsule train were required to extend the results. Consequently, a contract was signed between the Canadian Ministry of Transport, represented by the Transportation Development Agency and the Research Council for a three year research program, beginning January 1, 1971.

A major requirement of the contract was to produce experimental data from a series of test lines, one of which was to be sufficiently large to be representative of a practical line [1]. A ten inch diameter, four hundred foot long shuttle pipeline was designed and constructed on a site in south east Edmonton.

EXPERIMENTAL PIPELINE FACILITY

The 10 inch experimental pipeline facility was designed, constructed and instrumented to provide data on:

1) Capsule velocity
2) Capsule train pressure gradients
3) Capsule size, shape and surface
4) Specific gravities of capsules

relative to the velocity, pressure gradient and temperature of the carrier liquid. The size of the facility was too large to incorporate into existing Research Council facilities, and therefore was built on a separate site.

The main building which housed the equipment, control room and office was constructed from 24 gauge galvanized steel, sheeted with 22 gauge aluminum, and insulated.

The tunnel-like metal enclosure over the pipeline was $4\frac{1}{2}$ feet wide, 4 feet high and 415 feet long, and was heated with a 122,000 B.t.u.h. thermostatically controlled propane furnace.

Since water was used as the carrier liquid, the 10,000 Imperial gallon main reservoir was insulated and equipped with a 100,000 B.t.u.h. thermostatically controlled propane fired flue gas heater to keep it at operating temperature. All outside piping was traced with heating tape and covered with insulation and aluminum sheeting.

The 10 inch experimental line and the 8 inch return line were supported by pipe rolls at ten foot centres mounted on reinforced concrete blocks 12 inches wide by 12 inches high by 4 feet long, and supported on 10 inch diameter by 8 foot long friction piles. This provided a stable base for the pipeline and enabled levelling of the pipe to within ± 0.01 feet.

The nominal 10 inch main test line was 10.750 inches

outside diameter by 0.365 inch wall thickness and was 400 feet long. This provided sufficient length to achieve steady state conditions before the experimental test data were measured. Enough distance for slow deceleration of the capsules and liquid was also provided to permit reversing of the flow without the capsules colliding with the ends of the pipeline. Lengths of pre-selected Electric Resistance Weld pipe, joined with matched socket-weld flanges, were used in construction of the main test pipeline. The excess seam in the pipe and distortion in the pipe wall, due to welding of the flanges, were removed by grinding to give a smooth uniform bore.

The ends of the main test line and return pipe were fitted with Huber-Yale scraper trap closures. This permitted cleaning both lines with neoprene spheres and wire brushes.

A 42 foot section of the 10 inch test line was bent in a vertical "S" bend to achieve a 3 foot elevation for capsule injection and ejection. The opening was at the same elevation as a 20 foot roller conveyor fitted with a drip pan which was connected to a liquid return tank. During ejection the capsules moved along the conveyor while the water spilled into the return tank and was returned to the main reservoir with a centrifugal pump. The capsules were handled with a small electric fork lift.

Three centrifugal pumps, with capacities of 300 USGPM, 600 USGPM, and 1200 USGPM at a head of 50 psi, were connected to permit their operation individually or in combination. With the use of a 6 inch fish-tail butterfly control valve any liquid velocity from 0 feet per second to 9 feet per second could be selected.

The capsules were constructed from seamless mechanical tubing, cut to 4 foot lengths and fitted with 1.5 inch thick polyvinyl chloride (P.V.C.) end caps and O-ring seals. The removable end caps permitted loading with steel rods to achieve capsule specific gravities from 0.98 to 1.50. The chosen capsule diameters were 8.5 inches, 9.0 inches and 9.5 inches. Spheres of these diameters cast from aluminum and iron were also tested.

INSTRUMENTATION

The system was designed to permit several modes of control; manual, computer or a combination of both. The provision for the operator to take over manual control during the initial stages of the project and in times of difficulty proved useful. Normal operation was by computer control with the operator checking the data and accepting or rejecting them.

The control console was designed and constructed to permit operation of all equipment as well as provide a visual display of the performance of the equipment including the primary data sensing transducers. These were: pump discharge pressures, temperature of the carrier liquid at 5 locations, temperature along the pipeline enclosure at 3 locations, flow rate of the carrier liquid, flow-control valve setting, pressure transducers, photo detector operation and power supply outputs. A voltage to frequency converter and a digital counter were connected to all primary sensors with a selector switch for closer examination of their performance. The upper part of the console contained a schematic diagram of the pipeline with indicator lights and meters indicating the state of the photo detectors and providing a visual display of the location of the capsule train.

Valves not requiring frequent or rapid operation were manually operated, but the flow control valve, system by-pass valve and capsule collection valves were pneumatically operated either from the control console or by the computer (Figure 1).

The liquid flow was measured with a 6 inch magnetic flow transmitter connected to a flow to current converter which had a 4 step externally switched range selector.

The pressure drops for liquid flow and for capsule and liquid were measured using two differential pressure transducers with ranges of 0-5 inches and 0-50 inches of water, respectively.

Temperatures along the test pipeline, in the main storage tank, and inside the pipeline enclosure were measured with thermistor-resistor networks. These proved to be fast, stable and accurate.

The capsule detection system was constructed from a series of photo-sensitive detectors located diametrically opposite from helium-neon lasers. When the laser light source was activated and the beam directed on the detector, the phototransistor conducted with a resultant network output of +15 volts. When a capsule passed between the light source and detector, the detector ceased to conduct with a resultant network output of -15 volts. These signals interrupted the computer which was programmed to perform functions for each interrupt. Using carefully measured pipe distances, capsule velocities were determined by measuring the time between successive signals using a 5000 Hz crystal clock in the computer.

The computer used was a Digital Equipment of Canada PDP8/S with 4,096 words core memory. The primary sensor networks were interfaced to the computer with a multiplexed DEC Type AF01 Analog-to-Digital Converter. After all instruments were installed, they were carefully calibrated, against standards wherever possible, and these calibrations checked frequently. When a change in instrument performance occurred a new calibration was done.

Following the calibration of all primary instruments used for data collection, liquid velocity, liquid pressure and temperature measurements were taken and a Moody diagram plotted with the computer. The plot was compared with theoretical values and data from previous

runs. When a good comparison with theoretical values was achieved the system was considered calibrated and the experimental program continued.

Further discussion on calibration appears in the section on the computer program.

COMPUTER PROGRAM

The software for this project was designed so that basic operating decisions were the task of the operator, with the computer providing control of the equipment and fast and accurate execution of the tedious conversion and recording tasks. With the use of the computer, the operator was able to concentrate on proper operation of the pipeline, on determining the acceptability of data, and ensuring that the calibration of the system and other facets of data gathering remained valid over the period of time that the pipeline was operated.

The software consisted of three sets of programs: an operating data collection system, a calibration system, and a static data system, loaded as program overlays on a background program. The operating data system contained the operating program and the maintenance program, as well as auxiliary commands. The calibration system contained the calibration program, the calibration verification program, and the maintenance program. The static data system allowed the collection of data on a stationary train of capsules.

1. Operating Program

The operating program was used for data collection runs which consisted of a number of passes at various velocities of a capsule train from the injection point to the end of the line. The data collected were (1) the velocities of the liquid and the capsule, (2) pressure gradients for the liquid and the capsules, (3) temperature of the liquid at four places in the line, and (4) spacing, if any, of the capsules. The operator was in full command of the facility and determined whether or not to accept data generated by the program.

The operator had a variety of auxiliary commands available when the operating program was not running the pipeline. He could set the flow control valve to any percentage opening desired, manually operate the pumps and read temperatures, pressures and flow rates on command. He could change the value of floating point constants from the keyboard to update changes in various physical constants. These commands permitted the use of the computer's programs in the collection of data for non-standard runs.

A description of system operation is included in the next section.

(a) Capsule Pressure Gradient Calculation.

The capsule pressure gradient was calculated from the apparent pressure gradient with the capsules in the test section, and the fluid pressure gradient read when the capsules were at PC2 (see Figure 1). The fluid pressure gradient was assumed to remain constant and end effects were not considered. The pressure drop attributed to the capsules was calculated and divided by the length of the capsule train.

(b) Maintenance Program.

The maintenance program monitored the operation of the transducers and timers. In particular, the internal one second and five second time delays were checked against the internal 5 kHz clock for drift. The four pipeline temperatures were read and printed, the low and high range pressure transducer readings were printed. The isolation and bypass valves were not affected and so could be manipulated by the operator as desired.

The maintenance program was available in both the operating and calibration systems.

2. Calibration Program

There were three steps in the execution of the program: set-up, data collection, and conclusion.

The program set-up included the input and plotting of the date and the scaling of lower and upper values of the calibration range.

During data collection for thermistor and pressure cell calibrations, the operator typed in the true temperature or pressure in degrees Fahrenheit or inches of water, respectively, while the true value was impressed on the transducer and measured by a standard device. Any corrections for individual calibration instruments or temperatures were made in the "true" values read in from the keyboard, so that the calibration took into account all known factors. This procedure was repeated for each temperature or pressure.

For the flow meter ranges, the program collected the data automatically. An inflated neoprene sphere larger than the inside diameter of the experimental pipe was first inserted, the program then executed a series of passes of the sphere through the line at increasing flow rates. The time the sphere took to traverse the 10.00 foot test section was measured and converted to a flow rate in USGPM. This was the true input value, assuming no liquid bypassed the sphere. The averaged reading of the flow meter during the time the sphere was in the test section was taken as the measured value. Each reading consisted of the average of 64 transducer values, and these readings were taken 20 times per second.

The calibration program was concluded when the last

value of programmed flow was completed and the sphere returned, or when a negative number was typed in during calibration of the thermistor or pressure transducers. The values of the best fit linear coefficients found by a least squares analysis and the best fit straight line were plotted on the calibration chart, recording the calibration results. The calculated values of the coefficients were stored in the computer and the transducer was considered to be calibrated. The calibrations were then checked with a computer-plotted Moody Diagram, which is a logarithmic plot of Fanning Friction Factor against Reynolds Number.

For a programmed series of liquid flows, the program recorded the pressure and flow, calculated the Fanning Friction Factor and Reynolds number, recording their logarithms on the pre-printed chart. Flow and pressure readings were made 2048 times and averaged to reduce the effect of noise. When the set of liquid velocities were completed, the program stopped and waited for further information. No capsules were used in the process.

Examination of the results of this program allowed the operator to decide whether the dynamic operation of a pressure transducer or flow transducer was satisfactory or suggested recalibration.

The calculation of the friction factor at low flow values was sensitive to the errors in pressure from fluctuation and absolute error of the low pressure differential pressure cell. Since the friction factor was plotted on a logarithmic scale, small absolute errors caused large apparent errors. This method therefore served as an effective tool for checking instrument calibration and performance.

(a) Reading of Transducers.

Thermistors, differential pressure cells and flowmeter all used the same method for conversion of a transducer reading into calibrated engineering units. The transducer reading was converted by a linear transformation to a theoretical scale reading in engineering units. The calibrated value was found by application of the linear calibration parameters.

The calibration program determined the value of the slope and intercept for each transducer which best described the calibration curve of the device with a linear least squares fit.

The computer program used the calibration results to convert the quantities it could read (voltage) to engineering units, according to two linear transformations. These two linear transformations could be "reversed" if desired to generate the voltage measured to check the entire process. The computer routines written allowed updating of calibration curves independently for each device, and allowed a large amount of sharing of the stored programs to use core storage most effectively.

3. Static Data Program

This program was designed to collect data on the flow rate and pressure gradient of the capsule train before the capsules began to move. It consisted of a program loop reading data for five seconds, every six and a half seconds as long as required by the operator, while the photocell indicator lights were observed for movement of the capsule train. The data printed were liquid velocity, liquid pressure gradient, capsule pressure gradient and liquid temperature in two test sections.

Background Program

The background program contained some basic functions common to the three systems of programs. It was composed basically of a modification of the DEC Floating Point Package [2], an original plotter package for the plotting of axes and data on the charts, an interrupt servicing routine for the handling of input, output, clock and photocells, and system utility routines for handling common tasks.

The floating point package allowed a calculation accuracy to at least six significant figures.

The plotter package allowed the ordinary output routines for typing numerals and some special symbols to plot characters. The plotter calibration routine plots a 10 inch square, permitting scale and zero adjustment whenever desired. The interrupt servicing routine used the single-level interrupt structure in the PDP8/S to service interrupts in the following order: clock, photocell, teletype output and keyboard input.

The pipeline system routines were part of the background program. Included are such routines as transducer reading and scaling, time delays, flow control and valve control.

SYSTEM OPERATION AND DATA ACQUISITION

To inject the capsules, the scraper trap on the 10 inch line was vented, opened, and excess liquid allowed to drain into the return tank. The capsules were then pushed into the open line. When all capsules were inserted, the scraper trap was closed, the air vented and the train was ready for the test run or runs planned.

A new chart was put on the plotter, the plotter was calibrated and new capsule parameters were entered into the computer using a teletype. The computer printed these parameters on paper, plotted them on the graph and punched them in paper tape to identify the run. When these instructions and the date were properly recorded, the operator selected the velocity with which he wished to start the run and indicated the liquid velocity increments he wished the computer to use for the succeeding passes. This could be changed any time after a particular pass was completed.

As soon as the desired starting velocity and increments were typed in on the teletype the computer was ready to execute the commands (Figure 3). A pass through the test section was initiated when the appropriate command was entered on the teletype. The computer selected the right pump or pump combination, valve CCV_2 (capsule collection valve; see Figure 1) was opened and the preset flow rate was established with the direct digital control loop (DDC). The DDC loop used a 2 second time delay to compensate for mechanical time lags. The flow meter output was compared with the required flow rate and the valve opening adjusted till the required flow rate was attained. The flow valve opening was then "locked" to prevent change, and valve CCV_1 opened while valve CCV_2 closed. The liquid now entered behind the capsule train, moving it forward in the pipeline.

When the train passed PC_0 (photocell) all registers and flip-flops in the computer were cleared and the level lights on the control panel switched off.

Ten seconds after valve CCV_1 was opened the computer opened the transducer isolation valves (S_1 and S_2 ; S_4 and S_5) and closed the bypass valves (S_3 and S_6) to the pressure transducers and thus put them on line (see Figure 1).

As the train moved through the pipeline it passed PC_1 which functioned only as an indicator of the train movement. During this time the computer scanned the pressure transducer outputs. If the liquid gradient on the high range cell was greater than 4.5 inches of water it read the high range cell when the train arrived at PC_2 .

When PC_2 signalled the presence of the capsule train the computer read the 5 kHz clock and averaged 1024 readings of the flow meter output, read the output from the selected pressure transducer, as well as the average of 64 readings of the temperatures along the test line T_1 , T_2 , T_3 , T_4 , and then awaited a signal from PC_3 . When the signal from PC_3 was received the computer again read its internal 5 kHz clock and continued to read it every time an interrupt was received from the photocell as the train passed.

After the train had passed PC_3 the computer calculated the liquid velocity at PC_2 , the capsule velocity between PC_2 and PC_3 , the liquid pressure gradient over the test section, temperatures T_1 to T_4 , and the spacings between the capsules, if any. When these operations were completed and the low range cell isolated an interrupt from PC_4 was awaited. After the PC_4 interrupt the computer again read the clock and, since the distance and elapsed time interval between PC_3 and PC_4 were known, calculated the velocity of the lead capsule in the train. As soon as this was completed a signal from PC_5 was awaited. When the interrupt from PC_5 was received the clock was read again and the train velocity between PC_4 and PC_5 calculated. The reading of capsule velocity in 5 different pipe sections ensured that a stable capsule velocity was reached before data used for analysis were accepted. When the train reached PC_6 the clock, the liquid flow, the high range transducer, and all temperatures were read, and the high range transducer isolated. When the train reached PC_7 , the clock was read a sixth time. The flow control valve closed, the system bypass valve opened, the diverter valve switched to the return position, valves CCV_1 and CCV_2 opened, and the mechanical part of the system shut down while the computer calculated the velocity between PC_5 and PC_6 , the liquid velocity, the capsule pressure gradient, all temperatures and the velocity of the train between PC_6 and PC_7 . When all computations were completed, the following parameters were printed on the teletype (Figure 3):

Liquid velocity at PC_6
Liquid pressure gradient - when the train was at PC_2
Capsule velocity between PC_6 and PC_7
Capsule pressure gradient
Temperatures T_1 , T_2 , T_3 , T_4
Spacing, if any, between capsules
Velocities between PC_2 - PC_3 ; PC_3 - PC_4 ; PC_4 - PC_5; PC_5 - PC_6 ; and PC_6 - PC_7
Liquid velocity while the train was at PC_2 .

After the above was typed out the train was returned to the starting end of the pipeline at velocities between 3.5 and 4.0 feet per second.

While the train was returning the operator examined the data to ensure that the liquid velocities at PC_2 and PC_6 did not differ by more than 1%, that the train had not spread, or major variations in temperatures T_1 to T_4 had not occurred, also that the capsule train had achieved uniform velocity before reaching PC_6 . If all these conditions were met, the data were considered valid and were accepted; if not, a repeat pass was indicated or all instruments had to be checked to ascertain if they functioned properly.

Thirty seconds after the train returned to PC_0 the flow valve was closed, valves CCV_1 and CCV_2 were closed, the system bypass valve opened and the diverter valve switched to the forward position. The system bypass valve was then closed, and the mechanical part of the system assumed a waiting mode.

During the waiting mode the operator accepted the data. The data were again typed out (Figure 3), identified as accepted, punched in paper tape and plotted on the graph (Figure 2). When the plot was completed the operator initiated another pass. If the data were not acceptable, the operator repeated the pass. A run consisted of 16 to 23 passes at velocity increments of approximately 0.5 ft./sec. The data from a completed run were then checked and delivered for further processing, evaluation and correlation.

CONCLUSIONS

The system as designed and constructed has provided the flexibility necessary for a research program, as well as providing immediate data which were repeatable and accurate.

ACKNOWLEDGMENTS

The authors hereby wish to express their appreciation to Messrs. J. Green and J. Kruyer for their assistance and contributions to the design of the electronics and program, and to Messrs. M. Blachut, H. Dalpe and K. Wourms for operating the facility.

REFERENCES

[1] Jensen, E.J., et al., T.D.A.-R.C.A. Capsule Pipeline Project, Phase I Report. Research Council of Alberta Information Series Contribution No. 63.

[2] Programming Languages - 1970. Digital Equipment Corporation, Maynard, Massachusetts.

BIBLIOGRAPHY

[1] Anon. "Abstracts of Fluid Dynamics Research Papers." Published and continually revised by the Research Council of Alberta. Available on request.

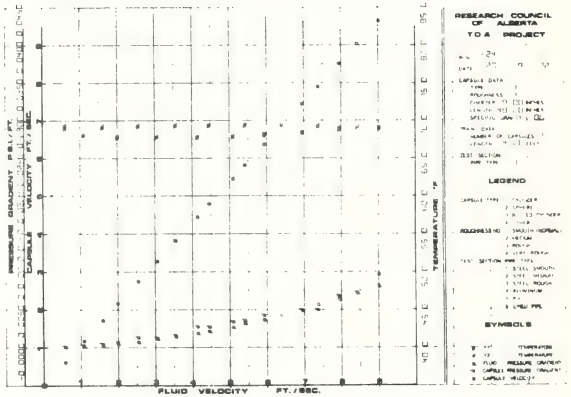

COMPUTER PLOT OF A RUN FIGURE 2

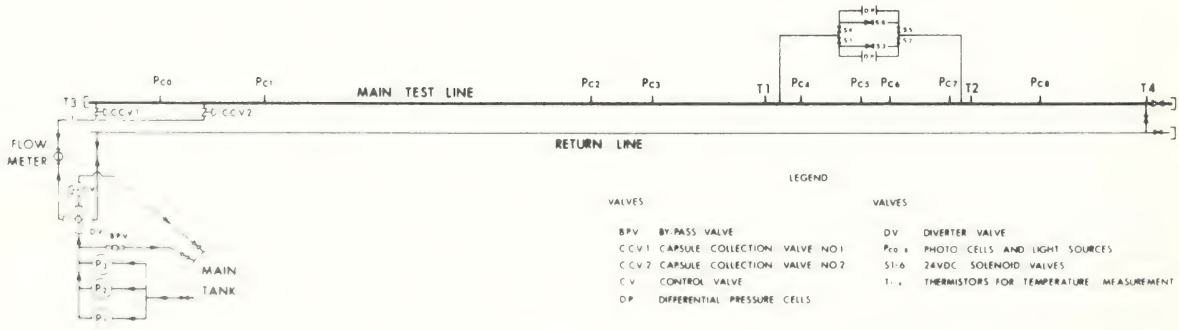

SCHEMATIC DIAGRAM OF THE TEN INCH PIPELINE

FIGURE 1

```
)CT
1

)RO
1

)CD
0.0

)CL
48.0

)CG
1.00

)NC
1

)TL
4.0

)PI
1

)TR
35 85

)PR
-.005 .045

)ST

RUN:: -524.

DATE:: D M Y  20 9 72
G 1.083 0.00017 1.167 0.00019 68.1 68.0 67.0 68.0 0.00 0.00 0.00 0.00
C 1.16 1.16 1.17 1.16 1.17   1.078

G 2.004 0.00052 2.164 0.00067 67.7 67.8 67.1 68.0 0.00 0.00 0.00 0.00
C 2.16 2.16 2.16 2.15 2.16   2.006

G 3.062 0.00114 3.276 0.00122 67.8 67.8 67.2 68.1 0.00 0.00 0.00 0.00
C 3.25 3.26 3.27 3.26 3.28   3.036

G 4.144 0.00188 4.431 0.00272 67.7 67.8 67.2 68.0 0.00 0.00 0.00 0.00
C 4.41 4.41 4.43 4.42 4.43   4.099

G 5.102 0.00262 5.442 0.00335 67.8 67.8 67.2 67.9 0.00 0.00 0.00 0.00
C 5.41 5.45 5.45 5.44 5.44   5.053

G 5.942 0.00361 6.357 0.00422 68.2 67.9 67.4 67.9 0.00 0.00 0.00 0.00
C 6.39 6.36 6.35 6.33 6.36   5.939

G 6.969 0.00485 7.438 0.00493 68.5 68.3 67.4 68.3 0.00 0.00 0.00 0.00
C 7.46 7.45 7.49 7.46 7.44   6.967

G 7.966 0.00629 8.517 0.00670 68.8 69.0 67.7 69.0 0.00 0.00 0.00 0.00
C 8.47 8.49 8.53 8.50 8.52   7.920

G 9.048 0.00809 9.651 0.00959 68.8 69.1 67.7 69.0 0.00 0.00 0.00 0.00
C 9.67 9.66 9.66 9.62 9.65   9.028

G 8.459 0.00715 9.046 0.00717 69.0 69.2 67.8 69.1 0.00 0.00 0.00 0.00
C 9.01 9.03 9.02 9.02 9.05   8.468

G 7.395 0.00564 7.901 0.00492 69.2 69.2 68.0 69.0 0.00 0.00 0.00 0.00
C 7.94 7.92 7.94 7.91 7.90   7.395

G 6.414 0.00432 6.868 0.00419 69.5 69.4 68.3 69.4 0.00 0.00 0.00 0.00
C 6.90 6.90 6.87 6.84 6.87   6.411

G 5.427 0.00310 5.811 0.00347 69.3 69.4 68.1 69.3 0.00 0.00 0.00 0.00
C 5.84 5.81 5.81 5.80 5.81   5.435

G 4.462 0.00216 4.762 0.00272 69.3 69.4 68.3 69.3 0.00 0.00 0.00 0.00
C 4.74 4.76 4.77 4.76 4.78   4.416

G 3.557 0.00144 3.820 0.00158 69.3 69.4 68.5 69.4 0.00 0.00 0.00 0.00
C 3.82 3.82 3.81 3.81 3.82   3.558

G 2.554 0.00075 2.737 0.00128 69.2 69.3 68.6 69.5 0.00 0.00 0.00 0.00
C 2.73 2.74 2.74 2.73 2.74   2.549

G 1.594 0.00032 1.711 0.00041 69.0 69.2 68.5 69.6 0.00 0.00 0.00 0.00
C 1.71 1.71 1.71 1.70 1.71   1.587

G 0.594 0.00024 0.621 0.00044 68.4 69.3 68.9 69.8 0.00 0.00 0.00 0.00
C 0.62 0.62 0.62 0.60 0.62   0.575
```

TELETYPE "PRINT-OUT" OF A RUN FIGURE 3

EXPLANATION TO FIGURE 3

)CT - Capsule Type
)RO - Capsule Roughness
)CD - Capsule Diameter
)CL - Capsule Length
)CG - Capsule Specific Gravity
)NC - Number of Capsules
)TL - Train Length
)PI - Pipe Index (test section type)

For further information on the above, see right hand side of graph of Figure 3

)TR - Temperature Range for Graph
)PR - Pressure Gradient Range for Graph
)ST - Starting symbol for computer

Run information:

Run: number
Date
G & C - prefixing each line of accepted data

From left to right:-

first number is velocity of liquid at PC_6 (see Figure 1)
second number is pressure gradient of liquid
third number is velocity of leading capsule between PC_6 and PC_7
fourth number is pressure gradient of capsule train
fifth number - Temperature 1 (T_1)
sixth number - Temperature 2 (T_2)
seventh number - Temperature 3 (T_3)
eighth number - Temperature 4 (T_4)

The last four numbers of first column are capsule spacings at PC_3.

Second line:

1st number - VC_{2-3} - Velocity of capsule train between PC_{2-3}
2nd number - VC_{3-4} " " " " PC_{3-4}
3rd number - VC_{4-5} " " " " PC_{4-5}
4th number - VC_{5-6} " " " " PC_{5-6}
5th number - VC_{6-7} " " " " PC_{6-7}
6th number - Velocity of liquid while capsule train is at PC_2.